Studies on the promiscuous xenobiotic receptor (PXR, NR1I2) in zebrafish: antibody characterisation and genetic variation in zebrafish embryos

Daniel James Hitchcock

Thesis submitted in partial fulfilment of the requirements for the degree of Master of Science

Department of Biology
University of Bergen, Norway
June 2014

Acknowledgements

The work presented in this thesis was performed in the Environmental Toxicology group at the Department of Biology at the University of Bergen. This project was funded by the Norwegian Research Council, Miljø 2015, Project 181888.

First I would like to thank my supervisors Anders Goksøyr and Roger Lille-Langøy for taking care of me during my time as a Masters student. Anders, thank you for letting me attend my first ever conference and helping me out during the writing stages of my thesis. Roger, thank you so much for all your technical assistance in the laboratory, your patience and dedication throughout my period as a student. It has been the utmost pleasure having you as my supervisor and I couldn't have wished for anyone better.

I would also like to thank everybody else in the Environmental Toxicology group, from Bachelors, Masters, PhD students, researchers and visitors who have made me feel a part of the group, and for creating a fun, upbeat social environment.

I also want to thank all the friends I've made along the way. Magnus, Ynghild and Rachael, a special shout out goes to you!

And last, but not least, thanks Mum for all the love and support you've given me from all the way on other side of the world. Thank you for all the phone calls, care packages and always checking up on me. You've been there through thick and thin and thanks to you I've made it through.

Bergen, 02 June 2014
Daniel James Hitchcock

Table of contents

Abstract

The promiscuous xenobiotic receptor (PXR, NR1I2, also denoted pregnane X receptor) is a nuclear receptor which regulates the transcription of genes involves in the biotransformation of endogenous and xenobiotic compounds. PXR is activated by ligands including steroids, natural products, as well as drugs and pollutants, making it an important subject of research in a pharmacological and ecotoxicological context. One method of studying this nuclear receptor is through the use of high quality, specific antibodies which can immunochemically detect the protein. In the first part of this study, the immunoreactivity of hybridoma supernatants obtained from cells of mice immunised with either human PXR (hPXR, *Homo sapiens*) or zebrafish Pxr (zfPXR, *Danio rerio*), suspected to contain monoclonal antibodies specific to each PXR ortholog, were tested against eukaryotically expressed hPXR and zfPXR, as well as prokaryotically expressed zfPXR. Hybridoma supernatants from mice immunised with hPXR were found to be immunoreactive against the hPXR antigen, however some of these supernatants were immunoreactive with an additional protein that was heavier than the PXR antigen. Hybridoma supernatants from mice immunised with zfPXR were not found to be immunoreactive against either eukaryotically or prokaryotically expressed zfPXR antigen. In a second aspect of this study, research has identified allelic variants in the amino acid sequence of zfPXR and this could have implications on the nuclear receptor's ability to function. A method for extracting RNA from individual zebrafish embryos was established in our laboratory, and *pxr* was sequenced from individuals (n = 24). However no genetic variation was found in this sample set, compared to what has been identified in literature and to online databases.

Abbreviations

Abbreviation	Full name
%	Percent
× g	Gravitational acceleration (relative to Earth)
µg	Microgram
µL	Microlitre
µm	Micrometre
µM	Micromolar
A	Absorbance
AB/Tu	AB/Tübingen
ABC	Adenosine triphosphate(ATP)-binding cassette
AF	Activation function
AGE	Agarose gel electrophoresis
AhR	Aryl hydrocarbon receptor
APS	Ammonium persulphate
BFR	Brominated flame retardant
bp	base pairs
BPA	Bisphenol A
BSA	Bovine serum albumin
BXR	Benzoate X receptor
CAR	Constitutive androstane receptor
CBB	Coomassie brilliant blue
CCD	Charge-coupled device
cDNA	Complementary DNA
CDR	Complimentarity determining region
ChIP	Chromatin immunoprecipitation
cm	Centimetre
CO_2	Carbon dioxide
COS-7	CV-1 (simian) in Origin containing SV40 genetic material, line 7
CXR	Chicken X receptor
CYP(450)	Cytochrome P450 monooxygenase
DBD	DNA binding domain
ddNTP	Dideoxynucleotide
DDT	Dithiothreitol
DEPC	Diethylpyrocarbonate
DMEM	Dulbecco's Modified Eagle Medium
DMSO	Dimethyl sulphoxide
DNA	Deoxyribonucleic acid
dNTP	Deoxyribonucleotide triphosphate
E. coli	*Escherichi coli*
E.g.	*Exampli gratia* (for example)
EC	Effective concentration
ECL	Enhanced chemiluminescence
EDC	Endocrine disrupting compound
EDTA	Ethylenediaminetetraacetic acid
ELISA	Enzyme-linked immunosorbent assay
Et al.	*Et alii* (and others)
EtBr	Ethidium bromide
Etc.	*Et cetera* (and so on)
EtOH	Ethanol
Fab	Fragment, antigen-binding
FBS	Fetal bovine serum

Fc	Fragment crystallisable
FL	Full-length
FXR	Farsenoid X receptor
g	Gram
GR	Glucocorticoid receptor
HCl	Hydrochloric acid
His	Histidine
hpf	Hours post fertilisation
HPLG	Heavy phase lock gel
hPXR	Human promiscuous xenobiotic receptor
HRE	Hormone response element
HRP	Horse radish peroxidise
i.e.	*Id est* (that is)
Ig	Immunoglobulin
IgG	Immunoglobulin G
IgM	Immunoglobulin M
IPTG	Isopropyl β-D-1-thiogalactopyranoside
kb	Kilobase
KCl	Potassium chloride
kD	Kilodalton
L	Litre
LB	Lysogeny broth
LBD	Ligand binding domain
LBP	Ligand binding pocket
LXR	Liver X receptor
M	Molar
MDR1	Multidrug resistant protein 1
MeOH	Methanol
mg	Milligram
min	Minutes
mL	Millilitre
mm	Millimetre
mM	Millimolar
mRNA	Messenger ribonucleic acid
MRP2	Multidrug resistance-associated protein 2
n	Number
NaCl	Sodium chloride
ng	Nanogram
NLS	Nuclear localisation signal
nm	Nanometre
nM	Nanomolar
NR	Nuclear receptor
º C	Celcius
OD	Optical density
PAGE	Polyacrylamide gel electrophoresis
PBS	Phosphate buffered saline
PBS-T	PBS Tween-20
PCB	Polychlorinated biphenyls
PCN	Prenenolone carbonitrile
PCR	Polymerase chain reaction
pDNA	Plasmid DNA
PDVF	Polyvinylidene fluoride
PPAR	Peroxisome proliferator-activated receptor
PXR	Promiscuous xenobiotic receptor
RAR	Retonoic acid receptor

RFLP	Restriction fragment length polymorphism
RIN	RNA Integrity Number
RNA	Ribonucleic acid
RNase	Ribonuclease
rpm	Revolutions per minute
rRNA	Ribosomal RNA
RT	Reverse transcriptase
RXR	Retinoid X receptor
s	Seconds
SDS	Sodium dodecyl sulphate
SNP	Single nucleotide polymorphism
SOB	Super optimal broth
SOC	Super optimal broth with catabolite repression
SRC-1	Steroid receptor coactivator 1
SULT	Sulphotransferase
SWT	Singapore wild-type
SWT	Singapore Wild-type
SXR	Steroid and xenobiotic receptor
TAE	Tris/Acetic/EDTA
TBE	Tris/Borate/EDTA
TBS	Tris-buffered saline
TBT-T	TBS Tween-20
TEMED	N,N,N',N'-tetramethyl-ethylenediamine
TGS	Tris/glycine/SDS
TL	Tupfel long fin
TR	Thyroid hormone receptor
Tris	Tris(hydroxymethyl)aminomethane
Tu	Tübingen
UGT	Uridine 5'-diphospho(UDP)-glucuronosyltransferase
UV	Ultraviolet
V	Volts
v/v	Volume to volume
VDR	Vitamin D receptor
w/v	Weight to volume
WB	Western blotting
XRE	Xenobiotic response element
ZFIN	Zebrafish Information Network
zfPXR	Zebrafish promiscuous xenobiotic receptor
β	Beta

1. Introduction

1.1 Background

The promiscuous xenobiotic receptor (PXR, NR1I2) is a nuclear receptor which is responsible for regulating genes involved in the biotransformation of endogenous and xenobiotic compounds (Blumberg *et al.*, 1998). When activated by ligands, PXR induces the transcription of genes which encode for enzymes involved in xenobiotic and steroid metabolism. Mammalian PXR is also known as the pregnane X receptor and steroid and xenobiotic sensing receptor (SXR), while the chicken and frog orthologs are chicken X receptor (CXR) and benzoate X receptor (BXR), respectively (Milnes *et al.*, 2008).

1.2 Nuclear receptors

1.2.1 Nomenclature, types and function

There are seven subfamilies of nuclear receptors and according to sequence similarity, PXR is placed in the nuclear receptor subfamily 1 group I member 2 (Nuclear Receptors Nomenclature Committee, 1999; Laudet, 1997). PXR is most closely related to the vitamin D receptor (VDR, NR1I1) and constitutive androstane receptor (CAR, NR1I3), which can be activated by calcitriol and steroids respectively (Krasowski *et al.*, 2011). These three nuclear receptors also belong to the thyroid-like receptors subfamily, which includes the thyroid hormone receptor (TR, NR1A), retinoic acid receptor (RAR, NR1B), peroxisome proliferator-activated receptor (PPAR, NR1C1, 1C2 and 1C3), liver X receptor (LXR, NR1H2 and 1H3) and the farsenoid X receptor (FXR, NR1H4 and 1H5) which are involved in other important processes in the body such as development, homeostasis, metabolism and bile acid synthesis (Robinson-Rechavi *et al.*, 2003; Germain *et al.*, 2006).

This thesis follows protein and gene nomenclature guidelines according to the *Genetics and Molecular Biology* journal. In humans and mammals, the protein form of NR1I2 is written as PXR; and as Pxr in zebrafish. The gene is written as *PXR* in humans; in mice it is written as *Pxr*; and as *pxr* in fish.

1.2.2 Nuclear receptor evolution

It has been proposed that the first nuclear receptor developed in metazoans over 600 million years ago (Escriva *et al.*, 2000), and ability for ligands to activate receptors occurred later in evolution (Escriva *et al.*, 1997). These first receptors were classified as orphan receptors,

because they either lacked an exclusive endogenous ligand or one had not yet been identified. Today, nuclear receptors are considered promiscuous to a wide range of endogenous and exogenous compounds, depending on which group they belong (Krasowski *et al.*, 2011).

1.3 Promiscuous xenobiotic receptor, PXR

1.3.1 Induction of cytochrome P450 monooxygenases

One important group of genes regulated by PXR is the cytochrome P450 (CYP) monooxygenases, and these represent enzymes involved in the oxidation of steroids and xenobiotic compounds in phase I biotransformation. CYP activity occurs mostly in the liver, small intestine and colon, where the highest level of xenobiotic detoxification takes place within the body (Bertilsson *et al.*, 1998; Nishimura *et al.*, 2004; Lamba *et al.*, 2004). CYP enzymes are divided into family, subfamily and gene number, and are an important enzyme group since they metabolise almost 75% of drug reactions (Figure 1.1; Nelson *et al.*, 1996; Guengerich, 2008). One important subfamily of CYP enzymes regulated by PXR activation in humans are the CYP3A4 enzymes, which have been said to metabolise about 50% of pharmaceutics (Guengerich, 2008). In zebrafish, Pxr is known to induce *cyp3a65* upon activation (Tseng *et al.*, 2005; Bresolin *et al.*, 2005).

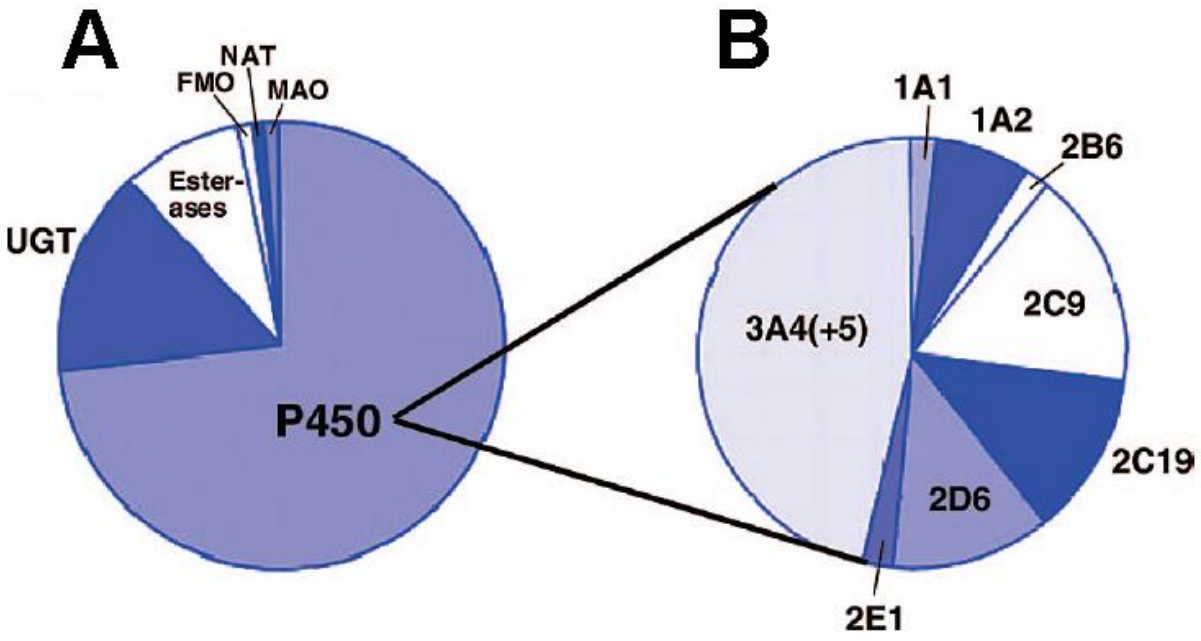

Figure 1.1. A pie chart depicting the percentage enzymes contribute to the metabolism of the top 200 prescribed drugs in the United States from 2002. A) The cytochrome P450 enzyme superfamily contributes to nearly 75% of drug metabolism; and B) The 3A subfamily contributes to almost 50%. Figure taken from Guengerich (2008).

1.3.2 Other roles of PXR

Apart from mediating CYP hydroxylation in phase I biotransformation, PXR has also been shown to induce the expression of other important genes involved in different stages of the detoxification process. For example, PXR can induce the transcription of conjugating enzymes UDP-glucuronsyltransferase (UGT) and sulphotransferase (SULT) in phase II biotransformation (Sonoda *et al.*, 2002; Rae *et al.*, 2001), and regulate the uptake and efflux of compounds through ATP-binding cassette (ABC) transporters in phase III biotransformation, including the multidrug resistant protein 1 (MDR1) and the multidrug resistance-associated protein 2 (MRP2) (Synold *et al.*, 2001; Kast *et al.*, 2002). PXR also plays an important role in lipid homeostasis (Dussault *et al.*, 2003; Sonoda *et al.*, 2005), and is known to interact with other steroid receptors, including CAR and FXR (Jung *et al.*, 2006; Xie *et al.*, 2000).

1.3.3 Ligand interaction

PXR has broad ligand specificity, meaning that it can become activated by a range of compounds. PXR is activated by endogenous compounds such as bile acids and steroid metabolites such as progesterone, oestrogen and corticosterone (Xie *et al.*, 2001; Kliewer *et al.*, 2002). PXR can also be activated by exogenous compounds, which include natural products such as St. John's wort, sulphoraphane, and vitamin E and K (Moore *et al.*, 2000; Zhou *et al.*, 2007; Landes *et al.*, 2003; Tabb *et al.*, 2003). These compounds are important when considering their combined effects with drug intake, since many of the PXR-related pathways associated with these products are also shared with pharmaceuticals.

This means that pharmaceutics also play an important role in the activation of PXR. Drugs such as rifampicin, RU486, taxol, SR12813 and ET-743 are all capable of regulating the activity of PXR (reviewed by Kliewer *et al.*, 2002). Most of these drugs are agonists, *i.e.* activators of PXR, whereas fewer compounds (*e.g.* ET-743) are antagonists, *i.e.* inhibitors of PXR. The degree of activation or inhibition largely depends on the compound's affinity towards PXR, meaning that different compounds will activate PXR more strongly than others and this has also been shown to vary between species (Lehmann *et al.*, 1998; Milnes *et al.*, 2008). For example, rifampicin has been shown to be a strong activator of PXR in human and rabbit, but not in rat or mouse (Jones *et al.*, 2000). This often makes it challenging to predict the degree to which a compound can activate PXR across species when deciding which model species to use (Milnes *et al.*, 2008).

1.3.4 Pollutants as ligands

The World Health Organization (2002) defines endocrine-disrupting compounds (EDCs) as: "an exogenous substance or mixture that alters function(s) of the endocrine system and consequently produces adverse health effects in an intact organism, or its progeny, or (sub)populations". EDCs have 3 modes of action: 1) compounds can act as hormone mimics, exhibiting either agonistic or antagonistic effects; 2) compounds can interfere with natural hormone pathways; and 3) compounds can interfere with the production and function of hormone receptors (Rotchell and Ostrander, 2003; Goksøyr, 2006). Because PXR is susceptible to a broad range of ligands, this means that EDCs are also be capable of activating this receptor. In mice, EDCs including phthalic acid and nonylphenol have been shown to activate PXR (Masuyama *et al.*, 2000). In humans, EDCs such as organophosphates, polychlorinated biphenyls (PCBs) (reviewed in Zhou *et al.*, 2009), brominated flame retardants (BFRs) (Pacyniak *et al.*, 2007), and bisphenol A (BPA) have all been shown to activate PXR (Sui *et al.*, 2012).

Studying the effects of pollutants as xenobiotics is an important aspect of toxicology. Many pollutants have been screened across PXR orthologs by studying their ability to activate the nuclear receptor (Milnes *et al.*, 2008; Kojima *et al.*, 2011). One common method for testing this is to clone the gene which encodes PXR and using recombinant expression to incorporate the transcript into a vector for transfection into a eukaryotic cell line. The luciferase assay is one way that toxicologists can test ligand activation in nuclear receptors (Grün *et al.*, 2002; Milnes *et al.*, 2008), and is a current focus in toxicological research.

1.3.5 Localisation of PXR

For humans, PXR is found in most cells but is localised mostly in the liver and small intestine, where the majority of steroid and xenobiotic metabolism takes place in the body (Blumberg *et al.*, 1998). However, the nuclear receptor has been shown to be expressed in the lungs and kidney (Miki *et al.*, 2005), bone (Tabb *et al.*, 2003) and even immune cells (Siest *et al.*, 2008; Dubrac *et al.*, 2010). The subcellular localisation of PXR is currently disputed (reviewed by Zhou *et al.*, 2009), and its exact location in the presence or absence of ligand varies according to species and even study (Saradhi *et al.*, 2005; Squires *et al.*, 2004; Koyano *et al.*, 2004).

1.3.6 Structure

Most nuclear receptors contain a modular structure that consists of domains labelled A to F, corresponding to the N and C terminals respectively (Figure 1.2). These include the DNA binding domain (DBD, C), the flexible hinge region (D) and the ligand binding domain (LBD, E) (Kumar and Thompson, 1999). Within the N-terminal is activation function 1 (AF-1), which is usually ligand independent, as opposed to activation function 2 (AF-2) found within the LBD, which is dependent on the presence or absence of ligand.

When PXR is activated by ligands, dimerisation of the nuclear receptor occurs at both the DBD and LBD. The DBD contains two zinc fingers which allow the transcription factor to bind to a target gene's xenobiotic or hormone response element (XRE / HRE). This response element is located in the promoter region of the target gene, and contain motifs recognised by the nuclear receptor which help regulate transcription (Goodwin *et al.*, 2002; Song *et al.*, 2004). The LBD binds to RXR, which helps promote transcription of the target gene.

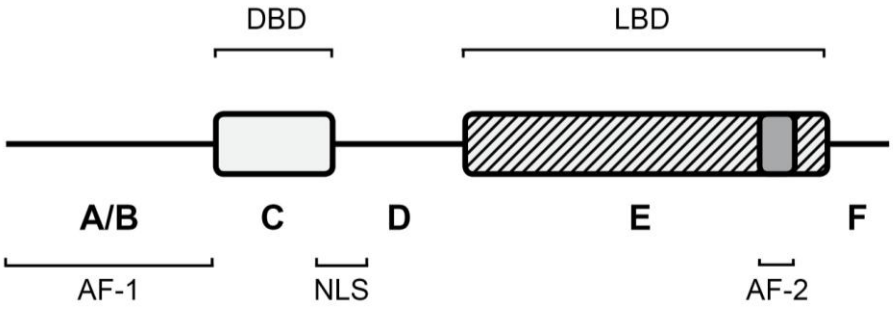

Figure 1.2. Modular structure of nuclear receptors, divided into its domains from the N to C terminals (A to F). The nuclear localisation signal (NLS) is located within the DBD (C) and hinge (D) domains. Figure modified from Escriva *et al.* (2000).

In humans, full length PXR protein is 434 amino acids long and has a molecular weight of approximately 50 kD. While the complete crystal structure of PXR has yet to be determined, the LBD of PXR is known to some extent (reviewed in Wu *et al.*, 2013). The LBD in PXR contains a flexible, hydrophobic and large ligand binding pocket (LBP), which has a low binding affinity with most ligands. The LBP has also been shown to interact with the same ligand in different conformations and in a different way to most other types of nuclear receptors (Watkins *et al.*, 2001; Xue *et al.*, 2007).

1.4 Variation in PXR orthologs

1.4.1 Species-specific variation

While the DBD in PXR is generally well conserved across species (Kliewer *et al.*, 2002), the LBD however has been shown to be poorly conserved (Moore *et al.*, 2002). Figure 1.3 shows how the amino acid sequence varies between species. Because of these differences, activation of PXR orthologs by the same ligand can lead to different levels of transcriptional response. For example, single amino acid differences in the LBD between human and mouse PXR have led to differences in its activation after ligand exposure (Östberg *et al.*, 2002).

Species	DBD	LBD	Reference
Human	100	100	
Rhesus monkey	100	95	Kliewer *et al.* (2002)
Polar bear	100	93	Lille-Langøy (unpub.)
Rabbit	94	82	Kliewer *et al.* (2002)
Mouse	94	82	Bainy *et al.* (2013)
Rat	66	80	Bainy *et al.* (2013)
Trout	66	56	Bainy *et al.* (2013)
Zebrafish	74	56	Bainy *et al.* (2013)
Fugu	61	52	Bainy *et al.* (2013)
Medaka	60	53	Milnes *et al.* (2008)
Frog	73	55	Bainy *et al.* (2013)
Chicken	64	49	Kliewer *et al.* (2002)

Figure 1.3. Amino acid sequence identity of PXR between humans and other species.

1.4.2 Genetic variation

1.4.2.1 Human PXR

The human *PXR* gene is 35 kilobases (kb) in length and is located on chromosome 3 (13q12-13.3). It consists of nine exons that when transcribed, give a coding sequence of 1305 base pairs (bp). Single polynucleotide polymorphisms (SNPs) are known to occur in the coding region of the human *PXR* sequence, whereby a single nucleotide is substituted with another. This leads to either a non-synonymous (amino acid change) or synonymous (amino acid remains the same) variants in the amino acid sequence. Fifteen of these SNPs in human *PXR*

are non-synonymous (Figure 1.4; Zhou *et al.*, 2009) and these are located throughout the sequence. One of these variants located on the DBD (R98C) has been shown to fail to both bind to the XRE and induce *CYP3A4* (Koyano *et al.*, 2004). SNPs located on the LBD have also been shown to affect human PXR (hPXR) activation and *CYP3A4* transcriptional response (reviewed in Zhou *et al.*, 2009).

Figure 1.4. A modular structure of the coding region of human *PXR* including the DBD and LBD. The location of the fifteen known non-synonymous SNPs and their associated amino acid substitutions are indicated by *. Figure adapted from Zhou *et al.* (2009).

1.4.2.2 Zebrafish Pxr

The zebrafish *pxr* gene is 96.5 kb long and is located on chromosome 9. It contains 7 exons which after transcription, give messenger RNA (mRNA) with a coding sequence 1293 bp long. Allelic variants have only been recently identified in zebrafish *pxr*, where 3 non-synonymous SNPs have been located in the hinge region and LBD (Figure 1.5; Bainy *et al.*, 2013). The effect of these variants on zebrafish Pxr (zfPXR) activation and *cyp3a65* expression is currently unknown, but Pxr from different strains of zebrafish has been contain to possess differing levels of ligand activation (Lille-Langøy, unpublished data).

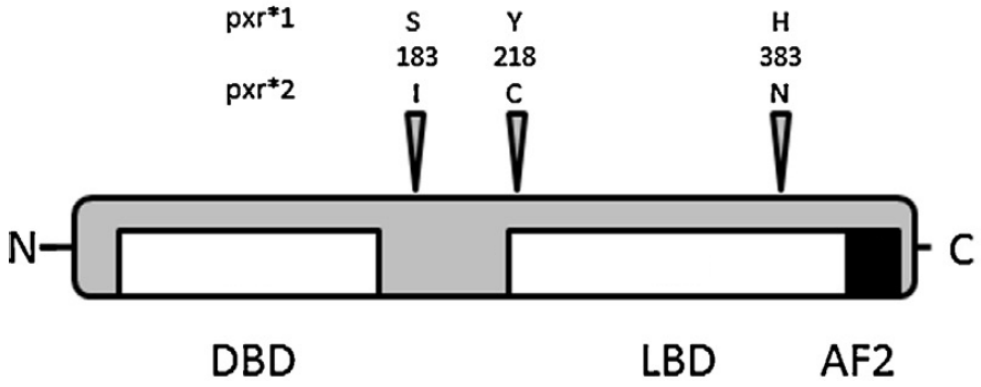

Figure 1.5. The modular structure of the coding region of zebrafish Pxr including the LBD, DBD and AF-2. The location of the three known non-synonymous SNPs and their associated amino substitutions are indicated by the grey arrow heads. Figure adapted from Bainy *et al.* (2013).

1.5 Zebrafish

Zebrafish (*Danio rerio*) are small freshwater fish which belong to the minnow family (Cyprinidae) (Figure 1.6). They are distributed throughout the Himalayas, but are kept in captivity as research animals across the world. Adults generally grow up to 4 cm in length under captivity, but individuals can grow as large as 6 cm. They thrive in tropical environments and can live up to 5 years, but usually live only between 2 and 3 years in captivity. Zebrafish are omnivorous and their diet consists of both phytoplankton and zooplankton (Spence *et al.*, 2008). Different strains have been classified for zebrafish, and these are maintained by the Zebrafish Model Organism Database (ZFIN) (Sprague *et al.*, 2006). Presently there are a total of 29 wild-type lines listed on the ZFIN database, including strains such as Tupfel long fin (TL), Tübingen (Tu), Singapore Wild-type (SWT) and AB/Tübingen (AB/Tu).

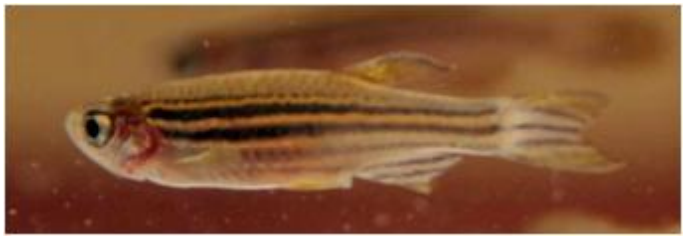

Figure 1.6. A zebrafish adult, approximately 2 years old. Photo by Daniel Hitchcock.

1.5.1 Zebrafish as a model organism

Zebrafish are notable for their fast generation time, where individuals can begin reproduction within 3 to 4 months. Embryos develop very quickly and fertilisation success can be seen by eye, whereby eggs become transparent. Females can lay up to a hundred eggs per mating and spawn a few times per week (Spence *et al.*, 2008). Their quick developmental period and ability to lay many eggs make zebrafish useful for research, since embryos can be acquired quickly and in large numbers.

In 2013 the zebrafish genome was sequenced, allowing researchers to determine similarities between humans and zebrafish (Howe *et al.*, 2013). Their early developmental period and response to human drugs has also been well-studied, making them a useful model species in toxicology and biomedicine (Kimmel, 1989; Alestrom *et al.*, 2006). Zebrafish have also been shown to respond to compounds in a similar manner as mammals and humans in toxicity testing, meaning that embryos and adults serve as ideal models (Guyon *et al.*, 2007; Driessen

et al., 2013). In fact, teratology assay models are commonly used in zebrafish embryos for drug discovery and screening (Rubinstein, 2003; Rubinstein, 2006).

The use of zebrafish as a model organism in toxicology makes them a valuable species for research and drug development (Barros *et al.*, 2008). For this reason, embryos serve as a good starting point for compound exposure, nuclear receptor activation and target gene induction.

1.5.2 Effects of clotrimazole on zebrafish

Clotrimazole (CAS number: 23593-75-1) is found in topical creams, is used to treat fungal infections and is listed on the World Health Organisation's list of essential medicines (Figure 1.7) (World Health Organization, 2013). However, this compound is also a pollutant since it is discharged into the aquatic environment and known to affect aquatic organisms (OSPAR Commission, 2013). In zebrafish, it has been reported that the compound's effective concentration for 20% of the exposed fish (EC_{20}) is 0.84 µM. At this concentration, affected fish exhibited "abnormal swimming behaviour", which is probably defined as any deviation from their normal upright position (Barros *et al.*, 2008). Clotrimazole is known to be a strong activator of Pxr and inducer of the transcription of *cyp3a65* (Bresolin *et al.*, 2005) and is known to act as an EDC to some extent, by altering levels of hormones involved in steroidogenesis (Baudiffier *et al.*, 2012).

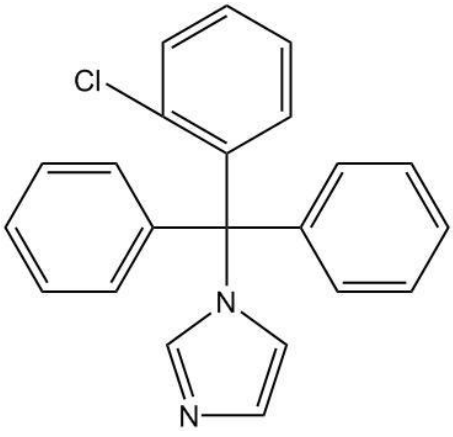

Figure 1.7. Chemical structure of clotrimazole.

1.6 Antibodies

Antibodies are Y-shaped proteins produced by the immune system that tag antigens for neutralisation (Figure 1.8). Immunoglobulin G (IgG) is the most commonly occurring isotype

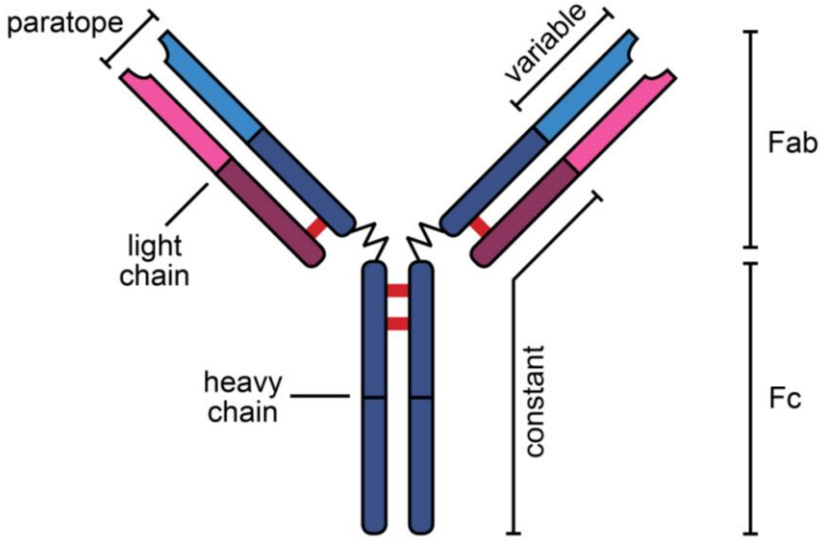

Figure 1.8. Structure of an antibody, including the symmetrical heavy (blue) and light (purple) chains linked to one another by cysteine disulphide bonds. The variable regions of the coupled light and heavy chain represent the paratope, the antigen binding site.

in serum (Murphy, 2012). IgG weighs approximately 150 kD and contains two identical heavy chains (approximately 50 kD) and two identical light chains (approximately 25 kD) (reviewed in Lipman *et al.*, 2005). For IgG, the two heavy chains are bound to one another by disulphide bonds and each of these is bound to a single light chain, with the number and specific location of disulphide bonds varying according to subclass (Liu and May, 2012). Each chain contains a constant and a variable region, and the combination of the light and heavy chain's variable region represents an antibody's paratope. The most important component of IgG that allows it to bind to antigens is the Fab (Fragment, antigen-binding) region, which constitutes the two arms of the Y, on which the variable regions containing the paratopes are called the complementarity determining regions (CDRs) (Murphy, 2012). The Fc (Fragment crystallisable) region represents the tail of the Y.

1.6.1 Antibody and antigen interaction

Antibodies are produced by the adaptive immune system after the body has been exposed to an antigen, either from within the body or a foreign source (Murphy, 2012). Antigens can be cells, microparticles or even proteins. Antibodies are mostly specific to a single antigen and bind to its epitope: a segment of the antigen to which the immune system has responded

(Abbas *et al.*, 2012). Interaction between an antibody and epitope depends on both the structure of an antibody's CDR and the epitope. For example, if the interaction between an antibody's CDR and epitope is strong and specific, then the antibody is monoreactive, *i.e.* it only binds to a single antigen. Polyreactive antibodies also exist, which are non-specific and capable of binding to different antigens (Notkins, 2004). The structure of the epitope is also important, since conformational epitopes are mostly only recognised by their tertiary structure, whereas linear epitopes are usually only recognised by their primary structure (Murphy, 2012).

1.6.2 Production of antibodies: immune response

Antibodies are an extremely useful tool in research, since they can be used to detect the presence of an antigen within a biological sample by binding to its epitope. For example, antibodies are a key tool in immunoreactive detection, *e.g.* in immunochemical detection of proteins, enzyme-linked immunosorbent assay (ELISA) and immunohistochemistry (see Methods 3.4.4).

Antibodies specific to antigens are often obtained from immunisation (Figure 1.9) (Murphy, 2012). This involves administering an antigen to an individual (primary exposure), usually by vaccine, causing the adaptive immune system to produce antibodies specific to that antigen (primary response). The primary response involves the differentiation of naïve B cells into antibody-producing effector B cells, which respond to the foreign antigen. Some naïve B cells also differentiate into long-lived, clonal memory B cells, which are capable of differentiating into effector B cells upon secondary exposure to the same antigen. For this reason, a secondary response to the same antigen will elicit a much stronger response than a primary exposure. The concept behind immunisation is used to acquire antibodies specific to desired antigens.

1.6.3 Monoclonal and polyclonal antibodies

Antibodies can be obtained from individuals in a number of ways. Depending on the method used, antibodies can vary in their specificity, being either monoclonal or polyclonal in nature. Polyclonal antibodies bind to multiple epitopes of a single antigen. They are obtained from the antiserum of blood of an immunised animal, and cross-reactive species can be removed using affinity purification (Robinson *et al.*, 1988). Polyclonal antibodies, including

commercial antibodies, are cheap and quick to obtain, but their cross-reactivity to multiple epitopes often makes them less sensitive (Lipman *et al.*, 2005).

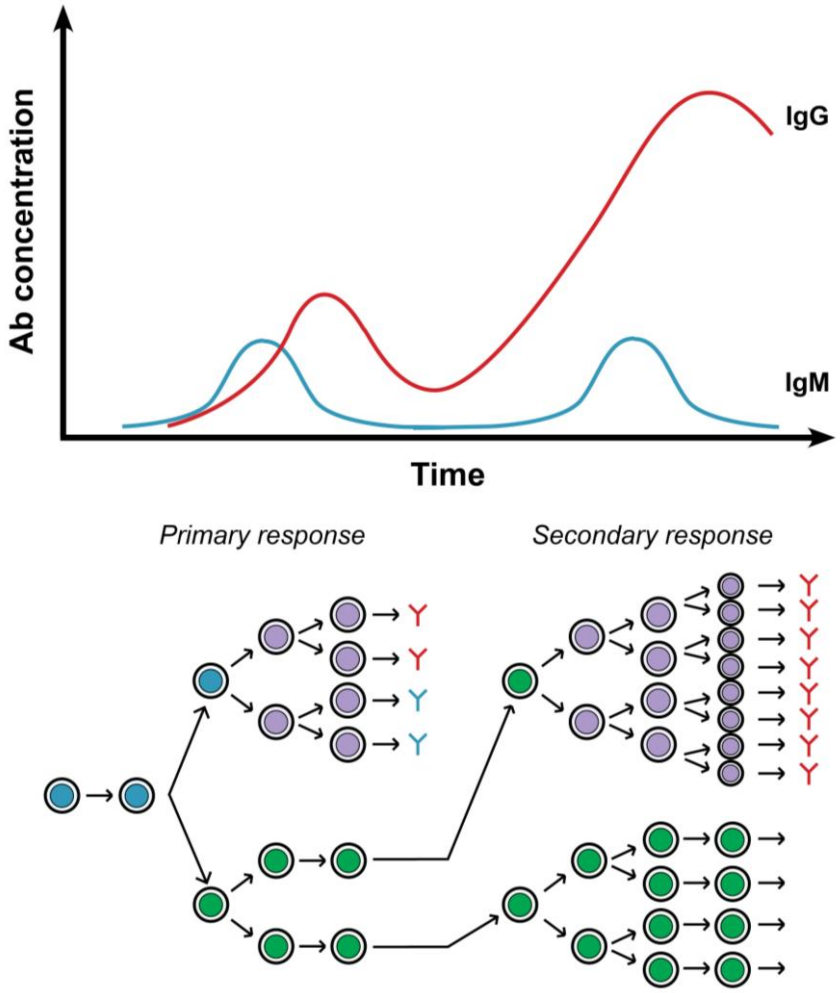

Figure 1.9. A representation of antigen exposure. During the primary exposure, naïve B cells (blue) differentiate both into effector B cells (purple) and memory B cells (green). Low-affinity IgM antibodies are produced by the effector B cells and are responsible for the majority of the primary response. Long-lived clonal memory B cells also remain in the body after the primary response. A secondary exposure to the same antigen elicits a faster and greater production of specific IgG antibodies due to the presence of memory B cells.

On the other hand, monoclonal antibodies bind only to a single epitope of a single antigen. They are highly specific, but can only be obtained by extracting B cells from an animal, making them more difficult and time-consuming to obtain. However, since monoclonal antibodies originate from a single clonal cell, antibodies obtained in this manner will always have the same affinity against the same epitope (Lipman *et al.*, 2005).

1.6.4 Hybridoma technology

Hybridoma technology, one method to obtain monoclonal antibodies, was first described by Köhler and Milstein (1975) (Figure 1.10). The process involves the immunisation of a mouse against a desired antigen, isolation of effector B cells from the spleen, and fusion of these cells with myeloma cells (immortal, cancerous effector B cells which have been modified to not secrete antibodies) (reviewed in Chiarella and Fazio, 2008). The fused cell is referred to as a hybridoma, and with limiting dilution, one can obtain single clonal cells which can be tailored to secrete antibodies indefinitely. Antibodies are collected in the supernatant and these are screened against the original antigen in order to determine correct specificity. In 2011, in a previous Master's project, hybridoma cell lines produced from spleen cells of mice immunised by either hPXR or zfPXR were developed (Davies, 2011).

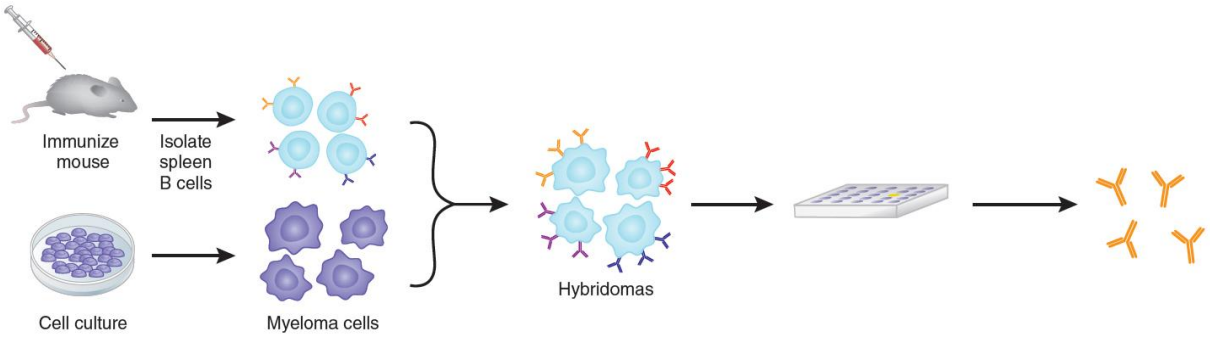

Figure 1.10. Production of hybridoma cells secreting monoclonal antibodies after immunisation of mice with a desired antigen. Adapated from Joyce and ter Meulen (2010).

1.6.5 Antibodies and PXR

Antibodies have been used to expand our understanding of PXR activity in cells. For example, monoclonal mouse antibodies have been used to determine the subcellular location of human PXR in breast cancer carcinomas (Miki *et al.*, 2006). In mice, polyclonal goat antibodies have been used to determine that PXR predominantly exists in the cytoplasm before ligand treatment and in the nuclei after exposure to pregnenolone carbonitrile (PCN) (Kawana *et al.*, 2003). The development of polyclonal rabbit antibodies has been used to demonstrate that PXR can be obtained and purified from a prokaryotic cell line by cloning the gene of the antigen into an expression vector (Saradhi *et al.*, 2005).

Another powerful tool which utilises antibodies is Chromatin immunoprecipitation (ChIP). ChIP is a tool that has been developed to determine which DNA binding sites are associated

with transcription factors (Orlando, 2000). This involves the binding of a desired transcription factor with chromatin, shearing of genomic DNA into fragments (300–500 bp), and purification of the DNA fragments for sequencing. So far, ChIP has only been carried out on mouse PXR (Cui *et al.*, 2010) and obtaining antibodies specific to PXR of other species could be used to further our understanding of PXR function.

1.7 Aims

Genetic variants of human *PXR* have been identified and now studies are focusing on how this variation might affect transcriptional variation of its target genes. However, the zebrafish *pxr* gene has received little attention, despite the species' and gene's importance and relevance in toxicology and biomedicine. In addition, the use of zebrafish embryos could prove to be a cheaper, easier and faster way of collecting data in this field of research. One of the main goals in this study is to develop a method for sequencing *pxr* from individual zebrafish embryos, and to compare these sequences with recently identified allelic variants.

Antibodies are of great importance in molecular biology and the establishment of hybridoma cell lines producing monoclonal antibodies specific to human and zebrafish PXRs can lead to many new and exciting possibilities. However, there is currently no commercial antibody available with specificity against zebrafish Pxr. Therefore, another main goal in this study is to evaluate the specificity of monoclonal antibodies, previously developed in this laboratory, against PXR orthologs.

2. Materials

2.1 General chemicals

Chemical name	Formula	Supplier / catalogue / product number
30% Acrylamide : Bis-acrylamide solution, 37.5:1		Sigma Aldrich / A3699
Ammonium persulphate (APS)	$(NH_4)_2S_2O_8$	Sigma Aldrich / A9164
Betaine solution		Sigma Aldrich / B0300
Chloroform	CH_3Cl	Sigma Aldrich / 34854
Clotrimazole	$C_{22}H_{17}CIN_2$	Sigma Aldrich / C6019
Coomassie brilliant blue G-250 (CBB G-250)	$C_{47}H_{48}NaO_7S_2$	Merck / 1.15444
Coomassie brilliant blue R-250 (CBB R-250)	$C_{45}H_{44}N_3O_7S_2Na$	Sigma Aldrich / B0149
Diethylpyrocarbonate (DEPC)	$C_6H_{10}O_5$	Sigma Aldrich / D5758
Dimethyl suphoxide (DMSO)	C_2H_6OS	Sigma Aldrich / D2650
Disodium hydrogen phosphate monohydrate	$Na_2HPO_4•H_2O$	Merck / 1.06346
Dithiothreitol (DDT)	$C_4H_{10}O_2S_2$	Sigma Aldrich / 43817
Ethanol (EtOH)	C_2H_5OH	Sigma Aldrich / 32221
Ethidium bromide (EtBr)	$C_{21}H_{20}BrN_3$	Sigma Aldrich / E1510
Ethylenediaminetetraacetic acid (EDTA)	$C_{10}H_{16}N_2O_8$	Merck / 324503
Formamide	CH_3NO	Sigma Aldrich / F9037
Glacial acetic acid	CH_3COOH	Merck / 1.00063
Glycerol 85%	$C_3H_8O_3$	Merck / 1.04094
Glycine	$C_2H_5NO_2$	Sigma Aldrich / G8898
HEPES	$C_8H_{18}N_2O_4S$	Sigma Aldrich / H3375
Hydrochloric acid	HCl	Sigma Aldrich / 339253
Isopropyl β-D-1-thiogalactopyranoside (IPTG)	$C_9H_{18}O_5S$	Sigma Aldrich / I6758
Isoamylalcohol	$C_5H_{12}O$	Merck / 1.00979
Isopropanol	C_3H_8O	Kemetyl / 200-661-7
L-glutamine	$C_5H_{10}N_2O_3$	Sigma Aldrich / G7513
Magnesium chloride hexahydrate	$MgCl_2•6H_2O$	Sigma Aldrich / M9272
Methanol	CH_3OH	Sigma Aldrich / 32212N
N,N,N',N'-tetramethyl-ethylenediamine (TEMED)	$C_6H_{16}N_2$	Sigma Aldrich / T9281
Ortho phosphoric acid 85%	H_3PO_4	Merck / 1.00573
Potassium chloride	KCl	Sigma Aldrich / P9541
Potassium phosphate dibasic trihydrate	$K_2HPO_4•3H_2O$	Sigma Aldrich / P5504
Rifampicin	$C_{43}H_{58}N_4O_{12}$	Sigma Aldrich / R3501
Sodium chloride	NaCl	Merck / 1.06404
Sodium dihydrogen phosphohate dihydrate	$NaH_2PO_4•2H_2O$	Merck / 1.06346
Sodium dodecyl sulphate (SDS) (20% w/v)	$NaC_{12}H_{25}SO_4$	Bio-Rad / 161-0418
Sodium pyruvate	$C_3H_3NaO_3$	HyClone / SH30231.01
Tris base (Trizma® base)	$C_4H_{11}NO_3$	Sigma Aldrich / T1503
β-mercaptoethanol	C_2H_6OS	Sigma Aldrich / M7154

2.2 General solutions, compounds, media and supplements

Chemical name	Formula	Supplier / catalogue / product number
0.25% trypsin-EDTA		Sigma Aldrich / T4049
0.5 M Tris-HCl buffer pH 6.8	$(HOCH_2)CNH_2$•HCl	Bio-Rad / 161-0799
1.5 M Tris-HCl buffer pH 8.8	$(HOCH_2)CNH_2$•HCl	Bio-Rad / 161-0798
Albumin from bovine serum		Sigma Aldrich / A4503
Ampicillin sodium salt	$C_{16}H_{18}N_3NaO_4S$	Sigma Aldrich / A9518
Dulbecco's Modified Eagle Medium (DMEM)		Sigma Aldrich / D5671
Fetal Bovine Serum (FBS)		Sigma Aldrich / F9665
Kanamycin	$C_{18}H_{36}N_4O_{11}$	Sigma Aldrich / K1876
Non-fat dried milk		Normilk AS
Opti-MEM® I (1×)		Gibco / 11058-021
Pencillin Streptomycin (Penstrep)		Gibco / 15140
SeaKem® LE Agarose		Lonza / 50004
Trypan bluestain	$C_{34}H_{28}N_6O_{14}S_4$	Cambrex / 17-492E
Tryptone (peptone from casein)		Merck / 1.11931
Yeast extract		Sigma Aldrich / 70161
QIAzol® Lysis Reagent		Qiagen
Lysozyme		Sigma
EDTA-free protease inhibitor × 100		Roche
cOmplete ULTRA Tablets, Mini, EDTA-free, *EASYpack*		Roche / 05 892791 001
5 × Boiling buffer		
TRI Reagent®		Sigma Aldrich / T9424
RNase-free water		Qiagen

2.3 Kits

Name	Description	Supplier / catalogue / lot number
Amersham™ ECL™ Prime Western Blotting Detection Reagent	Western blot chemiluminescence kit	GE Healthcare / RPN2232 / 9466590
TransIT®-COS Transfection Kit	Plasmid transfection kit into COS-7 cells	Mirus / MIR2190 / KLN6065
NucleoBond® Xtra Midi plasmid DNA repurification kit	Plasmid repurification of transformed *E. coli* cells	Marcherey-Nagel / 740410.50 / 1201/ 001
SuperSignal® West Pico Chemilumiscent Substrate	Western blot chemiluminescence kit	Thermo Scientific / 34080
Phase Lock Gel Heavy 1.5 mL	Gel separating RNA and DNA fractions during extraction	5 Prime / 2302810
RNA® MinElute™ Cleanup Kit	RNA clean up kit after phase separation	Qiagen / 74204
Protein G HP SpinTrap™	Purification of hybridoma supernatant	GE Healthcare / 28-9031-34
qScript™ cDNA Synthesis Kit	cDNA synthesis kit from RNA	Quanta Biosciences / 95047
GenElute™ PCR Clean-Up Kit	Cleanup of PCR product after amplification	Sigma-Aldrich / NA1020

2.4 Prokaryotic cell lines

Name	Description	Supplier
StrataClone™ SoloPack competent cells	Cells used for the heatshock transformation of plasmids containing PXR orthologs	Stratagene
E. coli Rosetta pET30b spotty FL zfPXR	Cells containing a pET30b plasmid encoding a 6×his-tagged full-length zfPXR	Roger Lille-Langøy
E. coli Rosetta	Non-transformed cells	Roger Lille-Langøy

2.5 Eukaryotic cell lines

Name	Description	Reference
COS-7	African green monkey cell line: CV-1 (simian) in Origin containing SV40 genetic material, line 7. Used to express PXR	Jensen *et al.* (1964); Gluzman (1981)

2.6 Plasmids

Name	Description	Supplier
pSG5 FL hPXR	Plasmid containing full length hPXR	Roger Lille-Langøy
pcDNA FL zfPXR	Plasmid containing full length zfPXR	Roger Lille-Langøy
pET30b His-tagged FL zfPXR	Plasmid containing fused His-tag and full length zfPXR	Roger Lille-Langøy

2.7 Hybridoma supernatants

Designation	Produced in	Isotype	Specificity	Supplier
5E4F9D9	Mouse	IgG	hPXR	Richard Davies, 2011
9F10D4B2	Mouse	IgG	hPXR	Richard Davies, 2011
12D5F6E6	Mouse	IgG	hPXR	Richard Davies, 2011
5E4B11D6	Mouse	IgG	hPXR	Richard Davies, 2011
8E2B8D7	Mouse	IgG	hPXR	Richard Davies, 2011
9E11D2C4	Mouse	IgG	zfPXR	Richard Davies, 2011
8F11C8C9	Mouse	IgG	zfPXR	Richard Davies, 2011
9E11C8D10	Mouse	IgG	zfPXR	Richard Davies, 2011

2.8 Molecular weight and size standards

Name	Description	Supplier / catalogue number
2-Log DNA Ladder	Concentration 50 ng / µL; range 0.1–10 kb. Dissolved in 5 mM TrisHCl and 1 mM EDTA. Used for agarose gel electrophoresis	New England Biolabs / N3200L
Precision Plus Protein™ Standards All Blue	Ten blue-stained proteins; range 10–250 kD. Used for SDS-PAGE.	Bio-Rad / 161-0373

2.9 Enzymes for amplification and sequencing

Name	Description	Supplier / product number
PrimeSTAR® GXL DNA Polymerase	Used for the PCR amplification of β-actin and zfPXR primers.	TaKaRa / R050A
BigDye® Terminator v3.1	Used for the PCR amplification of zfPXR primers for sequencing.	Applied Biosystems / 4337455

2.10 Primers

Name	Description	Sequence (5'–3')	Supplier
zf_actinF/811	Primer to determine successful synthesis of RNA to cDNA	GAGAAGATCTGGCATCACACC	Sigma
zf_actinR/812	Primer to determine successful synthesis of RNA to cDNA	GGTCTCGTGGATACCGCAAGA	Sigma
zfPXR(1)Ncol-F	Primer for the amplification of zfPXR from AA1	GTCACCATGGCAATGTCCCGCT TATATGAC	Sigma Aldrich
zfPXR-BamHI-R	Primer for the amplification of zfPXR from AA430	TTGTGGATCCGAGGACCTAGGT GTCTTTGC	Sigma Aldrich
zfPXR_seq_478_ Fwd	Primer for the sequencing of zfPXR	TTCGACATGACTTGTGCCCA	Sigma Aldrich
zfPXR_seq_1070 _Rev	Primer for the sequencing of zfPXR	TTGTGGTCTGTCACACCAGG	Sigma Aldrich

2.11 Commercial antibodies

Antibody	Produced in	Isotype	Reactivity	Supplier	Product number
Anti-human PXR	Mouse	IgG_{2A}	Monoclonal	Perseus Proteomics	PP-H4417-00
Anti-mouse IgG, HRP Conjugate	Goat	IgG	Polyclonal	Dako	P0447
Anti-mouse IgG (H+L), HRP Conjugate	Goat	IgG	Monoclonal	Molecular Probes Invitrogen™ / Life Technologies	G-21040
Anti-His, clone 2B5	Mouse	IgG_1	Monoclonal	OriGene	TA150088

2.12 Consumables

Name	Supplier	Product number
Immobilon®-P Transfer Membrane (pore size 0.45 µm)	Millipore™	IPVH00010

2.13 Instrumentation

Category	Name	Manufacturer
Blotting	Trans-Blot® SD Semi-dry Transfer cell	Bio-Rad
Cell density	Ultraspec 10	Amersham Biosciences
Centrifugation	CT15RE Himac	VRW
	Galaxy ministar	VRW
	Heraeus Multifuge X3R	Thermo Scientific
	Avanti J-26 XP	Bekman Coulter
Electrophoresis	PowerPac HC	Bio-Rad
Heating	Thermomixer compact	Eppendorf
	GD100	Grant
Homogenisation	XENOX motorised hand tool	XENOX
	Stainless steel pestle, cone diameter 8 mm	Carl-Roth
Imaging	Gel Doc™ EZ Imager	Bio-Rad
	ChemiDoc™ XRS+	Bio-Rad
Incubation	Galaxy 170 R	New Brunswick
	Infors HT Multitron Standard	VRW
		Termaks
	INCU-Line	VRW
Microscopy	DMIL LDE CMS GmbH	LEICA Microsystems
	SMZ-645	Nikon
Mixing		VWR International
	Rotator SB3	Stuart®
	HS 501 digital	IKA®-WERKE
pH measurement	pHM210 Standard pH Meter	MeterLab®
Plate reading	EnSpire® Multimode Plate Reader	PerkinElmer
Sequencing	3730XL DNA Sequencer	Applied Biosystems
Spectrophotometry	ND-1000	NanoDrop®
Sonication	4710 Series Ultrasonic Homogenizer	Cole-Pharmer Instrument Co.
Thermocycling	DOPPIO	VWR
Water supply	Advantage A10	Millipore
Weighing	S1-64	Denver Instrument
	EK-300i	AND

2.14 Water quality

MΩcm@25°C: 18.2
Ppb TOC: 5

Deionised type 1 ultrapure water, Milli-Q

2.15 Solutions, buffers and media

Heatshock transformation

Super optimal broth (SOB) medium
2% Tryptone (w/v)
0.5% Yeast extract (w/v)
10 mM NaCl
2.5 mM KCl

Super optimal broth with catabolite repression (SOC) medium
1 × SOB
5 mM $MgCl_2$
5 mM $MgSO_4$
20 mM Glucose

Bacterial growth

1× Lysogeny broth (LB) medium
1% Tryptone (w/v)
1% NaCl (w/v)
0.5% Yeast extract (w/v)

COS-7 maintenance

Dulbecco's modified Eagle medium (DMEM)++ medium
1 mM Sodium pyruvate
4 mM L-glutamate
100 U / mL Penstrep
10% mL Fetal Bovine Serum (FBS) (v/v)
-> add to 500 mL DMEM

Agarose gel electrophoresis (AGE)

5 × TBE
0.5 M Tris
0.5 M Boric acid
10 mM EDTA pH 8.0

1 × TAE
40 mM Tris
40 mM Acetic acid
1 mM EDTA pH 8.0

0.7% Agarose gel in TBE
0.7% Agarose (w/v)
0.5 × TBE

1% Agarose gel in TAE
1% Agarose (w/v)
1 × TAE

× 10 loading buffer
1% SDS
50% Glycerol
0.05% Bromophenol blue

Cytoplasmic and nuclear extraction

Buffer A
200 mM HEPES pH 7.9
100 mM KCl
10 mM $MgCl_2$•$6H_2O$
10 mM DTT
-> Add 1 × protease inhibitor before use

Buffer C
200 mM HEPES pH 7.9
10 mM $MgCl_2$•$6H_2O$
20% Glycerol
420 mM NaCl
10 mM EDTA
-> Add 1 × protease inhibitor before use

Bradford assay

Bradford Reagent
1 : 1 of A : B
A: 17% Phosphoric acid (v/v)
B: 0.08% Coomassie Brilliant Blue (CBB) G-250 (w/v)
10% EtOH (v/v)

Sodium dodecyl sulphate polyacrylamide gel electrophoresis(SDS-PAGE)

12.5% resolving gel (all amounts v/v)
29.8% deionised H_2O
25% 1.5 M Tris-HCl pH 8.8
1% 10% SDS
42% mL Acrylamide : Bis solution 37.5 : 1
2% 10% APS
0.2% µL TEMED

4% stacking gel (all amounts v/v)
59.1% deionised H_2O
25% mL 0.5 M Tris-HCl pH 6.8
1% µL 10% SDS
12.5% µL Acrylamide : bis solution 37.5 : 1
2% µL 10% APS
0.4% µL TEMED

10% resolving gel (all amounts v/v)
39% deionised H_2O
25% 1.5 M Tris-HCl pH 8.8
1% 10% SDS
33% mL Acrylamide : Bis solution 37.5 : 1
2% 10% APS
0.2% µL TEMED

10 × TGS pH 8.3
250 mM Tris
1920 mM Glycine
1% SDS

Coomassie staining

Coomassie staining agent
2 g / L CBB R-250 (w/v)
40% EtOH (v/v)
10% Acetic acid (v/v)

Coomassie destaining agent
40% EtOH
10% Acetic acid

Western blot buffers

10 × Pre-Semi-Dry Transfer Buffer
180 mM Tris
390 mM Glycine

10 × Pre-Wet Transfer Buffer
250 mM Tris base
1920 mM glycine

1 × Semi-Dry Transfer Buffer
1 × Pre-Semi-Dry Transfer Buffer
20% MeOH

1 × Wet Transfer Buffer
1 × Pre-Wet Transfer Buffer
20% MeOH

Phosphate buffered saline (PBS) buffers

10 × PBS
1370 mM NaCl
27 mM KCl
104 mM $Na_2HPO_4 \bullet 2H_2O$
11 mM $K_2HPO_4 \bullet 3H_2O$

1 × PBS 5% milk
1 × PBS
5 % Dry milk (w/v)

1 × PBS-Tween (PBS-T)
1 × PBS
0.05% Tween-20

Tris buffered saline (TBS) buffers

10 × TBS pH 7.6
200 mM Tris base
1370 mM NaCl

1 × TBS 5% milk
1 × TBS pH 7.6
5 % Dry milk (w/v)

1 × TBS-T
1 × TBS pH 7.6
0.05% Tween-20

Antibody purification

BINding buffer pH 7.0
20 mM Sodium phosphate
From: 8.9 mL 20 mM $NaH_2PO_4 \bullet H_2O$ in 50 mL deionised H_2O
11.1 mL 20 mM $Na_2HPO_4 \bullet 2H_2O$ in 50 mL deionised H_2O

NEUtralising buffer pH 9.0
1 M Tris

ELUtion buffer pH 2.7
0.1 M Glycine

Prokaryotic protein extraction

1 × PBS salt buffer
300 mM NaCl

Zebrafish media

60 × E3 medium
300 mM NaCl
100 mM KCl
20 mM $CaCl_2$
20 mM $MgSO_4$
0.1% methylene blue

E3 control medium (adults)
1 × E3
0.25% DMSO

E3 control medium (embryos)
1 × E3
1% DMSO

E3 treatment medium (adults)	**E3 treatment medium (embryos)**
1 × E3	1 × E3
1 μM clotrimazole	1 μM clotrimazole
0.25% DMSO	1% DMSO

Ribonuclease (RNase)-free solutions

Diethylpyrocarbonate (DEPC)-treated water

0.1% DEPC

3. Methods

3.1 Experimental overview

A strategy for screening hybridoma supernatants against PXR orthologs and identification of allelic variants in zebrafish was carried out according to Figures 3.1 and 3.2.

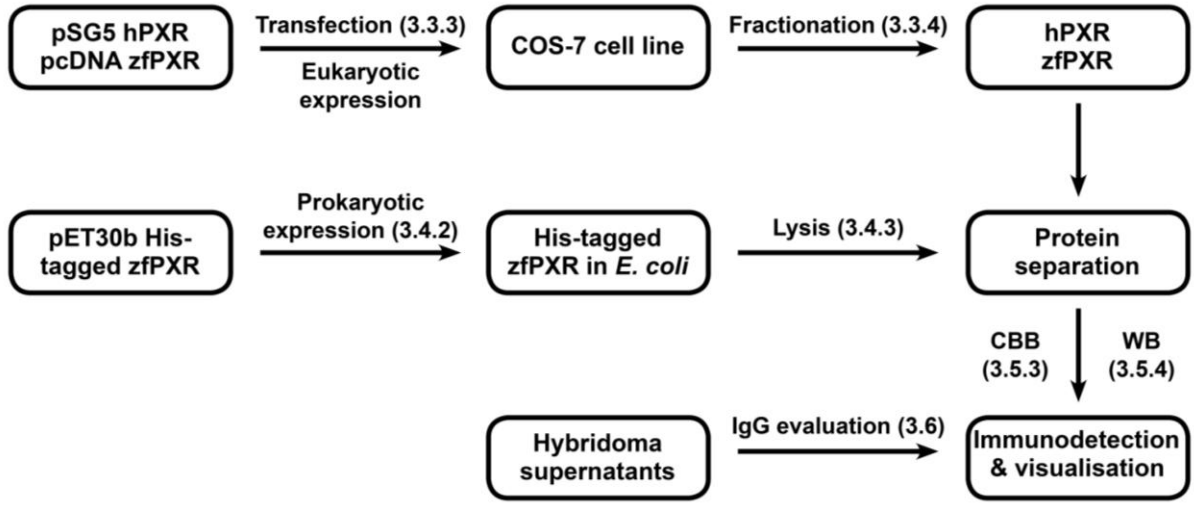

Figure 3.1. Strategy for the evaluation of hybridoma supernatant immunoreactivity. Details for each step are given in Sections 3.2 to 3.6.

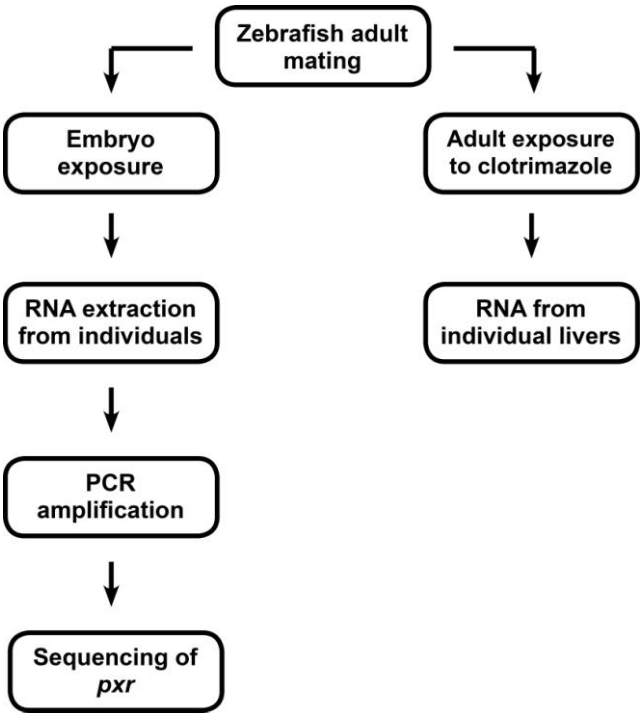

Figure 3.2. Strategy for identification of zebrafish *pxr* variants. Details for each step are given in Sections 3.7 to 3.9.

3.2 Plasmid purification

In order to produce PXR orthologs of high quality, *PXR* was previously cloned from both human and zebrafish and ligated into plasmids. This work was carried out by Roger Lille-Langøy at the University of Bergen. Repurification of these plasmids was necessary in order to carry out transfection into a eukaryotic cell line.

3.2.1 Heatshock transformation

Heatshock transformation is a technique that is used to genetically alter bacterium by introducing exogenous genetic material. Momentarily increasing the temperature of the cells induces the incorporation of exogenous DNA, *e.g.* plasmid DNA (pDNA). The mechanism behind this process is not fully understood, but it is known that topology of the plasmids is important when maximising transfer efficiency (Kreiss *et al.*, 1999).

StrataClone SoloPack competent cells were used to produce the pSG5 hPXR and pcDNA zfPXR plasmids. These plasmids contain recombinant genes including full length human *PXR* and zebrafish *pxr* respectively (Figure 3.3). Purified plasmids and cells were brought together by adding 20 ng of each plasmid to 25 µL of thawing competent bacterial cells (stored at –80 ºC) and incubating on ice for 20 minutes. Uptake of pDNA was facilitated by heatshocking the cells at 42 ºC in a water bath for 45 seconds then immediately cooling on ice for 2 minutes. 125 µL of SOC media (preheated to 42 ºC) was added to the heatshocked cells were added to and incubated at 250 rpm for 1 hour at 37 ºC to allow for the expression of the antibiotic resistance gene (AmpR/β-lactamase). Successfully transformed cells were selected for by cultivation on LB-agar with 100 µg/mL ampicillin. Two different volumes of the transformation reactions (100 µL and 10 µL) were inoculated to LB-agar plates and incubated for at 37 ºC overnight.

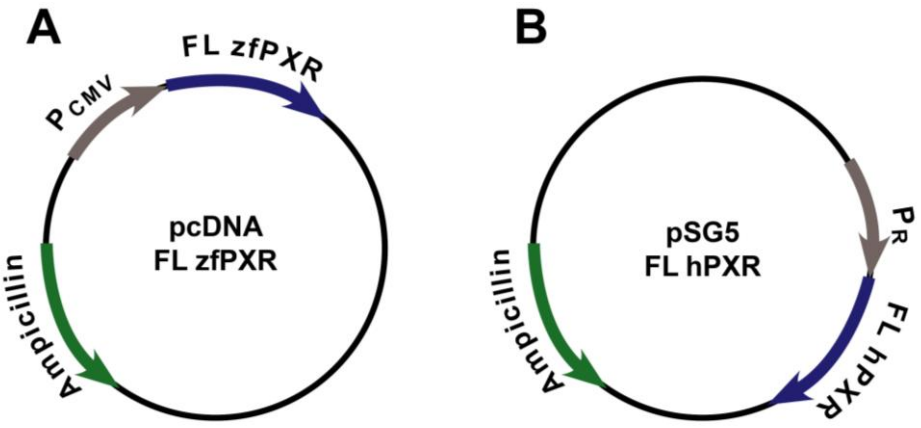

Figure 3.3. Maps of plasmids used in the eukaryotic expression of antigen. Plasmid pcDNA FL zfPXR (A) and pSG5 FL hPXR (B) were used in the transient transfection of COS-7 cells. P_{CMV} and P_R correspond to the promoter regions of each plasmid and ampicillin corresponds to the antibiotic resistance gene.

3.2.2 High quality plasmid preparation by medium scale purification of plasmid DNA

Plasmids can be purified through a column containing silica resin which binds to the phosphate backbone of DNA under acidic conditions (Bimboim and Doly, 1979). The application of a high salt elution buffer can shift the pH to alkaline conditions, allowing for the disassociation and collection of purified pDNA after centrifugation and wash steps.

Single bacterial colonies containing either the pSG5 hPXR or pcDNA zfPXR plasmid were then cultured for plasmid purification. An inoculation loop was used to scrape a single colony from the LB-agar plate to inoculate a 100 mL LB culture containing 100 µg/L of ampicillin. The culture was then incubated at 37 ºC at 250 rpm overnight. Because both plasmids contained genes resistant to ampicillin, only bacterial cells containing the plasmid could successfully replicate.

The NucleoBond® Xtra Midi plasmid DNA purification kit (Marcherey-Nagel) was used to extract the plasmids from the transformed bacteria cells. In the final step, 0.5 mL of deionised water (Type 1 ultrapure water, Milli-Q) was used to redissolve the precipitated pDNA pellet. The tube containing DNA pellet was shaken at 4 ºC overnight to ensure complete recovery of the pDNA. Dissolved pDNA was collected by centrifugation at 10000 × g for 1 minute at 4 ºC, giving the final purified plasmid product.

3.2.3 Quantification and evaluation of plasmid DNA by spectrophotometry

Plasmids were diluted to 1:20 in deionised water and the absorbance of each sample (1–2 µL) was measured at 260 nm in a NanoDrop® ND 1000 spectrophotometer. The concentration of plasmids was determined assuming that an absorbance of 1.0 at 260 nm corresponds to 50 µg/mL of DNA. The ratio between the absorbance of DNA (at 260 nm) and contaminants including proteins (at 280 nm) was also verified (Sambrook and Russell, 2001). An $A_{260/280}$ ratio greater than 1.8 suggests a high purity of DNA; however the usefulness of this ratio as a quality measurement is often debated (see Discussion 5.2.3).

3.2.4 Visualisation of nucleic acids by agarose gel electrophoresis

Plasmid quality was assessed using agarose gel electrophoresis (AGE). This method separates charged molecules in a gel matrix according to their length when subjected to an electric field. Linear nucleic acids contain an even distribution of negatively charged phosphates along their backbone, meaning that their migration through a gel depends on molecular size alone. A staining agent such as ethidium bromide (EtBr) is also added to the gel since EtBr binds to nucleic acids and fluoresces when exposed to ultraviolet (UV) light.

Double stranded pDNA however is circular and do not travel through a gel matrix in a linear fashion. This means that the size of pDNA cannot be determined by migration distance. Circular plasmids are capable of winding into coils, and high quality plasmids are often attributed as being supercoiled in topology. AGE can be used to determine plasmid quality since supercoiled plasmids are more compressed and travel further through a gel matrix than uncoiled plasmids, despite having the same molecular weight (Aaij and Borst, 1972).

200 ng of each plasmid and 2-log DNA ladder were loaded onto gels containing 0.7% agarose in 0.5 × TBE buffer and 50 µg/mL of EtBr. The size of gel matrices were either 7 × 5 cm or 7 × 10 cm depending on the number of samples loaded. Gels were run at 110 V in 0.5 × TBE buffer for 35 minutes. Nucleic acids were visualised under UV light using a Gel Doc™ EZ Imager and ImageReady software (v3.0).

3.3 Eukaryotic protein expression for antigen production

In order to test the immunoreactivity of PXR against hybridoma supernatants, a eukaryotic cell line was cultured and transfected with recombinant pDNA to produce either an hPXR or

zfPXR antigen. The COS-7 cell line was chosen because it is a continuous cell line which is easy to maintain, grows at a very rapid rate and is commonly used for recombinant protein expression. In addition, COS-7 cells have already been established in our laboratory as a model for the transient expression of proteins.

3.3.1 Preparation and maintenance of COS-7 cell lines

COS-7 cells stored in liquid nitrogen were thawed with pre-warmed DMEM++ media (Materials 2.15). The cells were pelleted by centrifugation (500 × g for 5 minutes) and the supernatant was carefully removed by pipetting. The pellet was resuspended in 10 mL of DMEM++ media, and this mixture containing the COS-7 cells was added to a 10 cm culture plate and incubated at 37 ºC with 5% CO_2. The COS-7 cells formed as a monolayer on the bottom of the plate.

Confluence was checked daily under a microscope and media was replaced every second to third day. Whenever confluence exceeded 70%, the cultures were split by trypsinisation. This involved the disassociation of COS-7 cells from the plate and the reseeding of these into subcultures (*i.e.* splitting). During splitting, DMEM++ media was removed and 10 mL of sterile PBS was added to remove any dead or unattached cells and serum-containing media which might inhibit trypsinisation. PBS was removed and 2 mL of 0.05 % trypsin-EDTA was added to disassociate the COS-7 cells the culture plate. Culture plates were incubated for 30 seconds at room temperature before excess trypsin was removed. The culture was then incubated for 5 minutes at 37 ºC with 5% CO_2. COS-7 cells were then resuspended with 10 mL of pre-warmed DMEM++ media to obtain a single cell suspension. Cells were reseeded to new culture plates in a dilution of 1:5 and maintained as described above.

3.3.2 Determining cell density using a haemocytometer

Cells in each culture plate were trypsinated as described above and resuspended using 5 mL of DMEM++ media. The resuspended cells were pooled and 25 µL of this culture was stained with 25 µL of tryphan blue. Stained cells were counted using a haemocytometer, a device which can determine cell concentration given the volume of the counting chambers is known.

3.3.3 Transient transfection of COS-7 cells

Transfection is a technique that is used to genetically alter eukaryotic cells by introducing exogenous genetic material, *e.g.* pDNA. Transfection of plasmids is more successful when

circular DNA is predominantly supercoiled and highly pure. The mechanism behind this process is not fully understood, but it is known that supercoiled plasmids are more readily taken up by cells than uncoiled plasmids (Kreiss *et al.*, 1999). Transfected cells express a recombinant protein, which can then be used for further studies. In our case, we wanted to use the transfected protein as an antigen for antibody analyses.

Fifteen culture plates containing COS-7 cells were cultured until each plate became approximately 70-80% confluent, and reseeded to twelve new culture plates at a concentration of 24.6×10^5 cells/plate the day prior to transfection (Table 3.1). Reseeded plates were adjusted to a volume of 10 mL using DMEM++ media.

The following day, COS-7 cells were transfected with either the pSG5 hPXR or pcDNA zfPXR expression vector by the *Trans*IT®-COS Transfection Kit (Mirus) (Table 3.1). Plates were resupplied with 14.5 mL of DMEM++ media. 15.5 µg of plasmids was added to 1.5 mL Opti-MEM I Reduced Serum Medium, followed by 46.5 µL *Trans*IT-COS Reagent and 15.5 µL COS Boss Reagent (COS reagents were warmed to room temperature and vortexed prior to use). Each plasmid mixture was then incubated at room temperature for 30 minutes before being distributed drop-wise to one of each culture plate. Four plates containing COS-7 cells without plasmids were maintained as a negative control. Cells were incubated overnight as described above.

Table 3.1
Experimental setup for the transfection of COS-cells.

Transfection plasmid	Cells/plate before 1 day before transfection	Number of plates	Ligand added to each plate 1 day after transfection
Negative	24.6×10^5	4	None
hPXR	24.6×10^5	4	Rifampicin (5 µM)
zfPXR	24.6×10^5	4	Clotrimazole (5 µM)

3.3.4 Nuclear and cytoplasmic fractionation from COS-7 cells

Fractionation of subcellular components from eukaryotic cells is important when the localisation of protein is ambiguous, which is the case for PXR (reviewed in Zhou *et al.*,

2009). Fractionation of both the cytoplasm and nuclei from transfected COS-7 cells allows for the immunochemical detection of PXR in each fraction.

24 hours after transfection, all culture plates were replenished with 10 mL of DMEM++ media. 5 µM of rifampicin was added to COS-7 cells containing hPXR plasmids and 5 µM of clotrimazole was added to COS-7 cells containing zfPXR plasmids (Table 3.1). PXR agonists were added to induce the translocation of PXR to the nucleus (Kawana *et al.*, 2003).

24 hours after ligand treatment, culture plates were placed on ice and washed twice with 4 ºC PBS. Cells were then scraped into 1.5 mL centrifuge tubes using 1 mL 4 ºC PBS and centrifuged at 1000 × g for 2 minutes at 4 ºC. Hypotonic lysis was then carried out fractionate cellular components, where a high solute buffer is added to make cells swell and cell membranes burst due to an increase in osmotic pressure (Abmayr *et al.*, 2006), but at the same time keep nuclei intact. The mixture was incubated in 300 µL of Buffer A for 10 minutes at 4 ºC. The mixture was vortexed for 10 seconds then centrifuged at 1000 × g for 2 minutes at 4 ºC. The supernatant containing the cytoplasmic fraction of the COS-7 cells was kept and frozen at –80 ºC. The addition of a second high-salt buffer causes the nuclear membrane to burst and so 300 µL of Buffer C was then added to the remaining cell pellet and incubated for 20 minutes at 4 ºC. The mixture was then centrifuged at 14000 × g for 3 minutes at 4 ºC. The supernatant containing the nuclear fraction of the COS-7 cells was kept and frozen at –80 ºC.

3.4 Prokaryotic protein expression for antigen production

A prokaryotic cell line was also cultured to produce histidine-tagged zfPXR from the plasmid pET30b zfPXR (Figure 3.4). This vector encodes a 6×histidine tag (His-tag) fused to the full length Pxr protein and a gene encoding resistance to the antibiotic kanamycin. A small sample was obtained from a glycerol stock previously prepared by Roger Lille-Langøy.

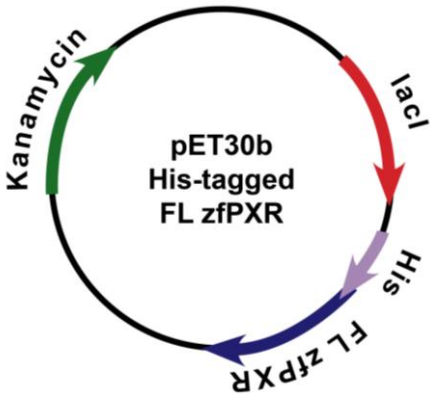

Figure 3.4. Map of plasmid used in the prokaryotic expression of antigen. Plasmid pET30b His-tagged FL zfPXR had previously been transformed into *E. coli* Rosetta cells. LacI corresponds to the promoter region and kanamycin the antibiotic resistance gene.

3.4.1 Expression culture of an *E. coli* cell line

Prokaryotic protein expression is useful such that it can be induced to express recombinant protein in high quantities. One disadvantage is that the final protein product is often incorrectly folded post-translation, making it dysfunctional compared to its native state.

E. coli Rosetta cells containing the pET30b His-tagged full length zfPXR were inoculated in a 5 mL starter culture of LB medium with 25 µg/mL of kanamycin and incubated at 37 ºC at 250 rpm overnight.

3.4.2 Protein induction

The following day, 2-3 mL of the starter culture was transferred into 100 mL of LB medium with 25 µg/mL of kanamycin. The expression culture was incubated at 37 ºC at 250 rpm for 2 hours before the cell density was determined spectrophotometrically (by its OD_{600}). The OD_{600} corresponds to the optical density of the culture at 600 nm. Production of histidine-tagged zfPXR was induced while the culture was in log phase growth ($OD_{600} \approx 0.6$-0.8) by the addition of IPTG to make a final concentration of 0.5 mM. Just prior to induction, a 1 mL of pre-induced sample was collected, spun down at 2500 × g for 5 minutes and its pellet was frozen at –20 °C for protein analysis. The remainder of the culture was incubated at 15 ºC at 250 rpm overnight.

3.4.3 Cell lysis and protein extraction by sonication

Unlike eukaryotes, prokaryotic cells require a more vigorous means of protein extraction. The presence of a cell wall means that shearing forces are often required to lyse cells. Sonication

is one means of achieving this, whereby ultrasonic frequencies are applied to cells in order to disrupt the cell membrane to achieve lysis.

The following day, the OD_{600} was measured and 1 mL of sample was collected and its pellet obtained as described above. The culture was then harvested by centrifugation for at 2500 ×g for 5 minutes. The sample was resuspended with 15 mL PBS with 300 mM NaCl containing 1 mg/mL lysozyme and 1 protease inhibitor tablet, before incubation at room temperature for 5 minutes. The suspension was then lysed by sonication on ice with a 10 s ON 10 s OFF cycle for 5 minutes immediately followed by a 20 seconds ON 10 seconds OFF cycle for another 5 minutes. The lysate was centrifuged at 37,000 × g for 30 minutes at 4 °C to separate soluble and insoluble protein fractions. The supernatant was collected and the pellet was resuspended in 5 mL PBS with 300 mM NaCl containing 1× protease inhibitor. 1 mL of both the soluble and insoluble fraction were stored at –20 °C and saved for protein analyses.

3.5 Protein analysis

Protein analyses were carried out to confirm the induction and concentration of the PXR protein, and to immunochemically detect their immunoreactivity towards commercial antibodies and to hybridoma supernatants potentially containing monoclonal PXR antibodies.

3.5.1 Quantification of total protein concentration by the Bradford protein assay

The Bradford protein assay is a colorimetric test that utilises the staining agent coomassie brilliant blue (CBB) G-250 (Bradford, 1976). This compound binds to amines and causes a colour shift from red to blue when proteins are present. Measuring the absorbance at 595 nm allows for the correlation between the absorbance of the sample and protein concentration. Setting up a standard curve based on protein samples of known concentration allows one to determine the concentration of samples given its absorbance lies within the standard curve.

The protein concentration from the cytoplasmic and nuclear fractions of transfected and non-transfected COS-7 cells was determined using the Bradford protein assay. Samples from each fraction were also pooled maximise protein concentration. A standard concentration curve was constructed using bovine serum albumin (BSA) as a colour standard. 2000 µg/mL of BSA was prepared in both Buffer A and Buffer C, and diluted along a concentration gradient ranging from 0 µg/mL (blank) to 1500 µg/mL. At the same time, a 1:10 dilution of each

cytoplasmic and nuclear fraction was prepared. Bradford reagent was prepared by mixing 1 part 17% phosphoric acid and 1 part CBB G-250. 4 µL triplicates of each standard and unknown were added into separate wells of a 96-well plate. 200 µL of bradford reagent was then added to each well and the mixture was shaken for 30 seconds and then incubated at room temperature for 15 minutes. The absorbance was measured at 595 nm using an EnSpire® Multimode Plate Reader. The protein concentration of unknown samples was then extrapolated from a line of best as determined by the standard concentration curve. Background signal from all standards and unknowns was adjusted by subtracting the absorbance value from blank standards.

3.5.2 Separation of protein by sodium dodecyl sulphate polyacrylamide gel electrophoresis (SDS-PAGE)

SDS-PAGE is a method which separates proteins according to their size (Laemmli, 1970). This is achieved by first denaturing proteins using β-mercaptoethanol at high temperature, which reduces disulphide bonds. Denatured proteins are oriented into a linear shape by binding with an anionic detergent (SDS), which adds a constant negative charge along the polypeptide chain. An electrical current is then applied, causing smaller proteins to migrate further along a gel matrix towards the negative anode than larger proteins.

The type of gel and the amount of sample loaded are described in Table 3.2. All samples were denatured in 1 × boiling buffer (containing β-mercaptoethanol) for 5 minutes at 95 ºC before being loaded into wells of an SDS mini-gel (7.5 × 8.5 × 0.75 mm). 5 µL of molecular weight standard (Precision Plus Protein™ Standards All Blue, BioRad) was added to each gel as a molecular weight standard. Gels were run in 1 × TGS buffer from 120 to 180 V and stopped when the boiling buffer had completely travelled through the gel.

3.5.3 Visualisation of proteins in SDS-PA gels by coomassie staining

Similar to the Bradford protein assay, coomassie staining involves the use of CBB R-250 to stain proteins. The exact binding nature of this chemical is not fully understood, but it is known to bind non-covalently with positively charged amine groups. A higher concentration of protein results in a higher number of bound dye molecules. The addition of a destaining agent (such as ethanol and acetic acid) is used to remove any unbound staining agent, leaving stained protein as chemically visible bands on the polyacrylamide gel.

After electrophoresis, polyacrylamide gels were briefly rinsed in deionised water to remove any excess SDS. Coomassie stain was then added and the gel was agitated slightly from one hour (room temperature) to overnight (4 ºC). The stained gel was then rinsed briefly in deionised water to remove any excess staining agent before being placed in destaining solution with slight agitation for 1 hour. The destaining solution was replaced when necessary until the gel became clear. The gel was rinsed again in deionised water before being viewed using a Gel Doc™ EZ Imager and ImageReady software (v3.0).

Table 3.2
Quantity of samples used for SDS-PAGE and the type of gel prepared.

Sample	Quantity loaded	Stacking gel (%)
COS-7 cell lysate, cytoplasmic fraction	9 µg	10
COS-7 cell lysate, nuclear fraction	9 µg	10
hPXR, cytoplasmic fraction	9 µg	10
hPXR, nuclear fraction	9 µg	10
zfPXR, cytoplasmic fraction	9 µg	10
zfPXR, nuclear fraction	9 µg	10
Hybdridoma supernatants	8 µL	12.5
Hybridoma supernatant wash	8 µL	12.5
IgG-enriched hybridoma supernatant	8 µL	12.5
E. coli Rosetta cells	12 µL, OD_{600} = 1.0*	10
Pre-induced *E. coli* Rosetta cells with His-tagged zfPXR	12 µL, OD_{600} = 1.0	10
Post-induced *E. coli* Rosetta cells with His-tagged zfPXR	12 µL, OD_{600} = 1.0	10
Supernatant of lysed *E. coli* Rosetta cells with His-tagged zfPXR	1.8 µL†	10
Pellet of lysed *E. coli* Rosetta cells with His-tagged zfPXR	1.35 µL‡	10

* In order to obtain an OD_{600} = 1.0 culture, 100 µL OD_{600} = 1.40 of cells for example was concentrated to 71.4 µL.
† Given that the supernatant containing the soluble fraction was × 6.66 times smaller in volume than the post-induced culture, then the volume required to equal 12 µL OD_{600} = 1.00 would be 1.8 µL
‡ Given that the supernatant containing the insoluble fraction was × 1.33 times smaller in volume than the supernatant containing the soluble fraction, the volume required to equal 12 µL OD_{600} = 1.00 would be 1.35 µL.

3.5.4 Immunochemical detection of proteins by Western blotting

Western blotting (WB) is a method which transfers proteins from a polyacrylamide gel to a membrane (polyvinylidene fluoride, PDVF) through an electrical current (Towbin *et al.*, 1979). Proteins transferred to the membrane can then be detected immunochemically using antibodies (Figure 3.5). First, the membrane is then blocked with proteins (such as milk) to prevent the non-specific binding of antibodies to the membrane. Primary antibodies specific to an epitope of the protein of interest are then added. Secondary antibodies specific to an epitope of the primary antibody are added. In this study, secondary antibodies were conjugated with horseradish peroxidase (HRP), an enzyme that converts a luminogenic substrate into a product which emits chemiluminescent light at a wavelength of 430 nm. This process is referred to as enhanced chemiluminescence (ECL). This light can then be detected using a CCD camera, and immunoreactive proteins will appear as a dark band using image processing software.

Figure 3.5. Representation of immunochemical detection of an immunoreactive protein transferred to a membrane by WB. Image adapted from Bio-Rad (2014).

3.5.4.1 Transfer of proteins from SDS-PAG to PDVF membranes

Various methods exist for WB, and two common methods used are semi-dry and wet blotting transfer. Semi-dry transfer involves the transfer of proteins in membrane and filter paper pre-soaked in a transfer buffer. It is faster and requires less transfer buffer, but is less efficient at transferring larger proteins. Wet blotting on the other hand transfers proteins immersed in the transfer buffer. It requires more time and a larger volume of transfer buffer, and is susceptible to overheating. Both types of blotting were used in this study.

The details for each type of Western blot transfer are detailed in Table 3.3. Proteins run through SDS-PAGE were transferred to a PDVF membrane using either the semi-dry or wet transfer method. For both types of transfer, PDVF membranes were activated in 100% methanol for 15 seconds before being transferred into water for 2 minutes and then into transfer buffer for 10-15 minutes. Semi-dry transfer was carried out in a Trans-Blot® SD Semi-dry Transfer cell (Bio-Rad) at 15 V for 25 minutes, and wet transfer at 100 V for 1 hour with an ice block to reduce overheating. Coomassie staining was carried out on the polyacrylamide gel after transfer to ensure successful protein transfer to the membrane.

Membranes were blocked in either PBS or TBS-T buffer containing 5% non-fat dry milk with slight agitation for one hour at room temperature (buffers used listed in Table 3.3). Membranes were washed in buffer two to four times for 5 minutes before being incubated with a primary antibody (diluted in buffer with 5% non-fat dry milk) with slight agitation overnight at 4 ºC. The following day, the membrane was washed four times with buffer for 5 minutes, then incubated with a secondary antibody (diluted in buffer with 5% non-fat dry milk) with slight agitation from one to two hours at room temperature. The membrane was then washed in buffer two to four times for 5 minutes.

3.5.4.2 Visualisation of immunoreactive proteins by horseradish peroxidase (enhanced chemiluminescence)

The probed PDVF membrane was then exposed to either the Amersham™ ECL™ Prime Western Blotting Detection Reagent (GE Healthcare) or the SuperSignal® West Pico Chemilumiscent Substrate (Thermo Scientific) (Table 3.3). For membranes exposed to the Amersham kit, the reagent was prepared as described in the protocol and added dropwise to the membrane and left to incubate for 5 minutes. Excess reagent was removed and the membrane was viewed using a ChemiDoc™ XRS+ imager and ImageReady software (v5.1). For membranes exposed to SuperSignal kit, reagent was prepared and added in the same manner, but an incubation step was omitted due to the sensitivity of the kit.

Table 3.3
Concentration of test antigens loaded for WB blotting and dilutions of commercial primary antibody and secondary antibodies used to detect immunoreactivity.

Sample	Quantity loaded	Transfer method	Buffer used	Primary antibody	Secondary antibody	Detection kit
COS-7 cell lysate, cytoplasmic fraction	1 µg/mm*	Semi-dry	PBS	1:1000 anti-hPXR	1:4000 anti-mouse IgG HRP-conjugated	Amersham
COS-7 cell lysate, nuclear fraction	1 µg/mm	Semi-dry	PBS	1:1000 anti-hPXR	1:4000 anti-mouse IgG HRP-conjugated	Amersham
hPXR, cytoplasmic fraction	1 µg/mm	Semi-dry	PBS	1:1000 anti-hPXR	1:4000 anti-mouse IgG HRP-conjugated	Amersham
hPXR, nuclear fraction	1 µg/mm	Semi-dry	PBS	1:1000 anti-hPXR	1:4000 anti-mouse IgG HRP-conjugated	Amersham
zfPXR, cytoplasmic fraction	1 µg/mm	Semi-dry	PBS	1:1000 anti-hPXR	1:4000 anti-mouse IgG HRP-conjugated	Amersham
zfPXR, nuclear fraction	1 µg/mm	Semi-dry	PBS	1:1000 anti-hPXR	1:4000 anti-mouse IgG HRP-conjugated	Amersham
E. coli Rosetta cells	OD_{600} = 1.0/5 mm†	Wet	TBS-T	1:4000 anti-His	1:10000 anti-mouse IgG HRP-conjugated	SuperSignal
Pre-induced *E. coli* Rosetta cells with His-tagged zfPXR	OD_{600} = 1.0/5 mm	Wet	TBS-T	1:4000 anti-His	1:10000 anti-mouse IgG HRP-conjugated	SuperSignal
Post-induced *E. coli* Rosetta cells with His-tagged zfPXR	OD_{600} = 1.0/5 mm	Wet	TBS-T	1:4000 anti-His	1:10000 anti-mouse IgG HRP-conjugated	SuperSignal
Supernatant of lysed *E. coli* Rosetta cells with His-tagged zfPXR	0.36 µL/mm‡	Wet	TBS-T	1:4000 anti-His	1:10000 anti-mouse IgG HRP-conjugated	SuperSignal
Pellet of lysed *E. coli* Rosetta cells with His-tagged zfPXR	0.27 µL/mm×	Wet	TBS-T	1:4000 anti-His	1:10000 anti-mouse IgG HRP-conjugated	SuperSignal

* 1 µg/mm corresponds to 1 µg of sample loaded per the length of the well. For example, combs with wells 5 mm long were loaded with 5 µg of sample and wells 70 mm long were loaded with 70 µg of sample.
† Given that 12 µL OD_{600} = 1.0of sample was loaded into a 5 mm well, then wells 70 mm long were loaded with 168 µL OD_{600} = 1.0.
‡ Given that 1.8 µL of sample was loaded into a 5 mm well, then wells 70 mm long were loaded with 126 µL of sample.
× Given that 1.35 µL of sample was loaded into a 5 mm well, then wells 70 mm long were loaded with 126 µL of sample.

3.6 Screening of hybridoma supernatants for immunoreactivity

After determining it was possible to probe PXR orthologs (or fused proteins) with commercial antibodies, characterisation of monoclonal antibodies was carried out using supernatants from hybridoma cultures established by fusing of splenocytes and myeloma cells from mice immunised with human and zebrafish PXRs (as described in Richard Davies's Master's thesis, 2011, listed in Materials 2.7 of this thesis).

3.6.1 IgG enrichment of hybridoma supernatants

The Protein G HP SpinTrap^{TM} (GE Healthcare) was used to obtain IgG-enriched antibodies from hybridoma supernatants. Antibodies were purified in a spin column containing sepharose resin, a compound which covalently binds to cysteine side chains at slightly basic pH values (Björck and Kronvall, 1984). Decreasing pH reduces the sepharose's affinity towards antibodies, thus allowing their extraction through a low pH eluent.

Samples were loaded into the spin column as described by the protocol. Ten volumes of 600 µL of hybridoma supernatant were loaded through the column followed by a wash step until 6 mL of sample had been passed through the column. After purification, spin columns were rinsed twice with 400 µL of elution buffer and then twice with 400 µL of 20% ethanol before a new batch of hybridoma supernatant was eluted through the column.

3.6.2 Screening the immunoreactivity of hybridoma supernatants using PXR antigen

Eukaryotically expressed hPXR and zfPXR, and prokaryotically expressed His-tagged zfPXR were immunochemically detected with hybridoma supernatants of different dilutions as well with IgG-enriched supernatants as described in Table 3.4. Each of type of antigen samples were subjected to SDS-PAGE and transferred to PVDF membrane (Methods 3.5.2 and 3.5.4.1). After transfer, the membrane was left to completely dry before being cut into 3 mm wide strips. The remainder were stored at –25 ºC.

Table 3.4
Concentration of antigens loaded for WB blotting and dilutions of unpurified and IgG-enriched hybridoma supernatants and secondary antibodies used to detect immunoreactivity.

Sample	Quantity loaded	Transfer method	Buffer used	Hybridoma supernatant	Secondary antibody	Detection kit
COS-7 cell lysate, cytoplasmic fraction	1 µg/mm*	Semi-dry	PBS	1:1, 1:10, 1:100, 1:1000 hybridoma supernatant	1:1000 anti-mouse IgG HRP-conjugated	Amersham
hPXR, cytoplasmic fraction	1 µg/mm	Semi-dry	PBS	1:1, 1:10, 1:100, 1:1000 hybridoma supernatant	1:1000 anti-mouse IgG HRP-conjugated	Amersham
zfPXR, cytoplasmic fraction	1 µg/mm	Semi-dry	PBS	1:1, 1:10, 1:100, 1:1000 hybridoma supernatant	1:1000 anti-mouse IgG HRP-conjugated	Amersham
COS-7 cell lysate, cytoplasmic fraction	1 µg/mm	Semi-dry	PBS	1:50 IgG-enriched supernatant	1:2000 anti-mouse IgG HRP-conjugated	Amersham
hPXR, cytoplasmic fraction	1 µg/mm	Semi-dry	PBS	1:50 IgG-enriched supernatant	1:2000 anti-mouse IgG HRP-conjugated	Amersham
zfPXR, cytoplasmic fraction	1 µg/mm	Semi-dry	PBS	1:50 IgG-enriched supernatant	1:2000 anti-mouse IgG HRP-conjugated	Amersham
E. coli Rosetta cells	OD_{600} = 1.0/5 mm†	Wet	TBS-T	1:1 hybridoma supernatant	1:10000 anti-mouse IgG HRP-conjugated	SuperSignal
Pellet of lysed *E. coli* Rosetta cells with His-tagged zfPXR	0.27 µL/mm×	Wet	TBS-T	1:1 hybridoma supernatant	1:10000 anti-mouse IgG HRP-conjugated	SuperSignal
E. coli Rosetta cells	OD_{600} = 1.0/5 mm†	Wet	TBS-T	1:50 IgG-enriched supernatant	1:10000 anti-mouse IgG HRP-conjugated	SuperSignal
Pellet of lysed E. coli Rosetta cells with His-tagged zfPXR	0.27 µL/mm×	Wet	TBS-T	1:50 IgG-enriched supernatant	1:10000 anti-mouse IgG HRP-conjugated	SuperSignal

* 1 µg/mm corresponds to 1 µg of sample loaded per the length of the well. For example, combs with wells 5 mm long were loaded with 5 µg of sample and wells 70 mm long were loaded with 70 µg of sample.
† Given that 12 µL OD_{600} = 1.0of sample was loaded into a 5 mm well, then wells 70 mm long were loaded with 168 µL OD_{600} = 1.0.
‡ Given that 1.8 µL of sample was loaded into a 5 mm well, then wells 70 mm long were loaded with 126 µL of sample.
× Given that 1.35 µL of sample was loaded into a 5 mm well, then wells 70 mm long were loaded with 126 µL of sample.

PDVF membrane strips of containing protein extract were blocked as described (Methods 3.5.4.2) and incubated with their respective hybridoma supernatants containing primary antibody and then secondary antibodies diluted in buffer (Table 3.4). Membrane strips were also washed between each step. Both the Amersham and SuperSignal kits were used to detect the presence of monoclonal antibodies from each hybridoma supernatant responding to PXR orthologs. Membranes were viewed using a ChemiDoc™ XRS+ imager and ImageReady software (v5.1).

3.7 Exposure experiment of zebrafish to clotrimazole

An initial effort was made to conduct an exposure experiment on both embryonic and adult zebrafish, extraction of total RNA from individuals, sequencing of the *pxr* gene to identity allelic variants and quantification of expression of a zfPXR target gene, *cyp3a65*. Due to time limitations this final goal was not achieved, however total RNA extraction was carried out on a small number of adult and embryo zebrafish, and *pxr* was sequenced from 24 individuals.

3.7.1 Rearing of adult zebrafish

Adult zebrafish (strain AB/Tu) were maintained at the zebrafish facility at the Institute of Biology at the University of Bergen in accordance with FOTS application 5799. Male and female adults (age = 335 to 809 days) were reared from cross breeding and maintained in water from the zebrafish facility at 28° C on a 14: 10 hour day: night cycle and fed *ad libitum* *Artemia salina* with ST-3 daily. Some of the adults were mated for embryo collection, the methods of which are described below.

3.7.2 Adult exposure experiment

Adult zebrafish (n = 160) were used for an exposure experiment. 20 adults were allocated to one of eight tanks, four representing control and four representing treatment (Table 3.5). Each tank contained 4 L of water from the zebrafish facility and 50% of this water was changed daily. Fish were left to acclimatise for 2 days after transfer to exposure tanks before beginning the exposures. On the third day, 0.25% DMSO was added to the control tanks and 1 µM clotrimazole dissolved in DMSO (final concentration of 0.25%) was added to the treatment tanks. On the fourth day, 50% of the treated water was replaced. 48 hours after exposure, zebrafish were anaesthetised in 200 mg/L tricaine mesylate and their livers were excised under a Nikon SMZ-645 stereomicroscope. Livers were snap frozen in liquid

Table 3.5
Experimental setup for the exposure of zebrafish adults.

Number of zebrafish	Fish per tank	Volume (L)	Treatment
80	20	4	0.25% DMSO control
80	20	4	1 µM clotrimazole, 0.25% DMSO

nitrogen, stored at –80 ºC and used for subsequent experiments. Weight, sex and any deaths during the exposure experiment were also noted.

3.7.3 Embryo collection

Ten male and ten female zebrafish adults were acclimated in the same tank for 24 hours, with a visible barrier separating the sexes. After the 24 hour period, the barrier was removed allowing males and females to mate, lay and fertilise eggs for up to one hour. Males and females were then returned to their respective tanks and eggs were collected using a sieve. Eggs were sorted onto a Petri dish and incubated in E3 medium overnight at 28.5 °C.

3.7.4 Embryo exposure experiment

Throughout the exposure experiment, all embryos were reared in E3 medium at 28.5 °C in a dark incubator. At 24 hours post fertilisation (hpf), any unfertilised eggs were discarded. At 48 hpf, eggs were checked again and allocated to one of two Petri dishes, one representing control and one representing treatment (Table 3.6). 1% DMSO was added to the control dish and 1 µM clotrimazole in 1% DMSO was added to the treatment dish. At 72 and 96 hpf, 50% of the treated medium was replaced and any hatched eggshells, debris or dead individuals were also removed. At 120 hpf, individual embryos were transferred to 1.5 mL centrifuge tubes. The treated water was removed completely and each tube was then snap frozen in liquid nitrogen and stored at –80 °C.

Table 3.6
Experimental setup for the exposure of zebrafish embryos.

Number of zebrafish	Embryos per dish	Volume (mL)	Treatment
60	60	30	1% DMSO control
60	60	30	1 µM clotrimazole, 1% DMSO

3.8 RNA extraction

Messenger RNA (mRNA) is more convenient to extract from biological samples than DNA due to its lack of introns, but ribonucleases (RNases) can become a major source of interference. Total RNA was extracted from select adult livers and individual embryos using different methods.

3.8.1 Total RNA extraction from adult zebrafish livers

Acid guanidinium thiocyanate-phenol-chloroform extraction is a commonly used method to extract RNA from homogenised sample (Chomczynski and Sacchi, 1987). Guanidinum thiocyanate is used to denature RNases (Gordon, 1972), and water-saturated phenol and chloroform are used separate the homogenate into three phases: an aqueous phase containing RNA; an interphase containing DNA an organic phase containing proteins and lipids.

Total RNA was extracted from the liver tissue of adult zebrafish using the TRI Reagent® (Sigma Aldrich) protocol as described by Sigma Aldrich. RNA was extracted from two single, and pools of five and nine individuals. RNA was resuspended in 100 µL RNase-free water (Qiagen) and its concentration was determined by spectrophotometry (Methods 3.2.3).

3.8.2 Denaturing agarose gel electrophoresis

Because RNA commonly forms secondary structures and is susceptible to degradation, a denaturing agent is required to keep the nucleic acids stable (Masek *et al.*, 2005). Denaturing AGE allows for the preparation and evaluation of intact RNA. In eukaryotes, intact RNA subject through denaturing AGE is indicated by the presence of heavy 28S and light 18S ribosomal RNA (rRNA).

RNA was denatured in 50% formamide containing 1 × loading buffer and heated to 65 ºC for 10 minutes. 100-200 ng of each sample and 2-log DNA ladder were loaded onto gels containing 1% agarose in 1 × TAE buffer and 50 µg/mL of EtBr. Gels were run and visualised as previously described (Methods 3.2.4).

3.8.3 Total RNA extraction from individual embryos

RNA extraction was conducted in accordance to the protocol developed by de Jong *et al.* (2010). Initially, centrifuge tubes containing individual embryos were transferred from –

80 °C to liquid nitrogen prior to homogenisation. A stainless steel pestle (Carl Roth) was pre-chilled in liquid nitrogen and then connected to a XENOX motorised hand tool. Each embryo was crushed at about 5000 rpm for 5-10 seconds. The pestle was lifted slightly and 200 µL of QIAzol® Lysis Reagent (Qiagen) was added. After the homogenate had been allowed to thaw, an additional 100 µL of lysis reagent was added to wash the pestle. Alternative methods, such as the use of TRI Reagent and types of pestles were also considered and are detailed in Table 3.7. After the optimal conditions were determined, TRI Reagent was used for the remainder of RNA extractions. The homogenate was vortexed for 15 seconds and left at room temperature for 5 min. Homogenates were spun down for 15 seconds before 60 µL of 24:1 chloroform : isoamyl alcohol was added. The homogenate was vortexed again for 15 s, left at room temperature for 3 min and spun down for 15 s. The entire homogenate was added to individual tubes containing 75-100 mg of heavy phase-lock gel (HPLG), which beforehand had been centrifuged at 12,000 × g for 30 seconds. The homogenate and gel was then centrifuged 12,000 × g for 15 minutes and the clear, aqueous phase was transferred to a new 1.5 mL centrifuge tube. Some sample was collected for use in a gel electrophoresis. Total RNA from adult zebrafish livers (500–4000 ng) was also run through the extraction to determine the yield of the method.

Table 3.7
Different methods used for total RNA extraction from individual embryos.

Pestle type	Pre-chilled?	Lysis reagent
Plastic	No	QIAzol
Plastic	Yes (–80 °C)	QIAzol
Metal	Liquid nitrogen	QIAzol
Metal	Liquid nitrogen	TRI Reagent

3.8.4 RNA cleanup using the RNA MinElute kit

After collecting the aqueous phase of the homogenate after HPLG separation, RNA cleanup was carried out in a silica-membrane column. The silica-membrane has a high affinity for RNA, and various wash steps with ethanol and buffer were used to remove contaminants such as phenol or proteins. RNA is disassociated from the column after a final high speed centrifugation step and collected in RNase-free eluent.

RNA was cleaned according to the RNA® MinElute™ Cleanup Kit (Appendix D of the QIAGEN protocol). In short, 1 volume of 70% ethanol was added to the RNA and the mixture was vortexed thoroughly. The volume was transferred to an RNeasy MinElute spin column and centrifuged at 8,000 × g for 15 s. 500 µL of RPE buffer was added and the column was centrifuged at 8,000 × g for 15 seconds. 500 µL of 80% ethanol was added and the column was centrifuged at 8,000 × g for 2 minutes. The column was then centrifuged at 14,000 × g for 5 minutes. 14 µL of RNase-free water was added to the centre of the column and centrifuged at 14,000 × g for 1 min. The eluate was added to the column a second time in order to maximise RNA yield. During two extractions of total RNA from individual embryos, flow-through was collected at each step and to determine whether any RNA was being lost during the cleanup process. Total RNA from adult zebrafish livers (500–4000 ng) was also initially subjected through RNA cleanup to determine the recovery of RNA.

RNA concentration from each individual was quantified using the NanoDrop® ND 1000 spectrophotometer (Methods 3.2.3), and the integrity of each sample was verified using denaturing AGE (Methods 3.8.2).

3.9 Sequencing of allelic variants of *pxr* in zebrafish

After successfully extracting total RNA from individual embryos, cDNA was synthesised from mRNA, the zebrafish *pxr* gene was amplified and then sequenced.

3.9.1 cDNA synthesis

Reverse transcription of mRNA to cDNA was carried out using oligo-dT primers which binds to the poly-A tail of mRNA. A qScript reverse transcriptase (RT) consists of a Moloney Murine Leukemia Virus Reverse Transcriptase (M-MLV RT) and RNase inhibitor protein, allowing for the synthesis of high quality cDNA with long mRNA templates.

The synthesis of cDNA was carried out according to the protocol by the qScript™ cDNA Synthesis Kit (Quanta Biosciences). 500 ng of total RNA was reverse transcribed to cDNA using the qScript RT enzyme. The reaction was carried out in a total volume of 20 µL.

3.9.2 Polymerase chain reaction

The polymerase chain reaction (PCR) is a well-established method that amplifies DNA fragments through the use of primers which recognise the desired ends of the fragment sequence (Mullis and Faloona, 1987). PCR amplification involves denaturation, annealing and extension steps along with the thermostable enzyme, DNA polymerase (Saiki *et al.*, 1988). In this study, PrimeSTAR® GXL DNA Polymerase was chosen as an enzyme for PCR amplification since it is reported to have a high fedility (*i.e.* accurate replication of the template). Amplification was carried out on beta-actin, in order to determine the success of cDNA synthesis (0.6 kb) and primers to produce a full-length zebrafish *pxr* amplicon to be used as template in sequencing (1.1 kb).

PCR reactions were set up and run according to Tables 3.8 and 3.9. For each reaction, a negative control containing no template was also prepared along with a positive control containing 20 ng of the pcDNA zfPXR plasmid. These controls were set up to ensure no contamination was occurring and that the PCR reaction was successful. 3 µL of each PCR product was run on a 1% agarose gel in 1 × TAE buffer for 110 V for 35 min on ice and analysed on a Gel Doc™ EZ Imager and ImageReady software (v3.0).

Table 3.8
PCR reaction mixture components.

Component	Final concentration	Volume (µL)
5× PrimeSTAR GXL Buffer	1 ×	10
dNTP Mixture	200 µM each	4
Forward Primer	0.25 µM	2.5
Reverse Primer	0.25 µM	2.5
Template cDNA (from 500 ng RNA)		2
PrimeSTAR GXL DNA Polymerase	1.25 U/50 µL	1
Deionised water		28
Total		50

Table 3.9
PCR reaction settings.

Temperature (° C)	Time	Cycles
98	10 s	
55	15 s	32
68	1 min/kb	
4	∞	

PCR product was cleaned according to the protocol of a PCR cleanup kit from Sigma Aldrich. Samples were collected in 50 µL of elution solution and PCR product concentration was measured using a NanoDrop® ND 1000 spectrophotometer. 100 ng of each sample was subjected to AGE (Methods 3.2.4, 1% agarose gel, 1 × TAE, 110 V for 35 min on ice) and analysed on a Gel Doc™ EZ Imager and ImageReady software (v3.0).

3.9.3 Sanger sequencing

Sanger sequencing is a method that utilises chain-terminating dideoxynucleotides (ddNTPs) in the presence of DNA polymerase (Sanger *et al.*, 1977). Dye-terminating ddNTPs contain four different fluorescent labels (ddA, ddC, ddG and ddT) which emit light at different wavelengths, allowing for the determination of nucleotide base pair along a given sequence.

10-40 ng of purified PCR product per sample was used as template in the sequencing reactions. Forward and reverse primers were selected to flank nucleotides 478 to 1070 in the zebrafish *pxr* gene because this region has been found to contain two non-synonymous mutations in zebrafish (Bainy *et al.*, 2013). A reaction mixture was prepared and run for each sample containing a forward and reverse primer (Table 3.10 and 3.11). After the reaction, an additional 10 µL of deionised water was added to reaction tube and samples were sequenced using the 3730XL DNA Sequencer (Applied Biosystems).

Chromatograms of each forward and reverse sequence were visualised in ApE (v2.0.47) and translated to amino acids. Consensus DNA sequences (contigs) were created from the forward and reverse sequences of each individual using BioEdit (v7.1.3.0). Sequences were aligned using ClustalW and visualised in JalView (v2.8.0b1).

Table 3.10
Sequencing reaction mixture components.

Component	Final concentration	Volume (µL)
BigDye v3.1	1 ×	1
Sequencing buffer	1 ×	1
Template	20-40 ng	2
Primer	320 nM	1
Betaine 5 M	1 M	2
Deionised water		3
Total		10

Table 3.11
Reaction settings for sequencing.

Temperature (° C)	Time	Cycles
96	5 min	1
96	10 s	35
50	5 s	
60	4 min	
4	∞	

4. Results

4.1 Characterisation of antibodies against PXR orthologs

Supernatants from hybridoma cultures were tested against human and zebrafish PXRs in order to determine their immunoreactive properties (Methods 3.6). This involved the eukaryotic and prokaryotic expression and evaluation of an antigen used to test the immunoreactivity of commercial antibodies and of the hybridoma supernatants (see Figure 3.1 for experimental overview).

4.1.1 Production and evaluation of the PXR antigen in COS-7 cells

Supercoiled plasmids were required in order for an efficient transfection into a eukaryotic cell line. This involved the transformation of plasmids into a prokaryotic cell line, incubation, purification and gel electrophoresis to confirm their topology (Methods 3.2, Figure 4.1). Since plasmids are capable of coiling, circular plasmids often do not travel through a gel according to size alone but also according to their topology. As a result, the circular plasmids which have travelled further through a gel are more supercoiled than those preceding them. The pure pSG5 hPXR and pcDNA zfPXR plasmid DNA obtained consisted mostly of plasmids of supercoiled topology (Figure 4.1).

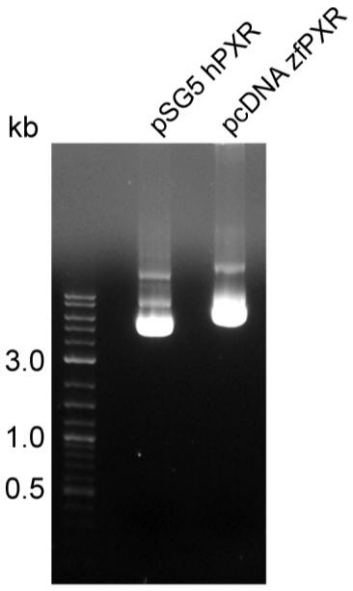

Figure 4.1. Evaluation of plasmid topology by agarose gel electrophoresis. The plasmids were pSG5 hPXR (lane 1) and pcDNA zfPXR (lane 2). 200 ng of 2-log DNA ladder and sample were subjected to AGE (0.7% agarose in 0.5 × TBE buffer for 35 min at 110 V).

The pSG5 hPXR and pcDNA expression vectors were transiently transfected into the COS-7 eukaryotic cell line (Methods 3.3). Endogenous PXR has been reported to translocate to the nucleus upon activation (Kawana *et al.*, 2003), so transfected COS-7 cells were exposed to well known agonists of human and zebrafish PXRs (rifampicin and clotrimazole respectively). However, it is not known whether recombinantly expressed PXR translocates in a similar manner to endogenous PXR, so both the cytoplasmic and nuclear fractions were collected from COS-7 cells. The Bradford protein assay was then used to determine the concentration of total protein within each sample (Methods 3.5.1). Total protein concentration varied between each fraction, but a much higher quantity of protein was found in non-transfected COS-7 cells than in those transfected with plasmids (Table A1, Appendix A).

5 µg of total protein from each fraction was subjected to SDS-PAGE and proteins were visualised by coomassie staining (Methods 3.5.2-3, Figure 4.2). Stained proteins appeared more intact in the cytoplasmic fraction of COS-7 cells than in the nuclear fraction. Despite this, Western blotting was still carried out on all samples (Methods 3.5.4.1). Samples were probed with a commercial anti-hPXR primary antibody before immunodetection with an HRP-conjugated secondary antibody (Methods 3.5.4.2, Figure 4.3). In both the cytoplasmic and nuclear fractions, an immunoreactive protein corresponding to a size of approximately 50 kD was detected, consistent with the size of human PXR. No immunoreactivity was detected for the non-transfected COS-7 cells and those transfected with zfPXR, indicating that the anti-hPXR antibody most likely did not cross-react with zebrafish Pxr, or with any endogenous PXR present in the COS-7 cells. Due to the lack of commercial antibody available for zfPXR, it was not possible at this stage to determine whether COS-7 cells had been successfully transfected with zfPXR or whether they were expressing a sufficient quantity of antigen for detection. Because the cytoplasmic fractions contained more intact protein and a higher concentration of immunoreactive protein, these samples were used to test the immunoreactivity of the hybridoma supernatants.

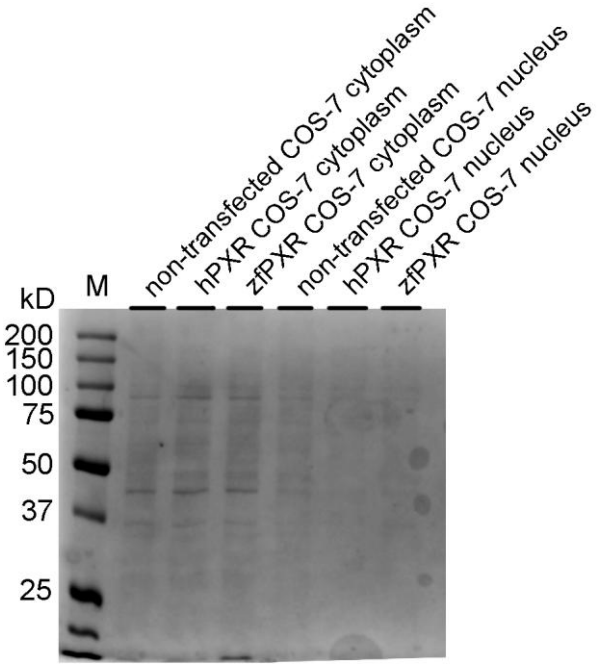

Figure 4.2. Separation of COS-7 protein fractions by SDS-PAGE. 5 µg of cytoplasmic and nuclear proteins were separated by SDS-PAGE and visualised by CBB staining. M represents 5 µL of the molecular weight standard; lanes 1–3 represent the cytoplasmic fraction of COS-7 cells transfected with: no plasmid, hPXR and zfPXR respectively; lanes 4–6 represent the nuclear fraction of cells transfected with: no plasmid, hPXR and zfPXR respectively.

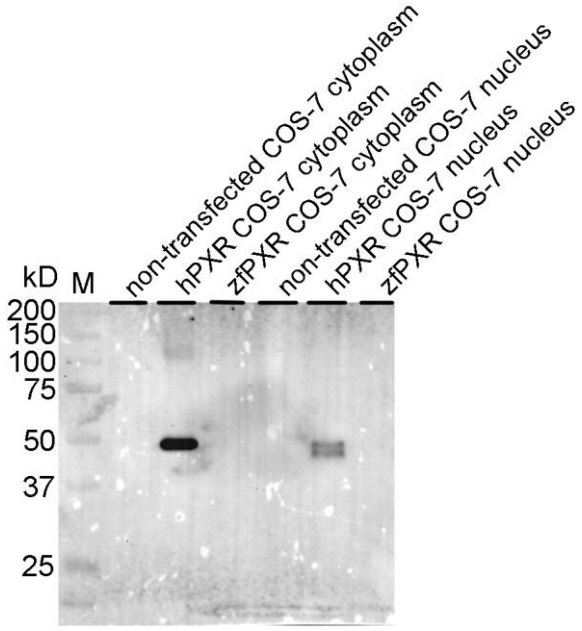

Figure 4.3. Immunochemical detection of immunoreactive protein in COS-7 fractions. Western blot of 5 µg of COS-7 cell cytoplasmic (lanes 1–3) and nuclear fractions (lanes 4–6) on a PDVF membrane. M the molecular weight standard; lanes 1 and 4 correspond to non-transfected COS-7 cells; lanes 2 and 5 correspond to cells transfected with hPXR; and lanes 3 and 6 to cells transfected with zfPXR. The membrane was probed with mouse anti-hPXR monoclonal IgG primary antibody (1:1000) and detected with a goat anti-mouse IgG HRP-conjugated secondary antibody (1:4000). Chemiluminescence was detected with the Amersham™ ECL™ Prime kit.

4.1.2 Immunoreactivity of unpurified hybridoma supernatants

In a previous Master's project, eight hybridoma cultures suspected to be secreting anti-PXR antibodies were identified (Davies, 2011). Final cell lines were selected according to their highest reactivity against a test antigen and the immunoreactivity of these was verified by immunochemically. In this study, six of the eight hybridoma supernatants chosen had previously not been tested for their immunoreactivity and the other two had only been tested with a lower quality of the PXR antigen.

The immunoreactivity of selected hybridoma supernatants potentially containing monoclonal antibodies specific to either hPXR or zfPXR was tested by chemical immunodetection against each cytoplasmic fraction of the COS-7 cells (Methods 3.6.2). Membranes were cut into 3 mm strips in order to probe the same protein with multiple hybridoma supernatants. Initially, only some of the supernatants were tested immunochemically (data not shown). However, an oversaturation of antibodies present in the supernatant made it difficult to separate signal from background noise, and so dilutions of select hybridoma supernatants were prepared and probed against each cytoplasmic fraction (Figure 4.4). Human PXR has a molecular weight of approximately 50 kD, but immunoreactive proteins corresponding to an unexpected size of at 55 kD were detected in the cytoplasmic fraction of cells expressing both human and zebrafish PXRs, as well as with the negative control.

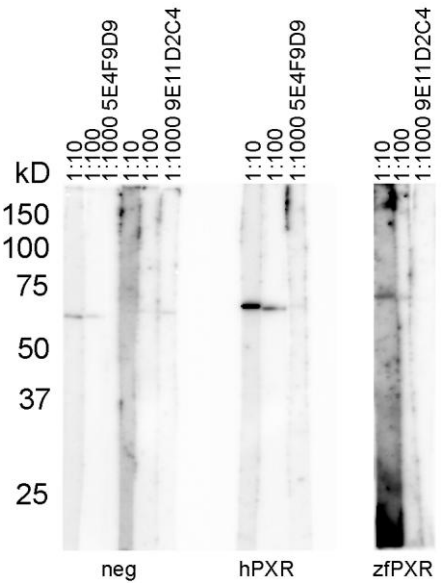

Figure 4.4. Immunochemical detection of diluted hybridoma supernatants. WB of 1 µg/mm of COS-7 cell cytoplasmic fraction on a PDVF membrane corresponding to: non-transfected COS-7 cells, cells transfected with hPXR, and cells transfected with zfPXR (Methods 3.5). Membranes were cut into 3 mm strips and probed with hybridoma supernatant 5E4F9D9 from cells of mice immunised with hPXR (1:10, 1:100, 1:1000); and hybridoma supernatant 9E11D2C4 immunised with zfPXR (1:10, 1:100, 1:1000) and then detected with polyclonal goat anti-mouse IgG HRP-conjugated secondary antibodies (1:1000). Chemiluminescence was detected with the Amersham™ ECL™ Prime kit.

4.1.3 Immunoreactivity of IgG-enriched hybridoma supernatants

In order to increase antibody concentration and reduce background noise from potentially cross-reacting species present within the unpurified hybridoma supernatants, the Protein G HP SpinTrap™ was used to enrich the quantity of IgG antibodies present in each supernatant (Methods 3.6.1). 6 mL of hybridoma supernatant was upconcentrated to a final volume of 400 µL. To evaluate this enrichment, each hybridoma supernatant, eluate wash and IgG-enriched hybridoma supernatant were subjected to SDS-PAGE and visualised by coomassie staining (Figure 4.5). The disulphide-linked heavy and light chains of an antibody become disassociated when the immunoglobulin is denatured and treated with β-mercaptoethanol, and so proteins migrating to a size of approximately 50 kD correspond to the heavy chain and approximately 25 kD to the light chain respectively. Proteins corresponding to the heavy chain of an IgG antibody were present in all samples, however proteins corresponding to the light chain were only observed in the unpurified hybridoma supernatants. In addition, the light chain-sized proteins were also visualised at lower quantities compared to the heavy chain bands at 50 kD. Protein concentration also appeared to decrease during the enrichment process, with the IgG-enriched hybridoma supernatants showing a lower concentration of

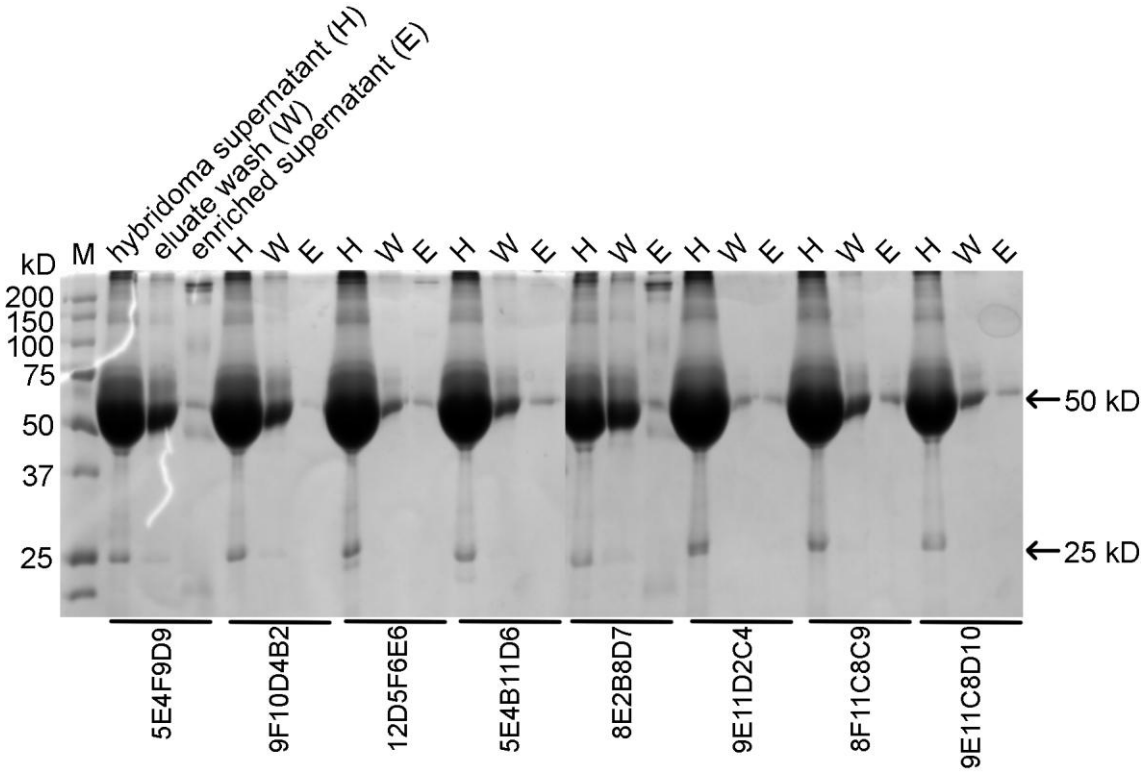

Figure 4.5. Evaluation of hybridoma supernatants subjected through IgG enrichment. 8 µL of each unpurified hybridoma supernatant (S), eluate wash (W) and IgG-enriched supernatant (P) was separated by SDS-PAGE and visualised by CBB staining. M represents 5 µL of the molecular weight standard; lanes 1–5 correspond to hybridoma supernatants containing hPXR and lanes 6–8 zfPXR. Within each lane, sublane 1 corresponds to unpurified hybridoma supernatant, sublane 2 the eluate wash and sublane 3 the IgG-enriched hybridoma supernatant.

total protein compared to the unpurified supernatants. It could be possible that the concentration of IgG antibody in unpurified hybridoma supernatant was low to begin with, leading to lack of visualisation of antibody in the IgG-enriched supernatants.

A 1:100 dilution of each IgG-enriched hybridoma supernatant was chosen to evaluate its immunoreactivity against antigen because enriched supernatants were suspected to contain a lower concentration of primary antibody compared to commercial antibodies. Dilutions of each IgG-enriched hybridoma supernatant were prepared and probed against each cytoplasmic fraction (Figure 4.6). No immunoreactive bands were observed in fraction from non-transfected COS-7 cells, indicating that the enrichment process was successful in removing antibodies with activity against proteins endogenous to COS-7 cells. Immunoreactivity was observed for the cytoplasmic fraction of COS-7 cells transfected with hPXR, but not for the non-transfected COS-7 cells or those transfected with zfPXR. All five IgG-enriched hybridoma supernatants from cells of mice immunised with hPXR detected an

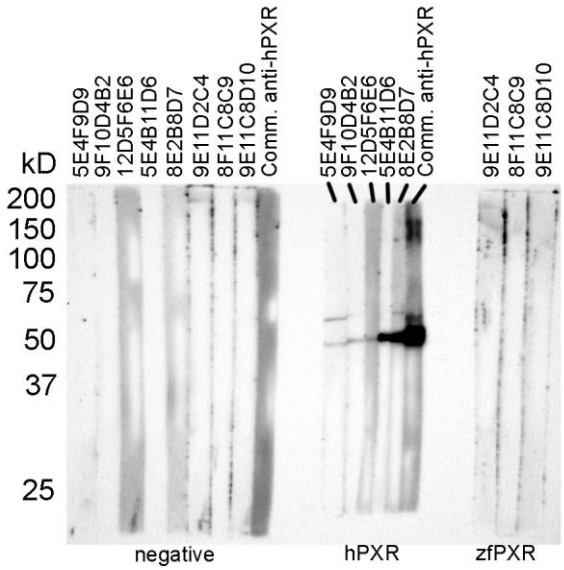

Figure 4.6. Immunochemical detection of IgG-enriched hybridoma supernatants. Western blot of 1 µg/mm of COS-7 cell cytoplasmic fractions on a PDVF membrane corresponding to: non-transfected COS-7 cells, cells transfected with hPXR, and cells transfected with zfPXR. Membranes cut into 3 mm strips and probed with purified hybridoma supernatants from either: cells immunised with hPXR (1:100) or from cells immunised with zfPXR (1:100). Non and hPXR transfected cells and were also probed with mouse anti-hPXR monoclonal IgG primary antibody (1:1000). All antibodies were detected with polyclonal goat anti-mouse IgG HRP-conjugated secondary antibodies (1:2000) and chemiluminescence was detected with the Amersham™ ECL™ Prime kit.

immunoreactive protein corresponding to a size of approximately 50 kD, corresponding to what was detected by the commercial anti-hPXR antibody (Figure 4.3). In addition, two of these hybridoma supernatants, 5E4F9D9 and 8E2B8D7, also detected a second immunoreactive protein corresponding to a size of 55 kD, alongside with the anti-hPXR commercial body.

4.1.4 Production and evaluation of the Histidine-tagged zfPXR test antigen in *E. coli*

Because no commercial antibody current exists for zfPXR, it was not possible to verify that the cytoplasmic fraction of COS-7 cells transfected with zfPXR were producing sufficient amounts of test antigen, and immunoreactivity could not be detected using either the anti-hPXR antibody or hybridoma supernatants. Therefore it was necessary to find another means of expressing zfPXR and effectively determining the presence of the protein before immunoprobing with hybridoma supernatants. In order to achieve this, a pET30b His-tagged zfPXR expression vector was used to transform *E. coli* Rosetta cells and an anti-histidine antibody was used to detect the expression of the resulting fusion protein (Methods 3.4). The expression of the fusion protein was induced by IPTG and degree of induction, as well as the

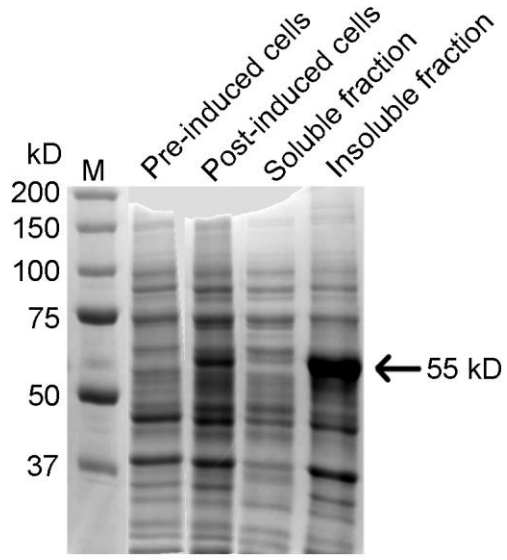

Figure 4.7. Evaluation of expression and solubility of the His-tagged zfPXR protein. Whole Rosetta cells from a 1 mL culture were adjusted so OD_{600} = 1.0, and corresponding amounts of soluble and insoluble fractions, were subjected to SDS-PAGE and proteins visualised by CBB staining. M represents 5 µL of the molecular weight standard; lane 1 represents *E. coli* Rosetta cells transformed with pET30b His-tagged zfPXR before induction; lane 2 represents cells post induction; lane 3 represents the soluble fraction of cells lysed after sonication; and lane 4 the insoluble fraction.

solubility of the fusion protein was evaluated by SDS-PAGE (Figure 4.7). His-tagged zfPXR weighs approximately 55 kD (Saradhi *et al.*, 2005), and proteins migrating to this size were observed for post-induced transformed Rosetta cells and in the insoluble fraction after lysis by sonication, but not in pre-induced cells or in the soluble fraction after sonication. This indicated that protein induction protein was successful and that the protein solubility was limited.

Each of these samples alongside non-transformed *E. coli* Rosetta cells was also transferred to a PDVF membrane for immunodetection against a commercial anti-his primary antibody (Figure 4.8). For the non-transformed Rosetta cells and for the pre-induced transformed Rosetta cells transformed with pET30b His-tagged zfPXR no immunoreactivity was observed. However, immunoreactivity corresponding to a protein of a size of 55 kD was detected in the post-induced cells and in both the soluble and insoluble fraction of cells after sonication. The presence of immunoreactive ghost bands in the insoluble fraction indicate that the signal became saturated from an overloading of too much sample or that chemiluminescent substrate was being depleted too quickly. Because a high concentration of immunoreactive protein was observed in both SDS-PAGE and Western blotting, this component was used for subsequent analyses.

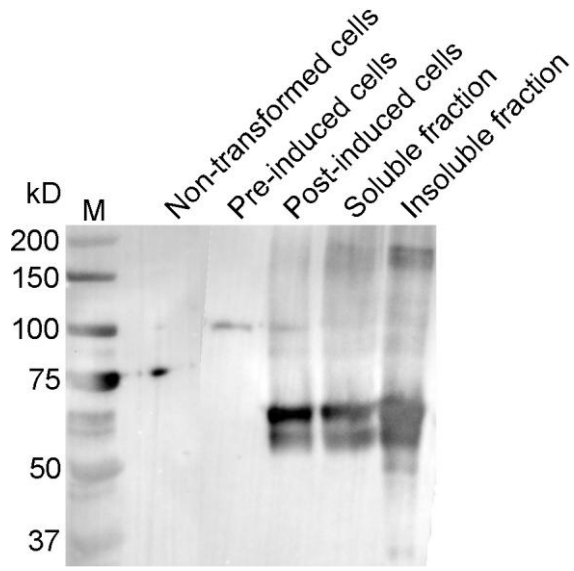

Figure 4.8. Immunological detection of histidine-tagged zebrafish Pxr expressed in *E. coli* Rosetta cells. Whole Rosetta cells from a 1 mL culture were adjusted so OD_{600} = 1.0, and corresponding amounts of soluble and insoluble fractions were transferred to a PDVF membrane. M represents 5 µL of the molecular weight standard; lane 1 represents non-transformed cells; lane 2 represents cells transformed with pET30b His-tagged zfPXR before induction; lane 3 represents cells post induction; lane 4 represents the soluble fraction of lysed cells; and lane 5 the insoluble fraction. Membranes were probed with mouse anti-his IgG primary antibody (1:4000) and detected with a goat anti-mouse IgG HRP-conjugated secondary antibody (1:2000). Chemiluminescence was detected with the SuperSignal® West Pico Chemilumiscent Substrate.

Due to the sensitivity of the SuperSignal® West Pico Chemilumiscent Substrate, various dilutions of the insoluble fraction were run through a SDS-PA gel, transferred to a PDVF membrane and probed with anti-His primary antibody in order to determine the optimal ratio between antibody and the insoluble fraction containing the test antigen. The gel was also subjected to coomassie staining after Western blotting in order to determine the efficiency of protein transfer. Samples containing a higher concentration of the insoluble fraction failed to transfer protein from gel to PDVF as successfully as samples with a lower concentration (Figure 4.9). Samples diluted to 1:4 were still visible on an SDS-PA gel even after transfer. Despite this, the presence of a highly immunoreactive protein migrating to a size of 55 kD was confirmed immunochemically, in accordance to what was expected for His-tagged zfPXR within all the dilutions of the sample (Figure 4.10). It was concluded that the 1:8 dilution of the insoluble fraction of lysed *E. coli* Rosetta cells containing His-tagged zfPXR resulted in a sufficiently strong signal. This dilution was used to test the immunoreactivity of hybridoma supernatants.

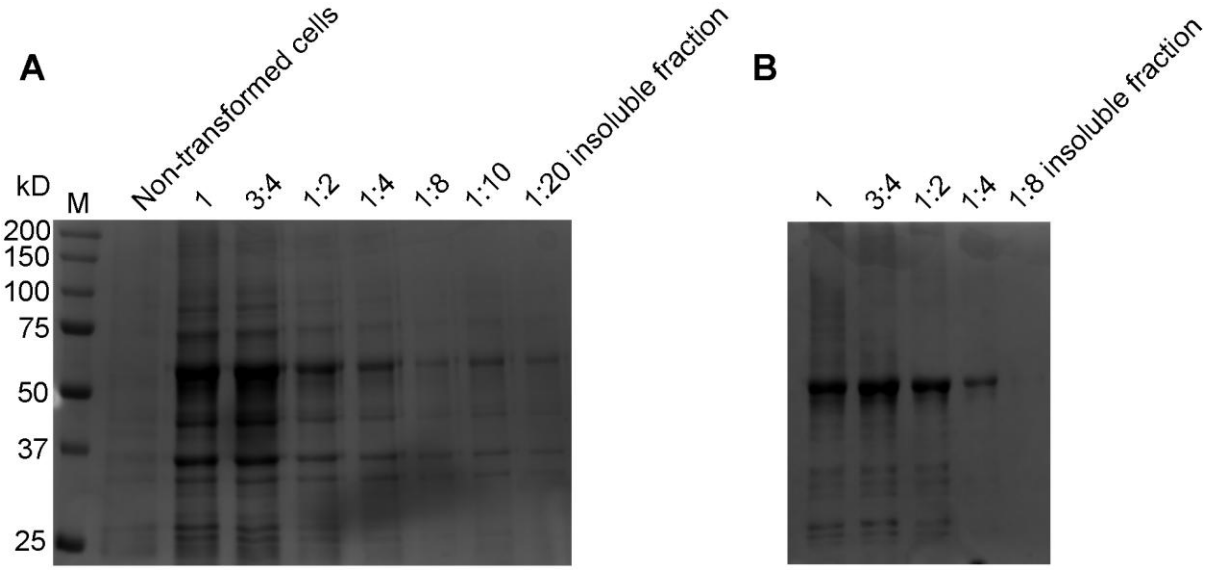

Figure 4.9. Separation of protein in *E. coli* Rosetta cells by SDS-PAGE and evaluation of protein transfer during WB. Coosmassie stain of whole Rosetta cells from a 1 mL culture were adjusted so OD_{600} = 1.0, and corresponding dilutions of the insoluble fraction (100%, 3:4, 1:2, 1:4, 1:8, 1:10 and 1:20 respectively) were run through SDS-PAGE before (A) and after (B) transfer to a PDVF membrane and visualised by CBB. M represents 5 µL of the molecular weight standard. A represents the separation of proteins within the insoluble fraction of transformed *E. Coli* Rosetta at different dilutions (100%, 3:4, 1:2, 1:4, 1:8, 1:10 and 1:20 respectively), alongside non-transformed cells. B represents the amount of visible protein visualised on an SDS-PA gel after transfer to a PDVF membrane.

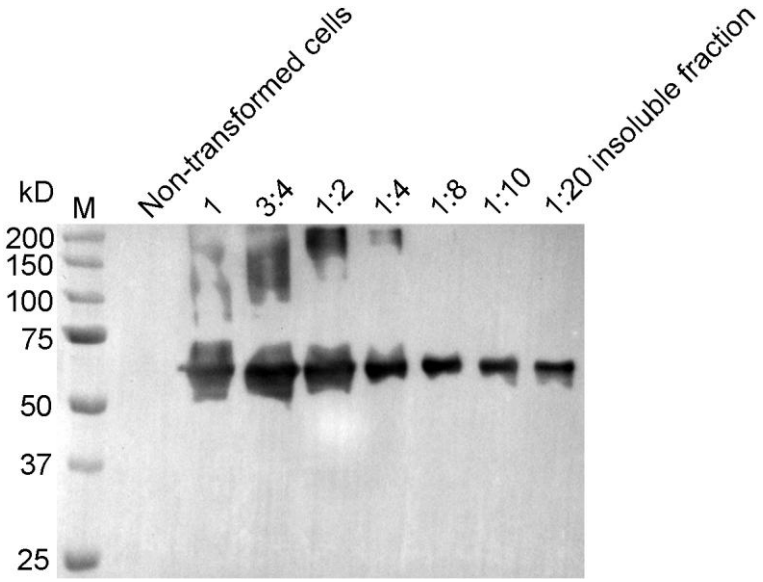

Figure 4.10. Immunochemical detection of His-tagged immunoreactive proteins in *E. coli* Rosetta cells. Whole Rosetta cells from a 1 mL culture were adjusted so OD_{600} = 1.0, and corresponding dilutions of the insoluble fraction (100%, 3:4, 1:2, 1:4, 1:8, 1:10 and 1:20 respectively) were transferred to a PDVF membrane. M represents 5 µL of the molecular weight standard; Membranes were probed with mouse anti-his IgG primary antibody (1:4000) and detected with a goat anti-mouse IgG HRP-conjugated secondary antibody (1:10000). Chemiluminescence was detected with the SuperSignal® West Pico Chemilumiscent Substrate.

4.1.5 Immunoreactivity of zfPXR hybridoma supernatants

Membranes containing the insoluble fraction from *E. coli* Rosetta cells expressing the His-tagged zfPXR fusion protein were initially probed with each unpurified hybridoma supernatant in order to evaluate their immunoreactivity. However, no immunoreactive proteins corresponding a size of 55 kD were observed. Difficulties emerged in optimising the immunodetection of His-tagged zfPXR using the anti-His primary antibody as a positive control (data not shown), so IgG-enriched hybridoma supernatants were used instead to detect immunoreactivity (Figure 4.11). In cells expressing His-tagged zfPXR, the anti-His antibody detected an immunoreactive protein ranging from 55 to 50 kD and an additional protein at approximately 30 kD. No immunoreactivity was observed for the whole non-transformed Rosetta cells or with the insoluble fraction containing His-tagged zfPXR.

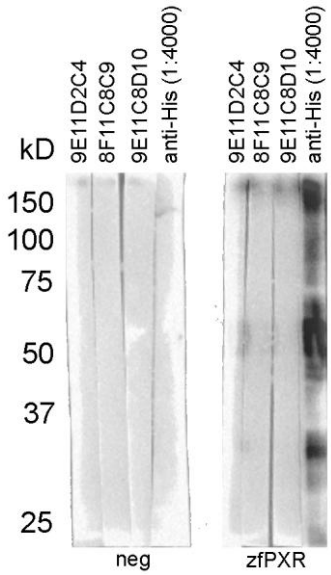

Figure 4.11. Immunochemical detection of IgG-enriched hybridoma supernatants. A Western blot of *E. coli* Rosetta cells corresponding to whole non-transformed cells and the insoluble fraction of lysed cells containing His-tagged zfPXR. A 1:40 dilution per mm of sample (corresponding to a 1:8 dilution per 5 mm well) was loaded into a 70 mm well and transferred to a PDVF membrane. Membranes cut into 3 mm strips and probed with purified hybridoma supernatants from mice immunised with zfPXR (1:50) and with mouse anti-His IgG primary antibody (1:4000) and detected with a goat anti-mouse IgG HRP-conjugated secondary antibody (1:10000). Chemiluminescence was detected with the SuperSignal® West Pico Chemilumiscent Substrate.

4.2 Zebrafish exposure experiment to clotrimazole

Embryonic and adult zebrafish were initially set up in an exposure experiment to clotrimazole (Methods 3.7) in order to determine whether there *pxr* exhibited functional variation, by measuring expression levels of *cyp3a65*. This was not completed due to time restraints.

However, data was obtained on the number of individuals exposed, weights, sex and number of deaths (Table 4.2).

The expression of *cyp3a65* in zebrafish has been recently studied in embryos exposed up to 10 μM of clotrimazole (Biancarosa, 2014), and so 40 adult zebrafish were initially exposed to 10 μM clotrimazole in 0.25% DMSO for a planned period of 48 hours. However 100% lethality was observed after 3 hours. Thus the exposure concentration of clotrimazole was reduced to 1 μM (in 0.25% DMSO). For the embryo zebrafish exposure experiment, embryos exposed to 1 μM of clotrimazole, and no deaths were observed after 72 hours.

Table 4.2.
Data of adult zebrafish used in the exposure experiment with clotrimazole.

Type of data	Males	Females	Total
Number survived	85	71	157*
Deaths from 0.25% DMSO	0	0	0
Deaths from 1 μM clotrimazole	—	—	3
Deaths from 10 μM clotrimazole	—	—	40
Weight (mg)	279	288	283†
Average age (days)	—	—	525

***** The sex of one individual was not identified.
† No significant difference was found in weight between sexes.

4.3 RNA extraction and sequencing of *pxr* from individual zebrafish embryos

Pxr from individual zebrafish embryos was sequenced in order to investigate genetic variation existed between individuals (see Figure 3.2 for experimental overview). The experimental strategy involved total RNA extraction from individual embryos, cDNA synthesis followed by PCR amplification of a select region of *pxr* for Sanger sequencing (Methods 3.8–9). Embryos were chosen because they were easy to obtain in large numbers and methods had been developed which allowed for total RNA extraction from individuals as young within the first few hours of fertilisation. Here, total RNA was extracted from individual embryos five days post fertilisation as part of an exposure experiment.

4.3.1 RNA extraction from zebrafish embryos

Initially, attempts to extract total RNA from individual embryos essentially as described by de Jong *et al.* (2010) proved unsuccessful. Briefly, this method involved the homogenisation of individual embryos pre-chilled in liquid nitrogen, HPLG separation to physically separate RNA from DNA and protein, and cleanup to remove any residual DNA or contaminants present in the unpurified RNA extract (Methods 3.8.2).

RNA extraction was first attempted with plastic pestles and QIAzol lysis reagent. In denaturing agarose gel electrophoresis, rRNA was clearly visible under UV light from RNA extracted from trout liver (at quantities as low as 50 ng), but absent in RNA extracted from individual embryos (Figure 4.12). This indicated that degradation was occurring in one of the three steps of the RNA extraction process, *i.e.* homogenisation, HPLG separation or cleanup. Plastic pestles were replaced with metal pestles and pre-chilled in liquid nitrogen before homogenisation and cleaned with 0.1% DEPC to minimise RNase activity, however samples lacked intact RNA (Figure 4.13). Eluate was also collected from each step of the cleanup process from two individuals and subjected through denaturing AGE (Figure 4.13). The cleanup involved two ethanol wash steps and one wash step with RPE buffer and eluates from each of these steps lacked intact rRNA compared to the non-degraded trout RNA, indicating that either: 1) RNA was already degraded before cleanup; or 2) RNA was being degraded in one or more steps during RNA cleanup. In addition, QIAzol lysis reagent was also replaced with TRI Reagent® to test whether one lysis reagent performed better than another, however RNA degradation still occurred (data not shown).

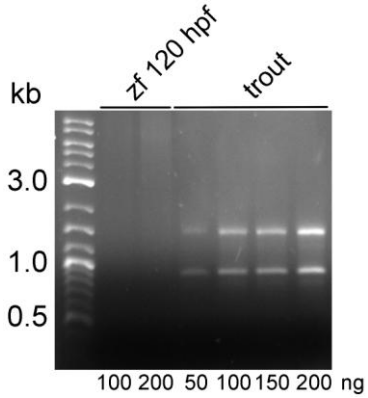

Figure 4.12. Evaluation of RNA quality by denaturing AGE. Total RNA was extracted from an individual zebrafish embryo homogenised with a plastic pestle and QIAzol lysis reagent. 200 ng of 2-log DNA ladder was also loaded. 100 and 200 ng of sample were denatured in 50% formamide for 5 min at 68 ºC, and subjected to denaturing AGE (1% agarose in TAE buffer at 35 min at 110 V). Pure trout RNA was loaded at different quantities (50, 100, 150 and 200 ng) and was used as a positive control to monitor degradation during the electrophoresis process.

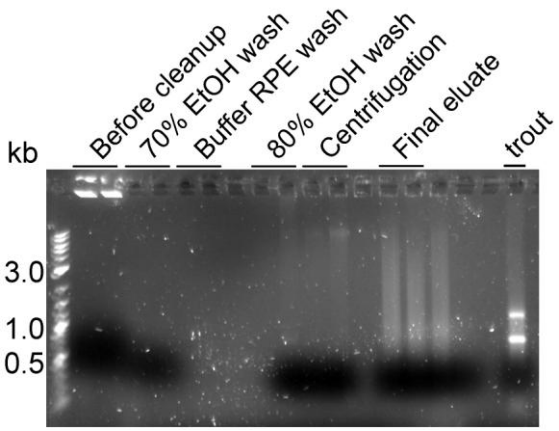

Figure 4.13. Evaluation of RNA extraction from individual zebrafish embryos during RNA cleanup. Eluate from two individual zebrafish embryos was collected during each step of RNA cleanup using the RNA® MinElute™ Cleanup Kit. Total RNA was initially extracted using a pre-chilled metal pestle in liquid nitrogen and QIAzol lysis reagent. 100 ng of ladder, 4 µL of each wash eluate, and 100 ng final eluate and trout RNA (intact RNA control) were subjected to denaturing AGE.

4.3.2 RNA extraction from adult zebrafish

Total RNA was also extracted from adult livers using TRI Reagent®, both from two individuals and pooled samples of five and nine individuals (Methods 3.8.1, Figure 4.14). RNA was visualised in denaturing agarose gels under UV light. The yield of total RNA from the two individual embryos was calculated to be 25.8 and 68.8 µg and even higher for the pooled embryos—253 and 415 µg respectively (Table 4.2). These values suggested that it was possible to obtain a high yield of RNA from individual adult livers and that pooling of samples increased the quantity of RNA obtained. For all samples, the $A_{260/280}$ ratio always exceeded 1.80. Total RNA from a single individual was then used as a positive control for subsequent denaturing gels as well as a means to quantify RNA degradation in the RNA cleanup process used for extracting RNA from individual zebrafish embryos.

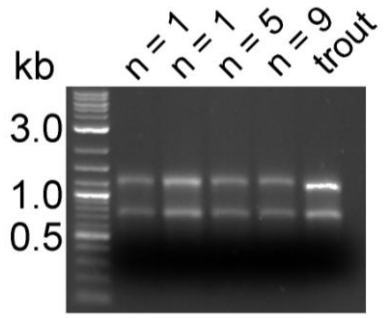

Figure 4.14. Evaluation of RNA quality by denaturing AGE. Total RNA from the liver of zebrafish adults was obtained from two individuals and two pools of five and nine individuals using the TRI Reagent protocol. 200 ng of 2-log DNA ladder, sample and trout liver RNA were subjected to denaturing AGE. Lanes 1–2 represent RNA obtained from individual livers (n=1) and lanes 3 and 4 represent five livers (n = 5) and nine livers (n = 9) respectively.

Table 4.2 Yield and integrity of total RNA obtained from liver of zebrafish adults.
Total RNA from the liver of zebrafish adults obtained from two individuals and two pools of five and nine individuals using the TRI Reagent protocol. RNA was extracted using the TRI Reagent protocol and collected in 100 µL of RNase-free water. Concentrations were calculated using a NanoDrop® ND-1000 spectrophotometer.

Number of livers	Concentration (ng/µL)	Total RNA (µg)	$A_{260/280}$
1	258	26	1.80
1	688	69	1.84
5	2526	253	1.88
9	4148	415	1.88

4.3.3 Optimisation of an RNA extraction method from zebrafish embryos

After determining it was possible to extract total RNA from individual adult livers, different quantities of zebrafish liver total RNA from a single individual were subjected through the HPLG separation and RNA cleanup steps in order to determine if RNA was being degraded before or during purification (Methods 3.8.2–3). Quantities of 4000, 2000, 1000 and 500 ng of RNA were prepared to determine whether final yield would vary depending on the initial amount of RNA loaded. However, denaturing AGE demonstrated that RNA was degraded during cleanup, so attention was directed towards optimising this procedure to remove any sources of degradation.

Wash solutions used in the RNA® MinElute™ Cleanup Kit were replaced, and different quantities of zebrafish liver total RNA (4000, 2000, 1000 and 500 ng) from a single

individual were subjected through RNA cleanup a second time, followed denaturing AGE (Methods 3.8.4, Figures 4.15). This time intact RNA was obtained, indicating that one of the wash solutions was responsible for RNA degradation and that RNase contamination had occurred. The final yield of RNA obtained from each input was measured using the NanoDrop® ND-1000 spectrophotometer (Table 4.3), and it was found that at least 37% of the RNA subjected through the cleanup process was retained. When 500 ng of RNA was subjected through cleanup, however, a recovery greater than the input was observed, and this could have been due to pipetting errors or uncertainties in quantifying RNA concentrations (see Discussion). 10 pg to 1 µg of total RNA is recommended for cDNA synthesis (depending on how much of the copy gene of interest is present in the sample), so 1000 ng of initial total RNA yield from an individual embryo was deemed sufficient for cDNA synthesis. Extraction of total RNA from individual embryos was therefore continued using metal pestles pre-chilled in liquid nitrogen, TRI Reagent (although QIAzol lysis reagent could have been used), HPLG separation and the RNA® MinElute™ Cleanup Kit.

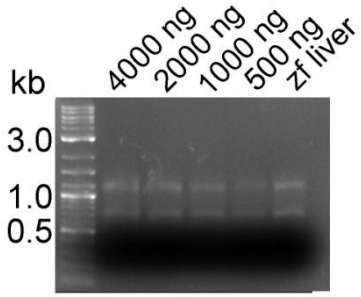

Figure 4.15. Evaluation of total RNA recovered from RNA cleanup. Total RNA obtained from the liver of zebrafish adults was subjected through RNA cleanup using the RNA® MinElute™ Cleanup Kit. Different quantities adult liver RNA (4000 ng, 2000 ng, 1000 ng and 500 ng) were loaded through the cleanup process and collected in eluate. 100 ng of 2-log DNA ladder, eluate from each loading and zebrafish liver RNA (intact positive control) was subjected to denaturing AGE.

Table 4.3. Recovery of total RNA subjected through RNA cleanup.
Yield and recovery of total RNA from zebrafish liver of a single individual subjected through RNA cleanup using the RNA® MinElute™ Cleanup Kit. Concentration was calculated using a NanoDrop® ND-1000 spectrophotometer and yields were calculated from 14 µL of final eluate.

Input of RNA (ng)	Yield of RNA (ng)	Recovery	$A_{260/280}$ ratio
4000	2230	56%	1.98
2000	748	37%	1.80
1000	577	58%	1.74
500	666	100%	1.58

4.3.4 Comparison of total RNA extraction methods from zebrafish embryos

After demonstrating that it was possible to obtain intact RNA from individual adult zebrafish livers using TRI Reagent®, this lysis reagent was used for the remainder of RNA extractions. In addition to the extraction total RNA from individual embryos using HPLG separation and RNA cleanup, total RNA was also extracted from embryos using the TRI Reagent protocol as carried out with adult livers (Figure 4.16 & Table 4.4). Total RNA was extracted from individuals as well as from pools of five and ten individual embryos. In all cases of RNA extraction using HPLG separation, it was possible to obtain total RNA concentration from each sample with yields greater than 1.4 µg. For pooled individuals however, RNA yield was higher in the pooled sample of five compared to ten embryos. The $A_{260/280}$ ratio in each sample was also greater than 1.90.

Extraction of total RNA using the TRI Reagent protocol led to mixed results (Figure 4.16 & Table 4.4). Total RNA extracted from three individuals indicated that RNA had degraded, due to the absence of 28S and 18S rRNA visualised under UV light. Only the extraction of total RNA from a single individual was successful. Extraction of RNA from individual zebrafish embryos using the TRI Reagent protocol was difficult and likely requires further technical optimisation to minimise the effect of RNA degradation. Extraction of RNA from five embryos gave a higher yield, but lacked intact rRNA after denaturing AGE. The pool of ten embryos gave a lower yield but contained intact rRNA after denaturing AGE. Caution should be taken when assessing RNA quality according to its yield, purity and rRNA.

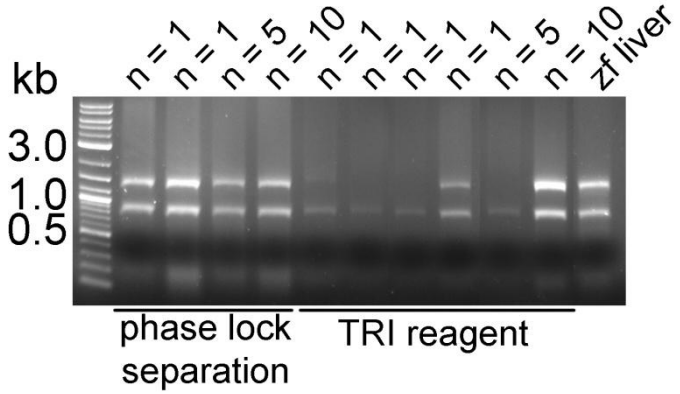

Figure 4.16. Evaluation of RNA quality extracted using HPLG separation and the TRI Reagent protocol. Total RNA from zebrafish embryos was obtained using both HPLG separation and the TRI Reagent protocol. Lanes 1–4 used HPLG separation to obtain RNA (lanes 1–2 from individual embryos and lanes 3–4 from pools of five and ten individuals). Lanes 5–10 used the TRI Reagent protocol to obtain RNA (lanes 5–8 from individual embryos and lanes 9–10 from pools of five and ten individuals). 200 ng of 2-log DNA ladder, sample and trout liver RNA were subjected to denaturing AGE.

Table 4.4. Yield and purity of total RNA obtained from liver of zebrafish adults.
Yield and $A_{260/280}$ ratios of total RNA extracted from individual and pooled embryos using both HPLG separation and TRI Reagent. Yield was calculated using a NanoDrop® ND-1000 spectrophotometer. Total RNA extracted from embryos using HPLG separation was eluted in 14 µL of RNase-free water and 20 µL of RNase-free water for RNA extracted using the TRI Reagent.

RNA extraction method	Number of individuals used	Yield (µg)	$A_{260/280}$ ratio
HPLG separation	1	1.6	1.90
HPLG separation	1	1.4	1.95
HPLG separation	5	13.9	1.98
HPLG separation	10	4.8	1.97
TRI Reagent	1	1.0	1.69
TRI Reagent	1	3.4	1.70
TRI Reagent	1	0.5	1.69
TRI Reagent	1	1.1	1.88
TRI Reagent	5	16.4	1.46
TRI Reagent	10	8.7	1.67

Extraction of total RNA from individual zebrafish embryos using HPLG separation was then scaled up to 24 individuals (Figure 4.17). The average yield of RNA extracted from individual embryos was 1969 ± 578 ng (Table A3, Appendix A). $A_{260/280}$ ratio was always greater than 1.80 (1.90 ± 0.06), except for two of the samples, suggesting that RNA was generally of high purity. Therefore, cDNA synthesis was continued with all samples, even when rRNA was difficult to visualise on denaturing agarose gel.

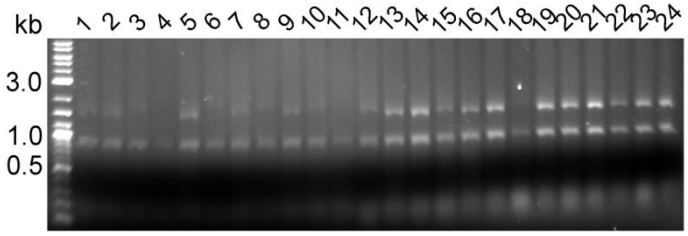

Figure 4.17. Evaluation of RNA quality by denaturing AGE. Total RNA was extracted from 24 individual embryos using HPLG separation and RNA cleanup. 200 ng of 2-log DNA ladder and each sample were subjected to denaturing AGE.

4.3.5 PCR amplification of zebrafish *pxr*

4.3.5.1 cDNA synthesis and control of cDNA quality

Complementary DNA was synthesised from 500 ng of RNA using the qScript™ cDNA Synthesis Kit (Methods 3.9.1). The quality of the cDNA was evaluated by amplification of the high copy gene beta-actin using the cDNA as template (Methods 3.8.2). As expected, a product of approximately 500 bp was amplified from all cDNA synthesised (Figure 4.18), indicating that mRNA within each sample of total RNA had been successfully reverse transcribed into cDNA.

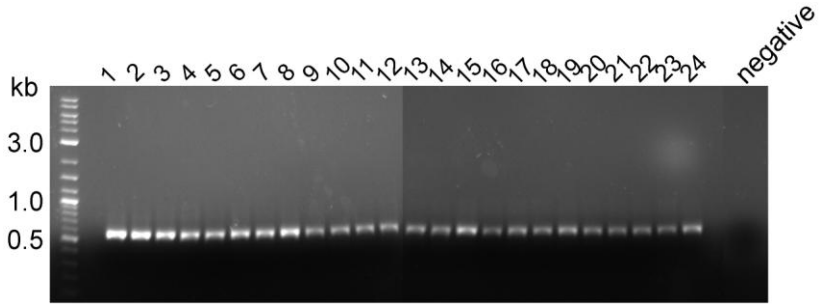

Figure 4.18. Evaluation of the beta-actin PCR product. cDNA from 24 individuals was amplified with primers flanking the zebrafish beta-actin gene. 250 ng of 2-log DNA ladder and 3 µL of each sample were subjected to AGE (1% agarose in 1 × TAE at 35 min at 110 V). The negative control represents a PCR reaction that did not contain a cDNA template.

4.3.5.2 Amplification of full length zebrafish pxr

The full open reading frame of the zebrafish *pxr* gene was amplified by PCR using the cDNA previously synthesised as a template (Methods 3.9.2). As expected the amplification product was approximately 1.3 kb in size (Figure 4.19).

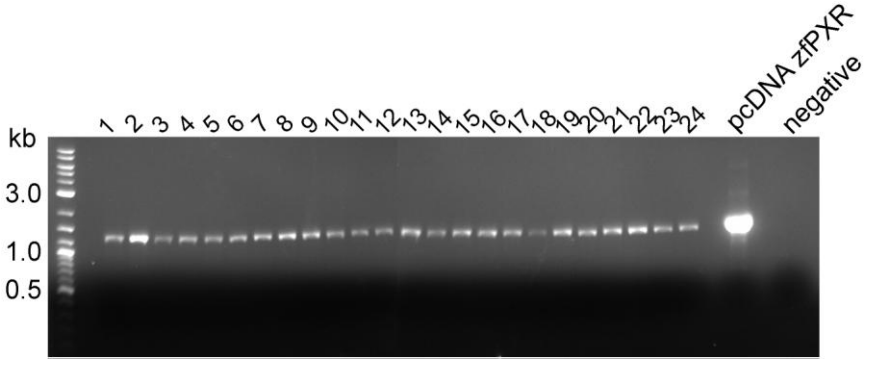

Figure 4.19. Evaluation of the full length zebrafish *pxr* PCR product. cDNA from 24 individuals was amplified with primers flanking the zebrafish *pxr* gene. 250 ng of 2-log DNA ladder and 3 µL of each sample were subjected to AGE. 20 ng of pcDNA vector containing zebrafish *pxr* was also amplified and 3 µL was used as a positive control. The negative control represents a PCR product which did not contain a cDNA template.

Following amplification, the total reaction volume of each PCR product (47 µL) was run through PCR cleanup using GenElute^{TM} PCR Clean-Up Kit and subjected to AGE (Figure 4.20). The average yield of PCR product obtained from each sample after cleanup was 783 ± 82 ng (Table A4, Appendix A). The size of the product (approximately 1.3 kb) was consistent with the product before cleanup.

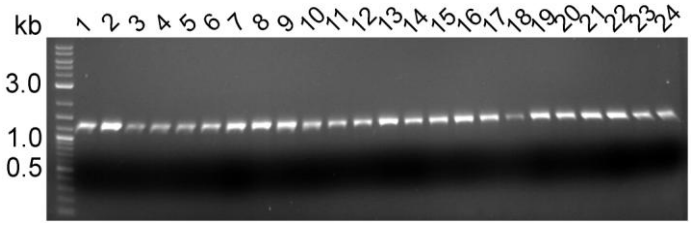

Figure 4.20. Evaluation of the full length zebrafish *pxr* PCR product after cleanup. PCR product of full length zebrafish *pxr* from 24 individuals after PCR cleanup. 100 ng of 2-log DNA ladder and each sample were subjected to AGE.

4.3.6 Sequencing of zebrafish *pxr*

40 ng of each purified PCR product was used a template for Sanger sequencing (Methods 3.9.3). A forward and reverse primer were selected to sequence the full open reading frame of the zebrafish *pxr* gene from nucleotides 478 to 1070, as this region includes two codons known to contain allelic variation. Contigs were created from forward and reverse sequences from each individual, translated and aligned using ClustalW. Consensus sequences representative of a section of *pxr* from each individual were compared with one another, however all 24 individuals contained identical sequences. The chromatogram, which contains specific peaks for each ddNTP along a stretch of a sequence, was also checked briefly to determine if any sequencing errors were present. Some individuals exhibited what appeared to be heterozygous peaks at some nucleotides of the *pxr* sequence, which could suggest that SNPs exist at these loci (Figure 4.21). Interpretations of findings made from the chromatograms are detailed in the Discussion.

The zfPXR sequence representative of all 24 individuals was also aligned with amino acids 180 to 338 of two zfPXR sequences from UniProtKB (identifiers: A5WYG8/unknown and F1R424/Tu) to determine whether there was any genetic variation (Figure 4.22). These online sequences corresponded to an unknown strain and Tu zebrafish. Five non-synonymous substitutions and one amino acid insertion were found and these substitutions corresponded

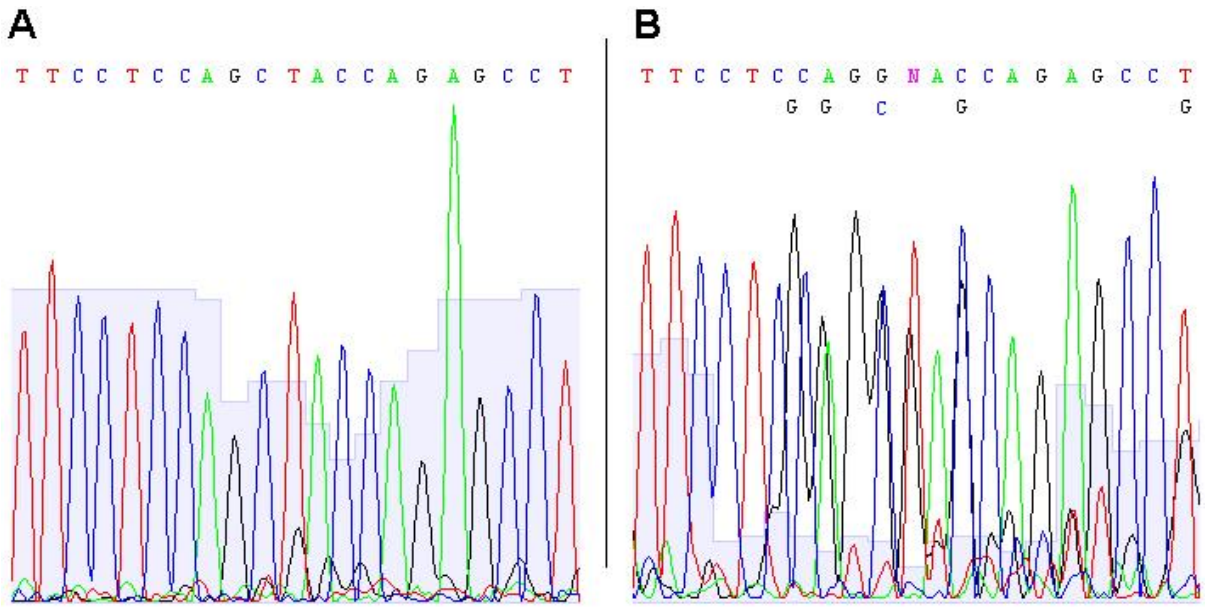

Figure 4.21. Chromatogram comparison in a region of zebrafish *pxr* between two individuals. Chromatogram (A) contains no overlapping base pair peaks; whereas chromatogram (B) contains several overlapping peaks which could represent the sequencing of a heterozygous gene (indicated below the main sequence.

to: substitutions L186V, M202V, P208S, N232S and S234T; and insertion N223. These substitutions corresponded to all the major (*i.e.* found in three or more individuals) variant residues found in *pxr*1* of TL zebrafish as described by Bainy *et al.* (2013), but to none in *pxr*2* of TL (containing allelic variants I184S and C218Y). This means that *pxr* sequence obtained from the 24 zebrafish embryos corresponds to the *pxr*1* allele. The Tu strain found online however did contain a sequence which corresponded to the *pxr*2* allele in the TL strain.

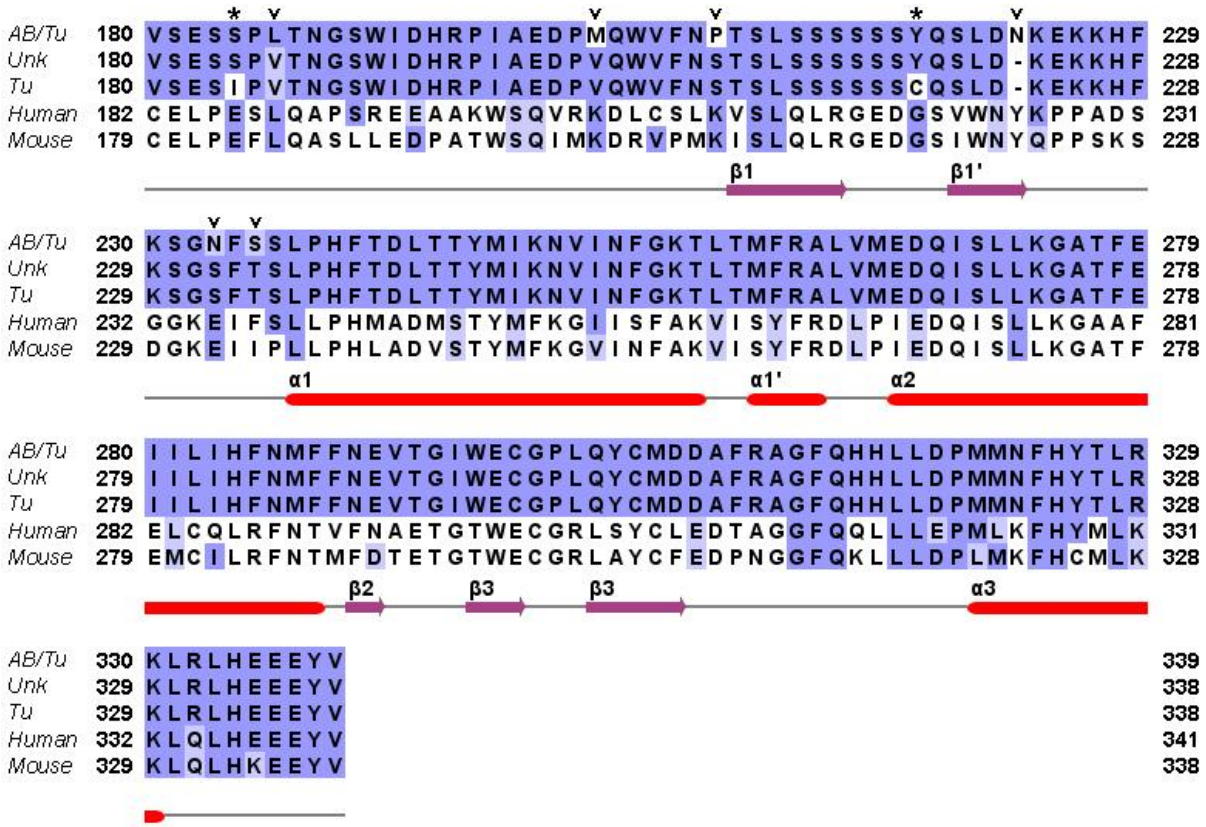

Figure 4.22. Multiple sequence alignment of zebrafish *pxr* variants and orthologs. Amino acid sequence alignment of AB/Tu strain zebrafish *pxr* from this study compared to an unknown strain (Unk) and the Tu strain of zebrafish from UniProtKB/TrEMBL (identifiers: A5WYG8/Unk and F1R424/Tu). The zebrafish *pxr* sequences were also compared to human *PXR* and mouse *Pxr* (UniProtKB/Swiss-Prot, identifiers: O75469/human and O54915/mouse). The secondary structure represents the hPXR LBD interacting with rifampicin (PDB Id: 1SKX). Sequences were aligned using Clustal Omega and visualised in Jalview (v2.8.0b1). Residues known to contain allelic variants in the TL strain by Bainy *et al.* (2013) are indicated by an asterisk; differences between AB/Tu and both the Unk and Tu strain are indicated by a caret.

5. Discussion

This study has focused on PXR, a nuclear receptor which regulates the transcription of genes for enzymes involved in the biotransformation of endogenous and xenobiotic compounds. Ligands for PXR include a wide range of steroids, natural products as well as pollutants. Understanding how a particular compound can activate PXR to induce gene expression is especially important from both an ecotoxicological and pharmacological perspective, and studies on this can be used to expand our knowledge on PXR function.

Studies on PXR can be achieved both *in vitro* and *in vivo*. Such studies can be used to help form the basis of risk assessment and decision making (Sheldon and Hubal, 2009), especially when considering compounds that interact with this nuclear receptor. Furthering our understanding of PXR function can help researchers draw more detailed conclusions when choosing appropriate animal species to use and compare to in toxicological testing.

In this study, we aimed to validate monoclonal antibodies against human and zebrafish PXRs due to the fact that commercial antibodies specific against this nuclear receptor are either limited (in the case of zfPXR, no commercial antibody exists) and/or generally polyclonal, *i.e.* antibodies bind to multiple epitopes of the same antigen. Hybridoma cells developed from mice immunised either with human PXR or zebrafish Pxr had been developed in a previous Master's project (Davies, 2011). Here, we further characterised these hybridomas by recombinant antigen expression and enrichment of the IgG fraction from the hybridoma supernatants. Monoclonal antibodies from cells of mice immunised with hPXR demonstrated good specificity to its antigen, whereas those from mice immunised with zfPXR detected no immunoreactivity against the denatured zfPXR antigen.

Another aspect of this study was to identify *pxr* variants in zebrafish embryos. Zebrafish are an extensively studied organism whose relevance in toxicology makes them a useful model species for studying response to newly discovered drugs, as well as to pollutants in the aquatic environment (Coe *et al.*, 2009; Rubinstein, 2006; Barros *et al.*, 2008). However, information about *pxr* in this species is limited, at least compared to what has been investigated in humans. This study focused on a region of *pxr* previously identified to contain genetic variation in the TL strain (Bainy *et al.*, 2013). RNA was extracted from individual embryos belonging to the AB/Tu strain and *pxr* was sequenced from 24 individuals. None of

the individuals exhibited genetic variation compared to those from TL strain, but amino acid differences were identified when compared to a sequence of the gene available in GenBank.

5.1 Immunoreactivity of hybridoma supernatants

For all IgG-enriched hybridoma supernatants from cells of mice immunised with hPXR, an immunoreactive protein was detected corresponding to an expected size of 50 kD when tested against the cytoplasmic fraction of COS-7 cells transiently expressing hPXR (Figure 4.6). However, two of the supernatants, 5E4F9D9 and 8E2B8D7, also unexpectedly detected an immunoreactive protein corresponding to a size of approximately 55 kD. The presence of this additional protein could be due to a number of reasons and is discussed in further detail in the following section.

5.1.1 Multiple isoforms of PXR

Splice variation refers to when the exons of a gene are spliced alternatively into an mRNA sequence. This can lead to gene variants possessing fewer exons than the original genomic sequence and thus different protein isoforms after translation (Venter *et al.*, 2001). For nuclear receptors, alternative splicing can lead to different levels of target gene expression, protein interaction and subcellular localisation (Keightley, 1998). In humans, seven splice variants or isoforms have been identified in PXR (Table 3.1), and some of these isoforms have been shown to have differing levels of ligand activation and target gene expression (Gardner-Stephen *et al.*, 2004; Fukuen *et al.*, 2002). PXR isoforms have also been identified in pigs (Pollock *et al.*, 2007).

In humans, isoform 1, consisting of 434 amino acids with an calculated molecular weight of 50 kD (Table 5.1), is referred to as "canonical" because it is the most functional and commonly occurring isoform in humans (Lamba *et al.*, 2004; Gardner-Stephen *et al.*, 2004). Isoform 3 contains an additional 39 amino acids, making it 473 amino acids long and approximately 54 kD. This isoform coincides to the second immunoreactive protein detected by two of the hybridoma supernatants and the commercial anti-hPXR antibody.

The detection of a second, heavier immunoreactive protein was also observed by Saradhi *et al.* (2005), where the immunoreactivity of polyclonal anti-hPXR antibodies from antiserum was tested against lysed COS-1 cells transfected with hPXR. Immunoreactive protein detected at 50 kD was observed in the COS-1 cell lysate, as well as an additional protein at

55 kD. The study suggested that the detection of additional immunoreactive proteins as well as the expected one detected at 50 kD could correspond to isoforms of PXR. Saradhi and co-authors refer to a study where the glucocorticoid receptor (GR, NR3C1), another type of nuclear receptor, was expressed in COS-1 cells and detected using an anti-GR antibody (Lu and Cidlowski, 2005). They conclude that the immunodetection of paralogous GR isoforms could help explain their own findings, but failed to acknowledge that the COS-1 cells were transfected with expression vectors coding for multiple isoforms of GR, rather than for a single isoform. Alternative splicing of recombinant DNA does not occur during transient transfection (unless the recombinant DNA also contains introns which is uncommon), indicating that the recombinant gene within pDNA is always translated into the same mRNA sequence and always transcribed to same final protein. This means that the appearance of multiple immunoreactive proteins observed in our study do not correspond to different isoforms of PXR as a result of alternative splicing of the gene located on the recombinant DNA.

Table 5.1
Isoforms of human PXR and their respective differences between one another.

Isoform	UniProtKB/Swiss-Prot identifier	Amino acid differences	Amino acids	Size (kD)
1A	O75469-1	Canonical	434	50
1B	O75469-2	Missing 1–55	379	44
1C	O75469-3	Additional 24	457	52
2A	O75469-4	Missing 174–210	397	46
2B	O75469-5	Missing 1–55 Missing 174–210	342	40
2C	O75469-6	Additional 24 Missing 174–210	420	48
3	O75469-7	Additional 39	473	54

5.1.2 Post-translational modification of PXR

Another explanation for the appearance of this heavier immunoreactive protein is that hPXR has undergone a post-translational modification. PXR has been demonstrated to undergo

different forms of post-translational modifications, including phosphorylation, SUMOylation, ubiquitination and acetylation (reviewed in Smutny *et al.*, 2013; Staudinger *et al.*, 2011). Post-translational modifications are also found in other nuclear receptors and are an important part of cell regulation (Rochette-Egly, 2003). For antigen probed with the commercial anti-hPXR antibody, it is interesting to note that the immunoreactivity of the protein is greater at 50 kD than 55 kD, suggesting that if post-translated PXR is being detected, it exists at a much lower concentration than its unmodified counterpart when expressed in COS-7 cells.

Alternatively, supernatants might have been reacting against an epitope of the protein which contained a modified site. Depending on the type of modification, it could be possible that this leads to a reduction or loss of binding towards antibodies in the supernatant (Jeltsch, 2013). One way of confirming the post-translational modification of PXR would have been to test the immunoreactivity of prokaryotically expressed hPXR towards a commercial antibody. This is because in prokaryotic systems, post-translational protein modifications occur less frequently than in eukaryotic expression systems (Walsh and Jefferis, 2006).

5.1.3 Cross-reactivity of anti-hPXR against PXR orthologs

In theory, it is possible that the COS-7 lysates contained endogenous isoforms of monkey PXR which were cross-reactive with the commercial anti-hPXR antibody. The commercial anti-hPXR antibody used in this study is reported to be specific to all isoforms of hPXR except those lacking the first 55 amino acids, *i.e.* isoform 1B and 2B (R&D systems). The antibody was prepared by immunising mice with a recombinant form of the human PXR isoform 1 containing the first 40 amino acids of the open reading frame of the sequence. It was not stated whether the anti-hPXR antibody was cross-reactive with closely related PXR orthologs. However, a comparison of the 40 amino acid sequence of hPXR with other species will indicate whether such cross-reactivity is likely to occur.

The sequence for Green monkey PXR has yet to be determined. However, *PXR* has been cloned and sequenced in Cynomolgus and Rhesus monkeys and shown to be highly homologous to human *PXR* (96%) (Kim *et al.*, 2010). Given these two species along with the Green monkey belong to same clade, family Cercopithecidae, the possibility of Green monkey *PXR* containing the same degree of similarity to human *PXR* is highly likely. In the study by Kim *et al.* (2010), the first 40 amino acids of the two monkey PXR sequence compared to hPXR varies only by five amino acids (Figure 5.1).

Figure 5.1. Sequence differences in the first 40 amino acids between *PXR* in human and the Cynomolgus monkey, Rhesus monkey and zebrafish. Figure adapted from Kim *et al.* (2010).

A minimum of fifteen amino acids residues of the epitope are required when binding with an antibody (Frank, 2002). Of these fifteen residues, only five strongly influence the antibody's binding affinity towards the epitope (Benjamin and Perdue, 1996). In theory, it could then be possible for anti-hPXR to be cross-reactive with monkey PXR, given that the exact location of the epitope lies within a conserved region of the sequence of the first 40 amino acids. The only way to confirm this would be through the immunochemical detection of the monkey PXR antigen towards the commercial antibody. In the case of zfPXR, the first 40 amino acids of the sequence resemble little similarity to its human counterpart, meaning that an anti-hPXR antibody targeting an epitope in this region is highly unlikely to cross-react with a zfPXR antigen.

Human PXR is expressed in low levels in the kidney (Nishimura *et al.*, 2004), and this could reflect what occurs in non-transfected COS-7 cells (Figure 4.6), since these originate from the kidney tissue of the Green monkey. Thus the absence of immunoreactive protein detected in non-transfected cells could have been due to: 1) endogenous PXR not being expressed; 2) endogenous PXR being expressed at levels too low for immunodetection; 3) anti-hPXR antibody not being cross-reactive with monkey PXR.

5.1.4 Cross-reactivity of anti-hPXR against closely related nuclear receptors

The nuclear receptors CAR and VDR are most closely related to PXR, and have been shown to be expressed at high levels in the human kidney (Nishimura *et al.*, 2004). This means that COS-7 cells could also contain higher levels of these proteins compared to endogenous PXR. As a result, hybridoma supernatants from cells of mice immunised with hPXR could also potentially be immunoreactive against monkey CAR and monkey VDR.

As discussed, the epitope of an antibody generally needs to be highly conserved for cross-reactivity to occur. For the anti-hPXR antibody, the epitope was located in the first 40 amino acids of the sequence, corresponding to a poorly conserved region between different nuclear

receptors (reviewed in Pawlak *et al.*, 2012). Therefore it is highly unlike that the commercial anti-hPXR antibody cross-reacted with endogenous CAR and VDR.

5.1.5 Epitope of antibodies from hybridoma supernatants

5.1.5.1 Antibodies specific against unexpected epitopes

No immunoreactivity was detected in the three hybridoma supernatants from cells immunised with zfPXR when tested against COS-7 cells transfected with zfPXR or against the insoluble fraction of lysed Rosetta cells containing His-tagged zfPXR (Figure 4.11). This is in contrast to findings made by Davies (2011), whereby three hybridoma supernatants from cells immunised with zfPXR detected an immunoreactive protein corresponding to a prokaryotically expressed His-tagged zfPXR antigen (Figure B1, Appendix B). In addition, Davies was also able to demonstrate cross-reactivity of these supernatants against an hPXR antigen.

It could be possible that hybridoma supernatants from cells immunised with zfPXR were only immunoreactive to the histidine tag fused to the Pxr protein. In Davies' study, mice were immunised to His-tagged zfPXR. This antigen was developed in a previous Master's project whereby His-tagged zfPXR was transformed in a prokaryotic cell line, expressed with IPTG and purified using a Ni-NTA column that binds to His-tagged proteins (Mork-Jannson, 2010). Given that the monoclonal antibodies in mice were generated in response to the His-tag itself, then it is possible that these would be immunoreactive against any recombinant protein fused with this tag. This could be confirmed by immunochemically determining whether the hybridoma supernatants respond against a His-tag protein not related to PXR. Interestingly, Davies detected immunoreactivity in most hybridoma supernatants against both His-tagged zfPXR and His-tagged hPXR. This could explain why no immunoreactivity was observed for COS-7 cells transfected with untagged zfPXR (Figure 4.6), but does not explain a lack of immunoreactivity detected against the Rosetta cells which contained His-tagged zfPXR (Figure 4.11).

5.1.5.2 The specificity of monoclonal antibodies

The production of hybridoma clones by limiting dilution does not always yield antibodies which are monospecific in nature (Underwood and Bean, 1988). When selecting hybridoma clones containing monoclonal antibodies, often the most reactive hybridoma cultures are chosen instead of those which are the most specific (Staszewski, 1984). It could be possible

that the most reactive hybridoma cultures initially selected were more reactive because they contained a higher level of cross-reactivity as opposed to mono-reactivity against the desired antigen. It is possible that some of the antibodies generated by the hybridomas from cells immunised with zfPXR may not have been monospecific.

For this reason, it could be argued that some of these antibodies may have only been immunoreactive against zfPXR in a conformational state. The initial expression of zfPXR by prokaryotic cells to be used for immunisation could have resulted in the production of antibodies which were only immunoreactive against a conformational epitope as a result of protein folding or misfolding, which is common for eukaryotic proteins expressed in prokaryotes. This could explain why no immunoreactivity was observed between hybridoma supernatants from cells of mice immunised with zfPXR and the zfPXR antigen probed in its linear, denatured state. In order to determine whether the epitope of these antibodies is conformational, the incorrectly folded proteins could be subjected to immunodetection towards the hybridoma supernatants with the omission of a heat denaturation step.

5.1.6 Proteasomal degradation of the test antigen

When testing the immunoreactivity of the commercial anti-His antibody against the lysed Rosetta cells containing His-tagged zfPXR, protein was detected ranging from 55 to 50 kD and approximately 30 kD (Figure 4.11). Initial attempts to optimise the immunodetection of the His-tagged positive control proved challenging, and this additional, lighter immunoreactive protein was present in many of these initial tests.

It could be possible that His-tagged zfPXR undergoes proteasomal degradation in prokaryotic cells despite the inclusion of protease inhibitors before and after cell lysis. In the case of degradation, it could have been problematic for hybridoma supernatants to cross-react with His-tagged zfPXR if there was antigen degradation to begin with. Moreover, if the epitope was retained in a partially degraded protein, this could explain the detection of immunoreactive proteins corresponding to a smaller size than expected. Protein degradation has also been suggested to occur for COS-1 cells transfected with zfPXR (Saradhi *et al.*, 2005), suggesting that cleavage of the protein could occur. Studies have shown that the stability and solubility of the PXR LBD in *E. coli* cells is poor and subject to degradation (Jones *et al.*, 2002; Wang *et al.*, 2008). This is because incorrect folding of the protein makes proteins more susceptible to degradation. Stability was improved however after cells were

coexpressed with a fragment of the nuclear receptor coactivator, steroid receptor coactivator 1 (SRC-1), a protein which assists in the transcriptional activity of PXR (Wang *et al.*, 2008). Since the stability of full length PXR tethered to SRC-1 has not yet been tested, then the coexpression of the PXR LBD with SRC-1 could have been considered in study, given that the epitope of the hybridoma supernatants are immunoreactive against the LBD.

5.1.7 Improvement of immunodetection by IgG enrichment

One of the unpurified hybridoma supernatants from cells immunised with hPXR, 5E4F9D9, was immunoreactive against a protein of a size of 55 kD in both non-transfected COS-7 cells and with COS-7 cells transfected with hPXR, indicating that the supernatant could react against COS-7 specific proteins. This apparent non-PXR specific immunoreactivity was also observed by Davies (2011). However, after IgG enrichment of the supernatant, the non-specificity was removed against the non-transfected cells, while reactivity against a 55 kDa protein in COS-7 cells expressing hPXR was retained. This indicates that IgG enrichment increase the specificity of the supernatants. In addition, Davies was unable to detect immunoreactivity of the unpurified hybridoma supernatant 12D5B5C8 against eukaryotically and prokaryotically expressed hPXR. However, in this study we were able to demonstrate that it was in fact possible to detect the immunoreactivity of this supernatant, but only after IgG enrichment.

These findings demonstrate that IgG enrichment of the hybridoma supernatants is a useful step. However, when IgG-enriched hybridoma supernatants were subjected to SDS-PAGE and visualised using CBB, proteins corresponding to the light and heavy chains of the antibody could not be detected (Figure 4.5). The absence of the light chain suggests that the amount of antibody subjected to SDS-PAGE was too low to be detected by staining, and this could be attributed to the fact that the light chain band was much weaker than the heavy chain band in the unpurified hybridoma supernatants also. Because destaining of SDS-PA gels depends on the sample loaded with the highest quantity of protein loaded (in this case the unpurified supernatant), it could be possible that CBB staining the light chains (in the IgG-enriched samples) was removed. Rerunning SDS-PAGE with a lower quantity of unpurified hybridoma supernatant and a higher quantity of IgG-enriched supernatant might improve this.

5.1.8 Subcellular localisation of PXR orthologs

As discussed previously, the subcellular localisation of PXR is a disputed topic (reviewed in Zhou *et al.*, 2009). In mice, endogenous PXR has been show to be localised exclusively in the nucleus in the presence and absence of a ligand such as PCN (Saradhi *et al.*, 2005). On the contrary, research has also demonstrated endogenous PXR in mice is localised in the cytoplasm prior to treatment with the PCN ligand (Squires *et al.*, 2004).

The ambiguity in the subcellular localisation of PXR before and after ligand treatment meant that it was an important step to fractionate both the cytoplasmic and nuclear fractions of COS-7 cells in order to determine where immunoreactivity was occurring. However, addition, it was not practical to compare studies between the localisation of endogenous and recombinant expressed PXR. In this study we demonstrated that for hPXR, localisation occurred both in the cytoplasm and nucleus of transfected COS-7 cells 24 hours after treatment with rifampicin, with the greatest immunoreactivity being detected in the cytoplasm (Figure 4.3). This contradicts findings made by Koyano *et al.* (2004), where they demonstrated that localisation in COS-7 cells transfected with hPXR occurred in the nucleus 48 hours after transfection and 24 hours after ligand treatment (vehicle control or rifampicin). However the negative control used in this study differs to the one used by Koyano and co-authors in three ways: 1) negative control COS-7 cells in this study were not transfected with hPXR; 2) non-transfected cells were not treated with either ligand or a vehicle control; and 3) localisation was determined by cellular fractionation and Western blotting (as opposed to immunocytochemistry of whole cells). The differences in the immunodetection of the subcellular localisation of PXR warrants further investigation and could form the basis of testing variation in immunoreactivity according to design and methodology.

It could also be possible that the localisation of recombinant PXR differs between COS-7 cells transfected with either hPXR and zfPXR. One possibility for the lack of immunoreactivity detected for COS-7 cells transfected with zfPXR is that the antigen could have translocated to the nucleus after treatment with clotrimazole, and these fractions were not used for subsequent analyses. Future studies could investigate PXR localisation in COS-7 cells by transfection of cloned PXR orthologs which have antibodies developed towards them (*e.g.* human, rodent, rabbit). Another option could be to tag recombinantly expressed PXR with protein tags such as green fluorescent protein (GFP, a protein which fluoresces when exposed to blue light), if antibodies specific to the nuclear receptor do not exist.

5.2 RNA extraction for sequence analysis

The extraction of total RNA from individual embryos proved difficult, due to degradation of genetic material. However, after the removal potential RNase contaminants, it was possible to extract total RNA from individuals with a high degree of success. The following section discusses how particular methods used in this process aided in the extraction of genetic material in both high quality and quantity.

5.2.1 Importance of homogenisation method

Obtaining total RNA from individual zebrafish embryos using the TRIzol Reagent protocol was challenging due to the embryo's small size, however a high quantity of RNA was obtained after the pooling of five and ten individual embryos. For many studies where the availability of biological sample is limited, a pooling of samples is often necessary (Linney *et al.*, 2004). This becomes impractical however when investigating sequences or gene expression levels resulting from individual variation (Jolly *et al.*, 2005; Mary-Huard *et al.*, 2007). On the other hand, pooling might be necessary when overall gene expression is more important than individual variation, and care should be taken in deciding whether analysing embryos individually or in pools is more important.

In this study, we were interested in identifying genetic variation in *pxr* between individuals, meaning that sequencing pooled samples would not have given us the results we were looking for. Various methods for extracting total RNA from individuals were evaluated in this study, including: choice of pestle, lysis reagent, phase separation and column purification.

5.2.2 Evaluation of total RNA extraction methods from individual zebrafish embryos

5.2.2.1 Facilitation of RNA extraction by pestle type

Zebrafish embryos possess a rubbery epidermis making it challenging to homogenise individuals completely. The use of plastic pestles to homogenise individual embryos proved unsuccessful. Therefore it was necessary to pre-chill embryos in liquid nitrogen and then crush individuals using a metal pestle pre-chilled in the same liquid. Crushing embryos in this manner allowed for the homogenisation of the sample into a fine powder, which helped facilitate RNA extraction and reduce RNA degradation. Similar methods have been developed for skin biopsies, which are tough and rich in RNases (Bruning *et al.*, 2011). The crushing of samples at liquid nitrogen temperatures has many applications and has also shown to be successful in smaller sized samples, including yeast cells (Yang *et al.*, 2011).

5.2.2.2 Choice of lysis reagent

In the study carried out by de Jong *et al.* (2010), total RNA was successfully extracted from individual zebrafish embryos using QIAzol lysis reagent. In our study, QIAzol was initially used as a lysis reagent but was replaced as a precaution with TRI Reagent when RNA degradation occurred. TRI Reagent and STAT-60 have been used to extract RNA from individual zebrafish embryos in other studies (van der Vaart *et al.*, 2013; Timme-Laragy *et al.*, 2012) and it is most likely that using QIAzol after optimisation of the RNA extraction protocol would not have affected the yield or quality of samples.

5.2.2.3 Importance of phase separation with small samples

While it was possible to extract RNA from individual embryos using the TRIzol Reagent protocol, the process was not always successful (Figure 4.16). Thus, a method combining both TRIzol Reagent and HPLG separation was evaluated. Although only five embryos were subjected to each of the two methods, the success rate of purifying RNA from single embryos using the combination of TRI Reagent and HPLG separation appeared to be higher than with TRI Reagent alone (Figure 4.1.6).

One difficulty faced when using the TRIzol Reagent protocol was that RNA pellets which were precipitated using isopropanol were extremely small in size and often did not pellet properly after an ethanol wash step. This could have been due to the limited amount of biological sample available from individual embryos, compared to the larger sized adult zebrafish livers, where RNA extraction using this protocol was no challenge. Adult zebrafish livers can weigh up to 6 mg in males and 13 mg in females (Kan *et al.*, 2009), compared to 120 hpf embryos which have a dry weight of < 1 mg (personal observation).

5.2.2.4 Importance of column purification with limited RNA

An alternative strategy to purify RNA was to use the RNA® MinElute™ Cleanup Kit. Instead of collecting RNA as a precipitate, RNA bound to a silica-membrane column, washed with buffer to remove contaminants such as phenol and proteins, and then collected in an RNase-free eluate. A possible improvement to extracting total RNA from individual embryos would have been to carry out RNA cleanup after separating of RNA, DNA and protein into its three phases (by HPLG). It might even be possible to extract RNA without the use of HPLG separation, but this has yet to be determined for zebrafish embryos. However, combining both

HPLG separation to completely separate limited RNA material and RNA cleanup to purify sample has been demonstrated to be successful in obtaining a high yields of RNA.

5.2.3 Evaluation of RNA quality

One important aspect of RNA extraction is evaluating the yield and quality of the resulting ribonucleic acids. This can be achieved by spectrophotometrically measuring the absorbance of light at a wavelength of 260 nm (A_{260}), evaluating RNA purity according to its $A_{260/280}$ ratio, and assessing RNA integrity by the visualisation of rRNA on denatured agarose gels. As mentioned earlier, the ratio between the absorbance of nucleic acids at 260 nm and 280 nm is often used to determine the purity of material. However the use of the word "purity" is often a misnomer when it comes to assessing RNA quality.

"Pure" RNA is said to have an $A_{260/280}$ ratio between 1.8 and 2.0 (Manchester, 1996). RNA has a maximum absorbance at 260 nm and an absorbance of 1.0 corresponds to 40 µg/mL of RNA. However, the absorbance at 280 nm can vary, according to the pH, which can be affected by contaminants (*e.g.* proteins) (Wilfinger *et al.*, 1997). For this reason, buffers are often recommended for storing RNA, since they stabilise fluctuations in pH. The presence of non-RNA material including phenol, ethanol and proteins can also interfere with the absorbance values and alter the $A_{260/280}$ ratio (Fleige and Pfaffl, 2006). In this study, all RNA samples were eluted in RNase-free water, and any contaminants affected by pH in the sample could have influenced any $A_{260/280}$ ratios obtaine. In the case of total RNA extracted using the TRI Reagent, RNA pellets were washed in ethanol, however additional wash steps could have aided in reducing sample contamination and potentially increase the $A_{260/280}$ ratio. Therefore using only this ratio to determine RNA quality is insufficient, but still can give some information on the contamination by proteins and phenol within RNA preparations.

Ribosomal RNA constitutes the majority (> 90%) of total RNA. Due to its abundance, rRNA will mask other forms of RNA when subjected to denaturing AGE. Thus, the evaluation of rRNA quality is used as another means of evaluating of total RNA quality (Sambrook and Russell, 2001). Intact rRNA contains the 28S and 18S forms in a ratio of 2.7:1, and the presence and intensity of both rRNAs in the denaturing AGE gel can be used to indicate whether degradation has occurred in the sample. However, this can also be subjective due to the running conditions, the amount of staining agent used and the quantity of RNA subjected through the gel.

Although extraction was only carried out on a limited number of samples, the $A_{260/280}$ ratio was generally lower compared to total RNA extracted from individual embryos using HPLG separation. However, it could be possible that using the TRIzol Reagent protocol leads to a final product with residual contaminants, such as phenols and proteins, which might affect the interpretation of the values, compared to HPLG separation and column purification which help facilitate in giving a more stable, final product.

In the study carried out by de Jong *et al.* (2010), the quality of total RNA obtained from individual zebrafish embryos was determined by its RNA Integrity Number (RIN), measured using a BioAnalyzer (Agilent Technologies). RIN is calculated by an algorithm which takes into account the fluorescence of RNA molecules in a sample and their respective sizes. A RIN equal or greater than 7.0 is the requirement for high quality RNA, where 10 represents intact RNA and 0 completely degraded RNA. The BioAnalyzer is highly sensitive and accurate, being able to measure RNA quality in samples with concentrations as low as 25 ng/µL (Mueller *et al.*, 2004). When the assessment of RNA quality is important (*e.g.* mRNA expression), it is recommended that this technology be utilised for a more objective determination of RNA quality, since it minimises any misinterpretations made on RNA quality according to $A_{260/280}$ ratio and rRNA ratio in denaturing AGE.

5.3 Sequencing zebrafish *pxr* in individuals

Genetic variation in *pxr* from different strains of zebrafish has been observed (Bainy et al., 2013; Lille-Langøy, unpublished data). In order to assess the intraspecies genetic variation of the AB/Tu strain, a *pxr* fragment encoding amino acids from180 to 338 was amplified and sequenced from 24 individual zebrafish embryos. The following section will discuss these findings in detail and their implications to the overall protein sequence of Pxr.

5.3.1 Absence of genetic variation between individuals

The region of *pxr* sequenced across the 24 individuals all contained an identical genotype (Figure 4.22). This differed to findings made by Bainy *et al.* (2013), where three alleles of full length zebrafish *pxr* were identified among individuals of the TL strain, with allelic determinants at S184, Y218 and H383. Variants containing S184, Y218 and H383 were

designated to possess the *pxr*1* allele and variants with I184, C218 and N384 the *pxr*2* allele. In this study, all individuals contained amino acids corresponding to the *pxr*1* allele.

5.3.1.1 Genetic variation dependent on allele frequency

In this study, *pxr* was sequenced from only 24 embryos, originating from a mating of ten males and ten females. A high number of adults was used for mating in order to maximise genetic variation in the offspring, and to increase the likelihood of an allele being detected. However, the likelihood of an individual possessing a particular genotype depends on the frequency of the allele in the population. For example, if the probability of both *allele a* (p) and *allele b* (q) in a given population is 0.5, then the likelihood of one of those alleles appearing in an individual would have been: $2pq = 2 \times 0.5 \times 0.5 = 0.5$. Of course, these probabilities depend on the Hardy-Weinberg equilibrium, where the frequency of all genotypes within a population is given by the formula: $p^2 + 2pq + q^2$. This principle assumes that mating is random and that there is no natural selection, mutation or migration (Hartl and Clark, 1997). Given subpopulation of 24 individuals, 12 hypothetically would have possessed one of each allele. However, if the probabilities were unequal, *i.e.* if the probability of *allele a* occurring in a given population is 0.9 and *allele b* is 0.1, then the number of individuals possessing only *allele b* would have been: $24 \times q^2 = 24 \times 0.01 < 1$ individual. In light of this, then it may have been difficult to detect alleles in individual zebrafish if the frequencies of alleles leading to non-synonymous substitutions were rare.

In a study by (Zhang *et al.*, 2001), 3 non-synonymous alleles were identified in human *PXR* (P27S, G36R and R122Q, Table 5.2). In Caucasians, the alleles giving rise to amino substitutions S27, R36 and Q122 occurred in frequencies of 0.00, 0.01 and 0.01 respectively. In African Americans, the same substitutions occurred in frequencies of 0.20, 0.03 and 0.00 respectively. In fact, most identified non-synonymous SNPs appear in very low frequencies in human *PXR*. If allelic determinants are present at such low frequencies, then it is no surprise that no alleles in zebrafish *pxr* were identified in 24 individuals, given the frequency of non-synonymous alleles present in human *PXR* and their probability of occurrence assuming Hardy-Weinberg equilibrium. Future studies would benefit from sequencing a larger number of individuals.

Table 5.2
12 of the 15 known non-synonymous SNPs identified in human *PXR* and their respective allele frequencies.

Substitution	Sample size	Heritage	Allele 1	Allele 2	Reference
E18K	300	Caucasian	1.00	0.00	Hustert *et al.* (2001)
	74	African American	0.85	0.15	Hustert et al. (2001)
P27S	150	Caucasian	1.00	0.00	Zhang *et al.* (2001)
	66	African American	0.80	0.20	Zhang et al. (2001)
G36R	150	Caucasian	0.99	0.01	Zhang et al. (2001)
	66	African American	0.97	0.03	Zhang et al. (2001)
R98C	205	Japanese	0.99	0.0024	Koyano *et al.* (2001)
R122Q	144	Caucasian	0.99	0.01	Zhang et al. (2001)
	22	African American	1.00	0.00	Zhang et al. (2001)
V140M	418	Caucasian	0.99	0.01	Hustert et al. (2001)
R148Q	205	Japanese	0.99	0.0024	Koyano et al. (2001)
Q158K	451	Chinese	0.98	0.02	Lim *et al.* (2005)
D163G	418	Caucasian	1.00	0.00	Hustert et al. (2001)
C379G	100	Mixed (93% Caucasian)	1.00	0.005	Bosch *et al.* (2006)
R381W	205	Japanese	0.99	0.0024	Koyano et al. (2001)
I403V	205	Japanese	0.99	0.0024	Koyano et al. (2001)

5.3.1.2 Genetic variation between strains

A major difference between the individuals sequenced in both studies was the strain of the fish, with AB/Tu being used in this study and TL being used by Bainy and co-authors. Studies comparing genetic variation between species strains have made use of genetic markers, which can assess relatedness or differentness between populations. Genetic variation between strains of zebrafish can be quite large (Guryev *et al.*, 2006), and it could be possible that alleles are more likely to be retained within strains than between them. In a study carried out by Coe *et al.* (2009), the average expected heterozygosity of laboratory maintained zebrafish was much lower in the AB/Tu strain (47%) than in wild zebrafish (86%). Differences in the degree of heterozygosity indicate that genetic variation differs from strain

to strain, and could be why the TL strain studied by Bainy and co-authors might contain allelic variants on the *pxr* gene, while the AB/Tu strain in this study does not, given this is the case.

5.3.1.3 Potential conservation in the sequenced region of pxr

It could be possible that allelic variants exist elsewhere on the *pxr* gene for the AB/Tu individuals. In this study, only 158 of the total 430 amino acids were sequenced in zebrafish *pxr*, and these amino acids encode for the hinge and the beginning of the LBD. In human *PXR*, none of the fifteen SNPs identified overlap with this region of zebrafish *pxr* sequenced in this study (Figure 1.4 & Table 5.2). This could imply that this region (hinge and the beginning of the LBD) in both strains remains relatively conserved.

In humans, SNPs have been predicted to occur in approximately 1% of amino acid coding sequences, with half of these leading to non-synonymous amino acid substitutions (Hinds *et al.*, 2005). SNPs in human *PXR* have been shown to occur much more frequently in the 5' and 3'-untranslated regions of the gene, and in introns more than exons (Zhang *et al.*, 2001; Bosch *et al.*, 2006). In the case of zebrafish however, the only way to confirm whether the sequenced region of *pxr* is conserved compared to the TL strain sequenced by Bainy *et al.* (2013) would be to sequence this region in other strains, and determine whether commonly occurring allelic variants are unique to the TL strain. Another solution would be sequence full length zebrafish *pxr*, to determine whether non-synonymous SNPs are more prevalent in other regions of the sequence.

5.3.2 Genetic variation of *pxr* compared to online sequences and its implications

When the *pxr* sequence from this study was compared to two zebrafish *pxr* sequences available on UniProtKB/TrEMBL (identifiers: A5WYG8 and F1R424), six amino acid differences were found (Figure 4.22). Five substitutions corresponded to L186V, M202V, P208S, N232S and S234T and one insertion to N223. From these two sequences, one was an unknown strain (A5WYG8) and the other corresponded to Tu (F1R424). Interestingly, the *pxr* sequence from the Tu strain corresponded to the *pxr**2* allele in the TL strain identified by Bainy *et al.* (2013).

Understanding how sequence variation in zebrafish *pxr* affects target gene expression is important if we are to use zebrafish as a model organism. This is especially important in

toxicological studies which study the activation of PXR by ligands acting as drugs or pollutants. One approach to this would be to clone *pxr* in the AB/Tu strain from this study, the TL strain from Bainy *et al.* (2013) and the Tu strain identified on UniProtKB and express these genes in a reporter assay. The luciferase reporter assay is a well established method in our laboratory and allows one to test a nuclear receptor's LBD ability to be activated by various ligands acting as drugs or pollutants. This has been done across a wide range of species (Milnes *et al.*, 2008). In fact, using this assay has found that zebrafish *pxr* variants from different strains (AB/Tu, TL and SWT) activate zfPXR in a variant dependent manner (Lille-Langøy, unpublished data; Figure B2, Appendix B). These findings could have implications on studies that use zebrafish and exposures to compounds acting through PXR.

5.3.3 The detection of SNPs from Sanger sequencing

Upon initial inspection of the chromatograms of each *pxr* sequence obtained from Sanger sequencing, some individuals exhibited what appeared to be heterozygosity in some of the base pairs of their sequence (Figure 4.21). This was indicated by the presence of a twin peak in the chromatogram, which appeared to be infrequent and be occurring at random.

A good chromatogram is defined as a sequence that contains evenly-spaced, intense peaks corresponding to each base pair and contains minimal baseline noise. Most of the sequences in this study had some baseline noise, but were mostly easy to interpret. Chromatograms containing weak peaks and high baseline noise will mask low frequency heterozygotes. However, from these sequences, no twin peaks corresponding to heterozygotes were identified.

As expected, all chromatograms lost intensity further along the sequence. For some sequences, this loss in intensity was "top-heavy", where the intensity of the peaks declined very early in the sequence, indicating that the optimal ratio between template and primer was not used. However, low baseline noise and evenly-spaced peaks made sequences still sufficient to interpret. For this reason, a cut-off point at beginning at V180 and ending V339 was set to prevent any misinterpretations on questionable regions of the sequence

The presence of twin peaks was only observed when the baseline noise was too strong or when the intensity of the actual sequence was weak. This only occurred in a few of the sequences and interpretation was still possible but proceeded with caution. Any peaks which

suggested the presence of a heterozygote were cross checked with the matching sequence in the opposite direction, which were always reliable to interpret. In all instances, the possibility of a base pair being heterozygous was ruled out.

5.4 Conclusions

Five hybridoma supernatants from the spleen cells of mice immunised with human PXR were shown to be immunoreactive against the eukaryotically expressed hPXR antigen. Two of these supernatants were also found to be immunoreactive againts a protein which could potentially correspond to a post-translational modification of PXR. Human PXR was also localised in both the cytoplasm and nucleus of transfected COS-7 cells after treatment with rifampicin, with a slightly higher concentration in the cyotplasm. In addition, IgG enrichment of hybridoma supernatants was shown to lead to an increase in the specificity of immunoreactivity of one hybridoma supernatant which had previously been shown to be non-specific. However, none of the hybridoma supernatants from spleen cells of mice immunised with zfPXR were found to be immunoreactive against COS-7 cells transfected with zfPXR or against prokaryotic cells expressing the His-tagged zfPXR antigen. Further analyses are required in order to determine whether non-specificity is due to antigen problems and/or the hybridoma supernatants.

Total RNA was extracted from individual zebrafish embryos using TRI Reagent, HPLG separation of phases followed by column purification of RNA. The use of zebrafish embryos and a method to extract total RNA from individuals could pave the way for exposure experiments where the quantification of genes involved in toxicological response is important.

RNA was obtained at yields high enough for cDNA synthesis and subsequent PCR amplification of a region of the zebrafish *pxr* transcript. We suspected that genetic variation in zebrafish *pxr* could lead to differences in Pxr function. However, no genetic variation was found from amino acids 180 to 338 in fragment of *pxr* sequenced from 24 individuals of the AB/Tu strain, despite allelic variants recently being identified in this region of TL strain zebrafish. Amino acid differences were found when sequences were compared to an unknown and Tu strain of zebrafish submitted to UniProtKB, showing that inter-strain variation of zebrafish *pxr* does exist. These differences could lead to functional variation.

Further analyses could focus on sequencing the full length gene from a larger sample size and determining if genetic variation exists elsewhere.

5.5 Future perspectives

One benefit of obtaining highly specific monoclonal antibodies is to utilise them in ChIP technology. As mentioned, the first study to utilise this technology using PXR was in mice, whereby its DNA-binding sites were investigated after activation with PCN and immunoprecipitation using anti-mouse PXR (Cui *et al.*, 2010). However, the induction of target genes by PXR depends on the type of ligands which activate the nuclear receptor (Song *et al.*, 2004). Therefore this area has potential for further research, especially when identifying which target genes become expressed after the activation of PXR by environmental pollutants. In addition, producing antibodies specific against PXR in other species (*e.g.* zebrafish) could reveal new target genes not previously attributed to PXR activation.

Hybridoma supernatants which have been characterised as immunoreactive against hPXR should be studied in further detail. Epitope mapping of the hybridoma supernatants could give insight on their exact target of specificity and this could be tested in a number of ways. The hybridoma supernatants could be tested again PXR fragments, such as the stable, tethered PXR LBD/SRC-1 complex (Wang *et al.*, 2008), or against other PXR fragments (*e.g.* N-terminal, DBD) fused to recombinant proteins which increase their stability. However, characterisation against PXR fragments might not give the exact location of the epitope, so one alternative is to probe antibodies against a microarray containing thousands of random peptides (Linnebacher *et al.*, 2012). Cross-reactivity of the supernatant against one or more of the peptides can be traced back to its original sequence and compared against PXR.

Identification of allelic variants in zebrafish *pxr* was not achieved in this study. Although no heterozygous genes were found from Sanger sequencing, it could still be possible that genetic variation does exist between individuals. Even if heterozygous alleles did exist, the chromatograms of sequences observed in this study were not completely reliable and frequently required cross-checking with their reverse complement. Given this degree of uncertainty, increasing the number of individuals sequenced could also increase the number of false positives. One option worth considering is restriction fragment length polymorphism

(RFLP) analysis, whereby a restriction enzyme targeting a site suspected to contain a heterozygous allele added to the amplified *pxr* product (Saiki *et al.*, 1985). Products subject to AGE can be used to determine the number of fragments and their respective sizes. Alleles in other transcription factors have been identified in this manner, including the Aryl hydrocarbon receptor (AhR), which is activated by planar aromatic hydrocarbons including planar PCBs (Wirgin *et al.*, 2011).

Given that zebrafish *pxr* variants can be identified, allelic variants could be used to determine whether functional variation exists between alleles. This could be tested by cloning a sequence and ligating it into an expression vector. The luciferase reporter gene assay could then be used to test whether *pxr* variants differentially transactivates *cyp3a* reporter genes (Koyano *et al.*, 2004). Additionally, quantification of gene expression from individuals exposed to PXR agonists *in vivo* could elucidate whether differential expression levels of Pxr target genes occurs as a result of *pxr* variation. For example, one could measure *cyp3a65* expression levels in individual embryonic or adult zebrafish exposed to clotrimazole.

References

Aaij, C., and Borst, P. 1972. The gel electrophoresis of DNA. *Biochimica et Biophysica Acta (BBA)-Nucleic Acids and Protein Synthesis* **269** (2):192-200.

Abbas, A. K., Lichtman, A. H., and S, P. (2012). *Cellular and Molecular Immunology*, 7 ed. Elsevier Saunders, Philadelphia.

Abmayr, S. M., Carrozza, M. J., and Workman, J. L. 2006. Preparation of nuclear and cytoplasmic extracts from mammalian cells. *Current Protocols in Pharmacology*.

Aleström, P., Holter, J. L., and Nourizadeh-Lillabadi, R. 2006. Zebrafish in functional genomics and aquatic biomedicine. *Trends in Biotechnology* **24** (1):15-21.

Bainy, A. C., Kubota, A., Goldstone, J. V., Lille-Langøy, R., Karchner, S. I., Celander, M. C., Hahn, M. E., Goksøyr, A., and Stegeman, J. J. 2013. Functional characterization of a full length pregnane X receptor, expression *in vivo*, and identification of PXR alleles, in zebrafish (*Danio rerio*). *Aquatic Toxicology* **142-143**:447-457.

Barros, T., Alderton, W., Reynolds, H., Roach, A., and Berghmans, S. 2008. Zebrafish: an emerging technology for *in vivo* pharmacological assessment to identify potential safety liabilities in early drug discovery. *British Journal of Pharmacology* **154** (7):1400-1413.

Baudiffier, D., Hinfray, N., Vosges, M., Creusot, N., Chadili, E., Porcher, J.-M., Schulz, R. W., and Brion, F. 2012. A critical role of follicle-stimulating hormone (Fsh) in mediating the effect of clotrimazole on testicular steroidogenesis in adult zebrafish. *Toxicology* **298** (1):30-39.

Benjamin, D. C., and Perdue, S. S. 1996. Site-directed mutagenesis in epitope mapping. *Methods* **9** (3):508-515.

Bertilsson, G., Heidrich, J., Svensson, K., Asman, M., Jendeberg, L., Sydow-Backman, M., Ohlsson, R., Postlind, H., Blomquist, P., and Berkenstam, A. 1998. Identification of a human nuclear receptor defines a new signaling pathway for CYP3A induction. *Proceedings of the National Academy of Sciences of the United States of America* **95** (21):12208-12213.

Biancarosa, I. (2014). Zebrafish (*Danio rerio*) emrbyos as *in vivo* model to test environmental endocrine disrupting compounds (EDCs). MSc Thesis, Dipartimento di Scienze della Vita e dell'Ambiente, Marche Polytechnic University.

Bimboim, H., and Doly, J. 1979. A rapid alkaline extraction procedure for screening recombinant plasmid DNA. *Nucleic Acids Research* **7** (6):1513-1523.

Bio-Rad. (2014). Chemiluminescence Chemistry. <http://www.bio-rad.com/webroot/web/images/lsr/products/electrophoresis/product_overlay_content/global/lsr_chemiluminescent_detection.jpg> Accessed 02/06/2014.

Björck, L., and Kronvall, G. 1984. Purification and some properties of streptococcal protein G, a novel IgG-binding reagent. *The Journal of Immunology* **133** (2):969-974.

Blumberg, B., Sabbagh, W., Jr, Juguilon, H., Bolado, J. J., van Meter, C. M., Ono, E. S., and Evans, R. M. 1998. SXR, a novel steroid and xenobiotic-sensing nuclear receptor. *Genes & Development* **12** (20):3195-3205.

Bosch, T. M., Deenen, M., Pruntel, R., Smits, P. H., Schellens, J. H., Beijnen, J. H., and Meijerman, I. 2006. Screening for polymorphisms in the PXR gene in a Dutch population. *European journal of Cinical Pharmacology* **62** (5):395-399.

Bradford, M. M. 1976. A rapid and sensitive method for the quantitation of microgram quantities of protein utilizing the principle of protein-dye binding. *Analytical Biochemistry* **72** (1):248-254.

Bresolin, T., de Freitas Rebelo, M., and Celso Dias Bainy, A. 2005. Expression of PXR, CYP3A and MDR1 genes in liver of zebrafish. *Comparative Biochemistry and Physiology Part C: Toxicology & Pharmacology* **140** (3):403-407.

Bruning, O., Rodenburg, W., Radonic, T., Zwinderman, A. H., de Vries, A., Breit, T. M., and de Jong, M. 2011. RNA isolation for transcriptomics of human and mouse small skin biopsies. *BMC Research Notes* **4** (1):438.

Chiarella, P., and Fazio, V. M. 2008. Mouse monoclonal antibodies in biological research: strategies for high-throughput production. *Biotechnology Letters* **30** (8):1303-1310.

Chomczynski, P., and Sacchi, N. 1987. Single-step method of RNA isolation by acid guanidinium thiocyanate-phenol-chloroform extraction. *Analytical Biochemistry* **162** (1):156-159.

Coe, T., Hamilton, P., Griffiths, A., Hodgson, D., Wahab, M., and Tyler, C. 2009. Genetic variation in strains of zebrafish (*Danio rerio*) and the implications for ecotoxicology studies. *Ecotoxicology* **18** (1):144-150.

Cui, J. Y., Gunewardena, S. S., Rockwell, C. E., and Klaassen, C. D. 2010. ChIPing the cistrome of PXR in mouse liver. *Nucleic Acids Research* **38** (22):7943-7963.

Davies, R. A. (2011). The establishment of hybridoma cell lines producing monoclonal antibodies against human and zebrafish steroid and xenobiotic receptor (SXR, NR1I2). MSc Thesis, Department of Molecular Biology, University of Bergen.

de Jong, M., Rauwerda, H., Bruning, O., Verkooijen, J., Spaink, H. P., and Breit, T. M. 2010. RNA isolation method for single embryo transcriptome analysis in zebrafish. *BMC Research Notes* **3**:73-73.

Driessen, M., Kienhuis, A. S., Pennings, J. L. A., Pronk, T. E., van de Brandhof, E.-J., Roodbergen, M., Spaink, H. P., van de Water, B., and van der Ven, L. T. M. 2013. Exploring the zebrafish embryo as an alternative model for the evaluation of liver toxicity by histopathology and expression profiling. *Archives of Toxicology* **87** (5):807-823.

Dubrac, S., Elentner, A., Ebner, S., Horejs-Hoeck, J., and Schmuth, M. 2010. Modulation of T lymphocyte function by the pregnane X receptor. *The Journal of Immunology* **184** (6):2949-2957.

Dussault, I., Yoo, H.-D., Lin, M., Wang, E., Fan, M., Batta, A. K., Salen, G., Erickson, S. K., and Forman, B. M. 2003. Identification of an endogenous ligand that activates pregnane X receptor-mediated sterol clearance. *Proceedings of the National Academy of Sciences* **100** (3):833-838.

Escriva, H., Delaunay, F., and Laudet, V. 2000. Ligand binding and nuclear receptor evolution. *Bioessays* **22** (8):717-727.

Escriva, H., Safi, R., Hänni, C., Langlois, M.-C., Saumitou-Laprade, P., Stehelin, D., Capron, A., Pierce, R., and Laudet, V. 1997. Ligand binding was acquired during evolution of nuclear receptors. *Proceedings of the National Academy of Sciences of the United States of America* **94** (13):6803-6808.

Frank, S. A. (2002). *Immunology and Evolution of Infectious Disease*. Princeton University Press.

Fukuen, S., Fukuda, T., Matsuda, H., Sumida, A., Yamamoto, I., Inaba, T., and Azuma, J. 2002. Identification of the novel splicing variants for the hPXR in human livers. *Biochemical and Biophysical Research Communications* **298** (3):433-438.

Gardner-Stephen, D., Heydel, J.-M., Goyal, A., Lu, Y., Xie, W., Lindblom, T., Mackenzie, P., and Radominska-Pandya, A. 2004. Human PXR variants and their differential effects on the regulation of human UDP-glucuronosyltransferase gene expression. *Drug Metabolism and Disposition* **32** (3):340-347.

Germain, P., Staels, B., Dacquet, C., Spedding, M., and Laudet, V. 2006. Overview of nomenclature of nuclear receptors. *Pharmacological Reviews* **58** (4):685-704.

Gluzman, Y. 1981. SV40-transformed simian cells support the replication of early SV40 mutants. *Cell* **23** (1):175-182.

Goksøyr, A. 2006. Endocrine disruptors in the marine environment: mechanisms of toxicity and their influence on reproductive processes in fish. *Journal of Toxicology and Environmental Health, Part A* **69** (1-2):175-184.

Goodwin, B., Redinbo, M. R., and Kliewer, S. A. 2002. Regulation of CYP3A gene transcription by the pregnane X receptor. *Annual Review of Pharmacology and Toxicology* **42** (1):1-23.

Gordon, J. A. 1972. Denaturation of globular proteins. Interaction of guanidinium salts with three proteins. *Biochemistry* **11** (10):1862-1870.

Grün, F., Venkatesan, R. N., Tabb, M. M., Zhou, C., Cao, J., Hemmati, D., and Blumberg, B. 2002. Benzoate X receptors α and β are pharmacologically distinct and do not function as xenobiotic receptors. *Journal of Biological Chemistry* **277** (46):43691-43697.

Guengerich, F. P. 2008. Cytochrome p450 and chemical toxicology. *Chemical Research in Toxicology* **21** (1):70-83.

Guryev, V., Koudijs, M. J., Berezikov, E., Johnson, S. L., Plasterk, R. H., Van Eeden, F. J., and Cuppen, E. 2006. Genetic variation in the zebrafish. *Genome Research* **16** (4):491-497.

Guyon, J. R., Steffen, L. S., Howell, M. H., Pusack, T. J., Lawrence, C., and Kunkel, L. M. 2007. Modeling human muscle disease in zebrafish. *Biochimica et Biophysica Acta (BBA)-Molecular Basis of Disease* **1772** (2):205-215.

Hartl, D. L., and Clark, A. G. (1997). *Principles of Population Genetics*, vol. 116. Sinauer associates Sunderland.

Hinds, D. A., Stuve, L. L., Nilsen, G. B., Halperin, E., Eskin, E., Ballinger, D. G., Frazer, K. A., and Cox, D. R. 2005. Whole-genome patterns of common DNA variation in three human populations. *Science* **307** (5712):1072-1079.

Howe, K., Clark, M. D., Torroja, C. F., Torrance, J., Berthelot, C., Muffato, M., Collins, J. E., Humphray, S., McLaren, K., and Matthews, L. 2013. The zebrafish reference genome sequence and its relationship to the human genome. *Nature* **496** (7446):498-503.

Hustert, E., Zibat, A., Presecan-Siedel, E., Eiselt, R., Mueller, R., Fuß, C., Brehm, I., Brinkmann, U., Eichelbaum, M., and Wojnowski, L. 2001. Natural protein variants of pregnane X receptor with altered transactivation activity toward CYP3A4. *Drug Metabolism and Disposition* **29** (11):1454-1459.

Jeltsch, A. 2013. Systematic specificity analysis of histone modification antibodies. *Materials and Methods*.

Jensen, F. C., Girardi, A. J., Gilden, R. V., and Koprowski, H. 1964. Infection of human and simian tissue cultures with Rous sarcoma virus. *Proceedings of the National Academy of Sciences of the United States of America* **52** (1):53.

Jolly, R. A., Goldstein, K. M., Wei, T., Gao, H., Chen, P., Huang, S., Colet, J.-M., Ryan, T. P., Thomas, C. E., and Estrem, S. T. 2005. Pooling samples within microarray studies: a comparative analysis of rat liver transcription response to prototypical toxicants. *Physiological Genomics* **22** (3):346-355.

Jones, S. A., Moore, L. B., Shenk, J. L., Wisely, G. B., Hamilton, G. A., McKee, D. D., Tomkinson, N. C. O., LeCluyse, E. L., Lambert, M. H., Willson, T. M., Kliewer, S. A., and Moore, J. T. 2000. The pregnane x receptor: A promiscuous xenobiotic receptor that has diverged during evolution. *Molecular Endocrinology* **14** (1):27-39.

Jones, S. A., Moore, L. B., Wisely, G. B., and Kliewer, S. A. 2002. Use of in vitro pregnane X receptor assays to assess CYP3A4 induction potential of drug candidates. *Methods in Enzymology* **357**:161-170.

Joyce, J. G., and ter Meulen, J. 2010. Pushing the envelope on HIV-1 neutralization. *Nature Biotechnology* **28** (9):929-931.

Jung, D., Mangelsdorf, D. J., and Meyer, U. A. 2006. Pregnane X receptor is a target of farnesoid X receptor. *Journal of Biological Chemistry* **281** (28):19081-19091.

Kan, N. G., Junghans, D., and Belmonte, J. C. I. 2009. Compensatory growth mechanisms regulated by BMP and FGF signaling mediate liver regeneration in zebrafish after partial hepatectomy. *The FASEB Journal* **23** (10):3516-3525.

Kast, H. R., Goodwin, B., Tarr, P. T., Jones, S. A., Anisfeld, A. M., Stoltz, C. M., Tontonoz, P., Kliewer, S., Willson, T. M., and Edwards, P. A. 2002. Regulation of multidrug resistance-associated protein 2 (ABCC2) by the nuclear receptors pregnane X receptor, farnesoid X-activated receptor, and constitutive androstane receptor. *Journal of Biological Chemistry* **277** (4):2908-2915.

Kawana, K., Ikuta, T., Kobayashi, Y., Gotoh, O., Takeda, K., and Kawajiri, K. 2003. Molecular mechanism of nuclear translocation of an orphan nuclear receptor, SXR. *Molecular Pharmacology* **63** (3):524-531.

Keightley, M.-C. 1998. Steroid receptor isoforms: exception or rule? *Molecular and Cellular Endocrinology* **137** (1):1-5.

Kim, S., Dinchuk, J. E., Anthony, M. N., Orcutt, T., Zoeckler, M. E., Sauer, M. B., Mosure, K. W., Vuppugalla, R., Grace, J. E., and Simmermacher, J. 2010. Evaluation of cynomolgus monkey pregnane X receptor, primary hepatocyte, and *in vivo* pharmacokinetic changes in predicting human CYP3A4 induction. *Drug Metabolism and Disposition* **38** (1):16-24.

Kimmel, C. B. 1989. Genetics and early development of zebrafish. *Trends in Genetics* **5**:283-288.

Kliewer, S. A., Goodwin, B., and Willson, T. M. 2002. The nuclear pregnane X receptor: A key regulator of xenobiotic metabolism. *Endocrine Reviews* **23** (5):687-702.

Köhler, G., and Milstein, C. 1975. Continuous cultures of fused cells secreting antibody of predefined specificity. *Nature* **256** (5517):495-497.

Kojima, H., Sata, F., Takeuchi, S., Sueyoshi, T., and Nagai, T. 2011. Comparative study of human and mouse pregnane X receptor agonistic activity in 200 pesticides using *in vitro* reporter gene assays. *Toxicology* **280** (3):77-87.

Koyano, S., Kurose, K., Ozawa, S., Saeki, M., Nakajima, Y., Hasegawa, R., Komamura, K., Ueno, K., Kamakura, S., and Nakajima, T. 2001. Eleven novel single nucleotide polymorphisms in the NR1I2 (PXR) gene, four of which induce non-synonymous amino acid alterations. *Drug Metabolism and Pharmacokinetics* **17** (6):561-565.

Koyano, S., Kurose, K., Saito, Y., Ozawa, S., Hasegawa, R., Komamura, K., Ueno, K., Kamakura, S., Kitakaze, M., and Nakajima, T. 2004. Functional characterization of four naturally occurring variants of human pregnane X receptor (PXR): one variant causes dramatic loss of both DNA binding activity and the transactivation of the CYP3A4 promoter/enhancer region. *Drug Metabolism and Disposition* **32** (1):149-154.

Krasowski, M. D., Ni, A., Hagey, L. R., and Ekins, S. 2011. Evolution of promiscuous nuclear hormone receptors: LXR, FXR, VDR, PXR, and CAR. *Molecular and Cellular Endocrinology* **334** (1):39-48.

Kreiss, P., Mailhe, P., Scherman, D., Pitard, B., Cameron, B., Rangara, R., Aguerre-Charriol, O., Airiau, M., and Crouzet, J. 1999. Plasmid DNA size does not affect the physicochemical properties of lipoplexes but modulates gene transfer efficiency. *Nucleic Acids Research* **27** (19):3792-3798.

Kumar, R., and Thompson, E. B. 1999. The structure of the nuclear hormone receptors. *Steroids* **64** (5):310-319.

Laemmli, U. K. 1970. Cleavage of structural proteins during the assembly of the head of bacteriophage T4. *Nature* **227** (5259):680-685.

Lamba, V., Yasuda, K., Lamba, J. K., Assem, M., Davila, J., Strom, S., and Schuetz, E. G. 2004. PXR (NR1I2): splice variants in human tissues, including brain, and identification of neurosteroids and nicotine as PXR activators. *Toxicology and Applied Pharmacology* **199** (3):251-265.

Landes, N., Pfluger, P., Kluth, D., Birringer, M., Rühl, R., Böl, G.-F., Glatt, H., and Brigelius-Flohé, R. 2003. Vitamin E activates gene expression via the pregnane X receptor. *Biochemical Pharmacology* **65** (2):269-273.

Laudet, V. 1997. Evolution of the nuclear receptor superfamily: early diversification from an ancestral orphan receptor. *Journal of Molecular Endocrinology* **19** (3):207-226.

Lehmann, J. M., McKee, D. D., Watson, M. A., Willson, T. M., Moore, J. T., and Kliewer, S. A. 1998. The human orphan nuclear receptor PXR is activated by compounds that regulate CYP3A4 gene expression and cause drug interactions. *Journal of Clinical Investigation* **102** (5):1016-1023.

Lim, Y.-P., Liu, C.-H., Shyu, L.-J., and Huang, J.-d. 2005. Functional characterization of a novel polymorphism of pregnane X receptor, Q158K, in Chinese subjects. *Pharmacogenetics and Genomics* **15** (5):337-341.

Linnebacher, M., Lorenz, P., Koy, C., Jahnke, A., Born, N., Steinbeck, F., Wollbold, J., Latzkow, T., Thiesen, H.-J., and Glocker, M. O. 2012. Clonality characterization of natural epitope-specific antibodies against the tumor-related antigen topoisomerase IIa by peptide chip and proteome analysis: a pilot study with colorectal carcinoma patient samples. *Analytical and Bioanalytical Chemistry* **403** (1):227-238.

Linney, E., Dobbs-McAuliffe, B., Sajadi, H., and Malek, R. L. 2004. Microarray gene expression profiling during the segmentation phase of zebrafish development. *Comparative Biochemistry and Physiology Part C: Toxicology & Pharmacology* **138** (3):351-362.

Lipman, N. S., Jackson, L. R., Trudel, L. J., and Weis-Garcia, F. 2005. Monoclonal versus polyclonal antibodies: distinguishing characteristics, applications, and information resources. *ILAR Journal* **46** (3):258-268.

Liu, H., and May, K. (2012). Disulfide bond structures of IgG molecules: Structural variations, chemical modifications and possible impacts to stability and biological function. In, *MAbs*. Landes Bioscience, pp. 17.

Lu, N. Z., and Cidlowski, J. A. 2005. Translational regulatory mechanisms generate N-terminal glucocorticoid receptor isoforms with unique transcriptional target genes. *Molecular Cell* **18** (3):331-342.
Manchester, K. 1996. Use of UV methods for measurement of protein and nucleic acid concentrations. *Biotechniques* **20** (6):968.
Mary-Huard, T., Daudin, J.-J., Baccini, M., Biggeri, A., and Bar-Hen, A. 2007. Biases induced by pooling samples in microarray experiments. *Bioinformatics* **23** (13):i313-i318.
Masek, T., Vopalensky, V., Suchomelova, P., and Pospisek, M. 2005. Denaturing RNA electrophoresis in TAE agarose gels. *Analytical Biochemistry* **336** (1):46-50.
Masuyama, H., Hiramatsu, Y., Kunitomi, M., Kudo, T., and MacDonald, P. N. 2000. Endocrine disrupting chemicals, phthalic acid and nonylphenol, activate pregnane X receptor-mediated transcription. *Molecular Endocrinology* **14** (3):421-428.
Miki, Y., Suzuki, T., Kitada, K., Yabuki, N., Shibuya, R., Moriya, T., Ishida, T., Ohuchi, N., Blumberg, B., and Sasano, H. 2006. Expression of the steroid and xenobiotic receptor and its possible target gene, organic anion transporting polypeptide-A, in human breast carcinoma. *Cancer Research* **66** (1):535-542.
Miki, Y., Suzuki, T., Tazawa, C., Blumberg, B., and Sasano, H. 2005. Steroid and xenobiotic receptor (SXR), cytochrome P450 3A4 and multidrug resistance gene 1 in human adult and fetal tissues. *Molecular and Cellular Endocrinology* **231** (1):75-85.
Milnes, M. R., Garcia, A., Grossman, E., Grün, F., Shiotsugu, J., Tabb, M. M., Kawashima, Y., Katsu, Y., Watanabe, H., and Iguchi, T. 2008. Activation of steroid and xenobiotic receptor (SXR, NR1I2) and its orthologs in laboratory, toxicologic, and genome model species. *Environmental Health Perspectives* **116** (7):880.
Moore, L. B., Goodwin, B., Jones, S. A., Wisely, G. B., Serabjit-Singh, C. J., Willson, T. M., Collins, J. L., and Kliewer, S. A. 2000. St. John's wort induces hepatic drug metabolism through activation of the pregnane X receptor. *Proceedings of the National Academy of Sciences of the United States of America* **97** (13):7500-7502.
Moore, L. B., Maglich, J. M., McKee, D. D., Wisely, B., Willson, T. M., Kliewer, S. A., Lambert, M. H., and Moore, J. T. 2002. Pregnane X receptor (PXR), constitutive androstane receptor (CAR), and benzoate X receptor (BXR) define three pharmacologically distinct classes of nuclear receptors. *Molecular Endocrinology* **16** (5):977-986.
Mork-Jannson, A. E. (2010). Steroid og xenobiotika-reseptor (SXR, NR1I2) i sebrafisk - variasjoner i aminosyresekvens og følger for ligandaktivering. MSc Thesis, Department of Molecular Biology, University of Bergen.
Mueller, O., Lightfoot, S., and Schroeder, A. 2004. RNA integrity number (RIN)–Standardization of RNA quality control. *Agilent Application Note, Publication*:1-8.
Mullis, K. B., and Faloona, F. A. 1987. Specific synthesis of DNA in vitro via a polymerase-catalyzed chain reaction. *Methods in Enzymology* **155**:335.
Murphy, K. (2012). *Janeway's Immunology*, 8 ed. Garland Science, Taylor & Francis Group, LLC, New York.
Nelson, D. R., Koymans, L., Kamataki, T., Stegeman, J. J., Feyereisen, R., Waxman, D. J., Waterman, M. R., Gotoh, O., Coon, M. J., and Estabrook, R. W. 1996. P450 superfamily: update on new sequences, gene mapping, accession numbers and nomenclature. *Pharmacogenetics and Genomics* **6** (1):1-42.
Nishimura, M., Naito, S., and Yokoi, T. 2004. Tissue-specific mRNA expression profiles of human nuclear receptor subfamilies. *Drug Metabolism and Pharmacokinetics* **19** (2):135-149.
Notkins, A. L. 2004. Polyreactivity of antibody molecules. *Trends in Immunology* **25** (4):174-179.
Nuclear Receptors Nomenclature Committee. 1999. A unified nomenclature system for the nuclear receptor superfamily. *Cell* **97** (2):161-163.
Orlando, V. 2000. Mapping chromosomal proteins *in vivo* by formaldehyde-crosslinked-chromatin immunoprecipitation. *Trends in Biochemical Sciences* **25** (3):99-104.
OSPAR Commission. 2013. Background document on clotrimazole. *Hazardous Substances Series*.
Östberg, T., Bertilsson, G., Jendeberg, L., Berkenstam, A., and Uppenberg, J. 2002. Identification of residues in the PXR ligand binding domain critical for species specific and constitutive activation. *European Journal of Biochemistry* **269** (19):4896-4904.

Pacyniak, E. K., Cheng, X., Cunningham, M. L., Crofton, K., Klaassen, C. D., and Guo, G. L. 2007. The flame retardants, polybrominated diphenyl ethers, are pregnane X receptor activators. *Toxicological Sciences* **97** (1):94-102.

Pawlak, M., Lefebvre, P., and Staels, B. 2012. General molecular biology and architecture of nuclear receptors. *Current Topics in Medicinal Chemistry* **12** (6):486.

Pollock, C. B., Rogatcheva, M. B., and Schook, L. B. 2007. Comparative genomics of xenobiotic metabolism: a porcine-human PXR gene comparison. *Mammalian Genome* **18** (3):210-219.

Rae, J. M., Johnson, M. D., Lippman, M. E., and Flockhart, D. A. 2001. Rifampin is a selective, pleiotropic inducer of drug metabolism genes in human hepatocytes: studies with cDNA and oligonucleotide expression arrays. *Journal of Pharmacology and Experimental Therapeutics* **299** (3):849-857.

Robinson-Rechavi, M., Garcia, H. E., and Laudet, V. 2003. The nuclear receptor superfamily. *Journal of Cell Science* **116** (4):585-586.

Robinson, P., Anderton, B., and Loviny, T. 1988. Nitrocellulose-bound antigen repeatedly used for the affinity purification of specific polyclonal antibodies for screening DNA expression libraries. *Journal of Immunological Methods* **108** (1):115-122.

Rochette-Egly, C. 2003. Nuclear receptors: integration of multiple signalling pathways through phosphorylation. *Cellular Signalling* **15** (4):355-366.

Rotchell, J., and Ostrander, G. 2003. Molecular markers of endocrine disruption in aquatic organisms. *Journal of Toxicology and Environmental Health Part B: Critical Reviews* **6** (5):453-496.

Rubinstein, A. L. 2003. Zebrafish: from disease modeling to drug discovery. *Current Opinion in Drug Discovery & Development* **6** (2):218-223.

Rubinstein, A. L. 2006. Zebrafish assays for drug toxicity screening. *Expert Opinion on Drug Metabolism & Toxicology* **2** (2):231-240.

Saiki, R. K., Gelfand, D. H., Stoffel, S., Scharf, S. J., Higuchi, R., Horn, G. T., Mullis, K. B., and Erlich, H. A. 1988. Primer-directed enzymatic amplification of DNA with a thermostable DNA polymerase. *Science* **239** (4839):487-491.

Saiki, R. K., Scharf, S., Faloona, F., Mullis, K. B., Horn, G. T., Erlich, H. A., and Arnheim, N. 1985. Enzymatic amplification of beta-globin genomic sequences and restriction site analysis for diagnosis of sickle cell anemia. *Science* **230** (4732):1350-1354.

Sambrook, J., and Russell, D. W. (2001). *Molecular Cloning: A Laboratory Manual*, vol. 1, 3 ed. Cold Spring Harbor Laboratory Press, New York.

Sanger, F., Nicklen, S., and Coulson, A. R. 1977. DNA sequencing with chain-terminating inhibitors. *Proceedings of the National Academy of Sciences* **74** (12):5463-5467.

Saradhi, M., Krishna, B., Mukhopadhyay, G., and Tyagi, R. K. 2005. Purification of full-length human Pregnane and Xenobiotic Receptor: polyclonal antibody preparation for immunological characterization. *Cell Research* **15** (10):785-795.

Sheldon, L. S., and Hubal, E. A. C. 2009. Exposure as part of a systems approach for assessing risk. *Environmental Health Perspectives* **117** (8):1181-1194.

Siest, G., Jeannesson, E., Marteau, J.-B., Samara, A., Marie, B., Pfister, M., and Visvikis-Siest, S. 2008. Transcription factor and drug-metabolizing enzyme gene expression in lymphocytes from healthy human subjects. *Drug Metabolism and Disposition* **36** (1):182-189.

Smutny, T., Mani, S., and Pavek, P. 2013. Post-translational and post-transcriptional modifications of pregnane X receptor (PXR) in regulation of the cytochrome P450 superfamily. *Current Drug Metabolism* **14** (10):1059-1069.

Song, X., Xie, M., Zhang, H., Li, Y., Sachdeva, K., and Yan, B. 2004. The pregnane X receptor binds to response elements in a genomic context-dependent manner, and PXR activator rifampicin selectively alters the binding among target genes. *Drug Metabolism and Disposition* **32** (1):35-42.

Sonoda, J., Chong, L. W., Downes, M., Barish, G. D., Coulter, S., Liddle, C., Lee, C.-H., and Evans, R. M. 2005. Pregnane X receptor prevents hepatorenal toxicity from cholesterol metabolites. *Proceedings of the National Academy of Sciences of the United States of America* **102** (6):2198-2203.

Sonoda, J., Xie, W., Rosenfeld, J. M., Barwick, J. L., Guzelian, P. S., and Evans, R. M. 2002. Regulation of a xenobiotic sulfonation cascade by nuclear pregnane X receptor (PXR). *Proceedings of the National Academy of Sciences* **99** (21):13801-13806.

Spence, R., Gerlach, G., Lawrence, C., and Smith, C. 2008. The behaviour and ecology of the zebrafish, Danio rerio. *Biological Reviews* **83** (1):13-34.

Sprague, J., Bayraktaroglu, L., Clements, D., Conlin, T., Fashena, D., Frazer, K., Haendel, M., Howe, D. G., Mani, P., and Ramachandran, S. 2006. The Zebrafish Information Network: the zebrafish model organism database. *Nucleic Acids Research* **34** (suppl 1):D581-D585.

Squires, E. J., Sueyoshi, T., and Negishi, M. 2004. Cytoplasmic localization of pregnane X receptor and ligand-dependent nuclear translocation in mouse liver. *Journal of Biological Chemistry* **279** (47):49307-49314.

Staszewski, R. 1984. Cloning by limiting dilution: an improved estimate that an interesting culture is monoclonal. *The Yale Journal of Biology and Medicine* **57** (6):865-868.

Staudinger, J. L., Xu, C., Biswas, A., and Mani, S. 2011. Post-translational modification of pregnane X receptor. *Pharmacological Research* **64** (1):4-10.

Sui, Y., Ai, N., Park, S.-H., Rios-Pilier, J., Perkins, J. T., Welsh, W. J., and Zhou, C. 2012. Bisphenol A and its analogues activate human pregnane X receptor. *Environmental Health Perspectives* **120** (3):399-405.

Synold, T. W., Dussault, I., and Forman, B. M. 2001. The orphan nuclear receptor SXR coordinately regulates drug metabolism and efflux. *Nature Medicine* **7** (5):584-590.

Tabb, M. M., Sun, A. S., Zhou, C., Grün, F., Errandi, J., Romero, K., Pham, H., Inoue, S., Mallick, S., Lin, M., Forman, B. M., and Blumberg, B. 2003. Vitamin K-2 regulation of bone homeostasis is mediated by the steroid and xenobiotic receptor SXR. *Journal of Biological Chemistry* **278** (45):43919-43927.

Timme-Laragy, A. R., Karchner, S. I., Franks, D. G., Jenny, M. J., Harbeitner, R. C., Goldstone, J. V., McArthur, A. G., and Hahn, M. E. 2012. Nrf2b, novel zebrafish paralog of oxidant-responsive transcription factor NF-E2-related factor 2 (NRF2). *Journal of Biological Chemistry* **287** (7):4609-4627.

Towbin, H., Staehelin, T., and Gordon, J. 1979. Electrophoretic transfer of proteins from polyacrylamide gels to nitrocellulose sheets: procedure and some applications. *Proceedings of the National Academy of Sciences* **76** (9):4350-4354.

Tseng, H.-P., Hseu, T.-H., Buhler, D. R., Wang, W.-D., and Hu, C.-H. 2005. Constitutive and xenobiotics-induced expression of a novel CYP3A gene from zebrafish larva. *Toxicology and Applied Pharmacology* **205** (3):247-258.

Underwood, A. P., and Bean, P. A. 1988. Hazards of the limiting-dilution method of cloning hybridomas. *Journal of Immunological Methods* **107** (1):119-128.

van der Vaart, M., van Soest, J. J., Spaink, H. P., and Meijer, A. H. 2013. Functional analysis of a zebrafish myd88 mutant identifies key transcriptional components of the innate immune system. *Disease Models & Mechanisms* **6** (3):841-854.

Venter, J. C., Adams, M. D., Myers, E. W., Li, P. W., Mural, R. J., Sutton, G. G., Smith, H. O., Yandell, M., Evans, C. A., and Holt, R. A. 2001. The sequence of the human genome. *Science* **291** (5507):1304-1351.

Walsh, G., and Jefferis, R. 2006. Post-translational modifications in the context of therapeutic proteins. *Nature Biotechnology* **24** (10):1241-1252.

Wang, W., Prosise, W. W., Chen, J., Taremi, S. S., Le, H. V., Madison, V., Cui, X., Thomas, A., Cheng, K.-C., and Lesburg, C. A. 2008. Construction and characterization of a fully active PXR/SRC-1 tethered protein with increased stability. *Protein Engineering Design and Selection* **21** (7):425-433.

Watkins, R. E., Wisely, G. B., Moore, L. B., Collins, J. L., Lambert, M. H., Williams, S. P., Willson, T. M., Kliewer, S. A., and Redinbo, M. R. 2001. The human nuclear xenobiotic receptor PXR: Structural determinants of directed promiscuity. *Science* **292** (5525):2329-2333.

Wilfinger, W., Mackey, K., and Chomczynski, P. 1997. Effect of pH and ionic strength on the spectrophotometric assessment of nucleic acid purity. *Biotechniques* **22** (3):474-476, 478-481.

Wirgin, I., Roy, N. K., Loftus, M., Chambers, R. C., Franks, D. G., and Hahn, M. E. 2011. Mechanistic basis of resistance to PCBs in Atlantic tomcod from the Hudson River. *Science* **331** (6022):1322-1325.

World Health Organization. 2002. IPCS global assessment of the state-of-the-science of endocrine disruptors. *WHO/PCS/EDC/02.2*:35-50.

World Health Organization. 2013. WHO Model List of Essential Medicines.

Wu, B., Li, S., and Dong, D. 2013. 3D structures and ligand specificities of nuclear xenobiotic receptors CAR, PXR and VDR. *Drug Discovery Today* **18** (11-12):574–581.

Xie, W., Barwick, J. L., Simon, C. M., Pierce, A. M., Safe, S., Blumberg, B., Guzelian, P. S., and Evans, R. M. 2000. Reciprocal activation of Xenobiotic response genes by nuclear receptors SXR/PXR and CAR. *Genes & Development* **14** (23):3014-3023.

Xie, W., Radominska-Pandya, A., Shi, Y., Simon, C. M., Nelson, M. C., Ong, E. S., Waxman, D. J., and Evans, R. M. 2001. An essential role for nuclear receptors SXR/PXR in detoxification of cholestatic bile acids. *Proceedings of the National Academy of Sciences* **98** (6):3375-3380.

Xue, Y., Moore, L. B., Orans, J., Peng, L., Bencharit, S., Kliewer, S. A., and Redinbo, M. R. 2007. Crystal structure of the pregnane X receptor-estradiol complex provides insights into endobiotic recognition. *Molecular Endocrinology* **21** (5):1028-1038.

Yang, F., Tan, H., Zhou, Y., Lin, X., and Zhang, S. 2011. High-quality RNA preparation from Rhodosporidium toruloides and cDNA library construction therewith. *Molecular Biotechnology* **47** (2):144-151.

Zhang, J., Kuehl, P., Green, E. D., Touchman, J. W., Watkins, P. B., Daly, A., Hall, S. D., Maurel, P., Relling, M., Brimer, C., Yasuda, K., Wrighton, S. A., Hancock, M., Kim, R. B., Strom, S., Thummel, K., Russell, C. G., Hudson, J. R., Jr, Schuetz, E. G., and Boguski, M. S. 2001. The human pregnane X receptor: genomic structure and identification and functional characterization of natural allelic variants. *Pharmacogenetics* **11** (7):555-572.

Zhou, C., Poulton, E.-J., Grün, F., Bammler, T. K., Blumberg, B., Thummel, K. E., and Eaton, D. L. 2007. The dietary isothiocyanate sulforaphane is an antagonist of the human steroid and xenobiotic nuclear receptor. *Molecular Pharmacology* **71** (1):220-229.

Zhou, C., Verma, S., and Blumberg, B. 2009. The steroid and xenobiotic receptor (SXR), beyond xenobiotic metabolism. *Nuclear Receptor Signaling* **7**.

Appendix A

Table A1
Protein concentration of COS-7 cell lysate components according to the Bradford protein assay.

COS-7 cells transfected with	Fraction	Concentration (µg/ml)
No plasmid	Cytoplasmic	1959
No plasmid	Nuclear	1435
pSG5 hPXR	Cytoplasmic	741
pSG5 hPXR	Nuclear	1096
pcDNA zfPXR	Cytoplasmic	1218
pcDNA zfPXR	Nuclear	1032

Table A2
Concentration and purity of RNA obtained from individual zebrafish embryos using phase lock gel separation.

Individual	Concentration (ng / µL)	$A_{260/280}$	Yield (ng)
1	158.1	1.76	2213
2	186.2	1.91	2607
3	140.5	1.89	1967
4	98.0	2.00	1372
5	127.7	1.92	1788
6	202.3	1.98	2832
7	187.8	1.79	2629
8	197.1	1.84	2759
9	178.7	1.93	2502
10	211.6	1.92	2962
11	197.4	1.87	2764
12	168.9	1.96	2365
13	100.9	1.86	1413
14	96.8	1.83	1355
15	144.4	1.89	2023
16	111.8	1.94	1565
17	114	1.91	1596
18	113	1.89	1582
19	103.6	1.94	1450
20	126.5	1.91	1771
21	94.2	1.92	1319
22	140.7	1.82	1970
23	90.3	1.92	1264
24	84.9	1.98	1189

Table A3
Concentration of PCR product (full length zebrafish *pxr*) obtained after PCR reaction with zfPXR primers and cleanup.

Individual	Concentration (ng / µL)	$A_{260/280}$	Yield (ng)
1	15.2	1.69	760
2	21.0	1.60	1050
3	15.4	1.70	770
4	16.5	1.55	825
5	14.1	1.75	705
6	15.3	1.60	765
7	15.0	2.15	750
8	16.1	1.88	805
9	18.1	1.60	905
10	15.5	1.83	775
11	14.9	1.57	745
12	14.1	1.84	705
13	16.8	1.90	840
14	15.0	1.88	750
15	15.3	2.43	765
16	15.7	1.83	785
17	14.6	1.54	730
18	13.1	2.24	655
19	16.8	2.04	840
20	15.8	1.66	790
21	16.2	1.74	810
22	17.4	1.63	870
23	14.1	1.94	705
24	13.7	1.83	685

Consensus DNA sequence of *pxr* (mRNA coding sequence, cds) and translated Pxr in AB/Tu strain zebrafish from this study.

```
GTGTCCGAGTCGAGTCCACTCACAAACGGCAGCTGGATCGATCACAGACCCATCGCTGAAGAC
CCAATGCAGTGGGTCTTCAATCCCACTTCGCTCTCGTCCTCTTCCTCCAGCTACCAGAGCCTT
GACAATAAAGAGAAGAAGCACTTTAAAAGTGGCAACTTCTCCTCTCTGCCACACTTCACAGAC
CTCACCACGTACATGATCAAGAATGTCATCAACTTCGGGAAGACGCTGACAATGTTTAGGGCT
CTGGTTATGGAGGACCAGATCTCGCTGCTGAAAGGTGCCACCTTTGAGATCATTCTGATTCAC
TTCAACATGTTCTTTAATGAAGTGACGGGAATTTGGGAGTGTGGCCCCTTGCAGTACTGCATG
GATGATGCCTTTCGAGCTGGTTTTCAGCACCATCTGCTGGACCCAATGATGAATTTCCATTAC
ACACTGCGTAAGCTGCGTTTGCATGAGGAGGAGTATGTGCT


VSESSPLTNGSWIDHRPIAEDPMQWVFNPTSLSSSSSSYQSLDNKEKKHFKSGNFSSLPHFTD
LTTYMIKNVINFGKTLTMFRALVMEDQISLLKGATFEIILIHFNMFFNEVTGIWECGPLQYCM
DDAFRAGFQHHLLDPMMNFHYTLRKLRLHEEEYV
```

Nucleotide sequence of *pxr* (cds) and amino acid sequence of Pxr in an unknown strain of zebrafish from EMBL (DQ069792) and UniProtKB (accession: A5WYG8).

```
GTGTCCGAGTCCAGTCCAGTCACAAACGGCAGCTGGATCGATCACAGACCCATCGCTGAAGAC
CCAGTGCAGTGGGTCTTCAACTCCACTTCGCTCTCGTCCTCTTCCTCCAGCTACCAGAGCCTT
GACAAAGAGAAGAAGCACTTTAAAAGTGGCAGCTTCACCTCTCTGCCACACTTCACAGACCTC
ACCACGTACATGATCAAGAATGTCATCAACTTCGGGAAGACGCTGACAATGTTCAGGGCTCTG
GTTATGGAGGACCAGATCTCGCTGCTGAAAGGTGCCACCTTTGAGATCATTCTGATTCACTTC
AACATGTTCTTTAATGAAGTGACGGGAATTTGGGAGTGCGGCCCCCTGCAGTACTGCATGGAT
GATGCCTTTCGAGCTGGTTTTCAGCACCATCTGCTGGACCCAATGATGAATTTCCATTACACA
CTGCGTAAGCTGCGTTTGCATGAGGAGGAGTATGTGCT


VSESSPVTNGSWIDHRPIAEDPVQWVFNSTSLSSSSSSYQSLDKEKKHFKSGSFTSLPHFTDL
TTYMIKNVINFGKTLTMFRALVMEDQISLLKGATFEIILIHFNMFFNEVTGIWECGPLQYCMD
DAFRAGFQHHLLDPMMNFHYTLRKLRLHEEEYV
```

Amino acid sequence of Pxr in Tu strain zebrafish from UniProtKB (accession: F1R424). Nucleotide sequence not available.

```
VSESIPVTNGSWIDHRPIAEDPVQWVFNSTSLSSSSSSCQSLDKEKKHFKSGSFTSLPHFTDL
TTYMIKNVINFGKTLTMFRALVMEDQISLLKGATFEIILIHFNMFFNEVTGIWECGPLQYCMD
DAFRAGFQHHLLDPMMNFHYTLRKLRLHEEEYV
```

Nucleotide sequence of *PXR* (cds) and amino acid sequence of PXR in human from EMBL (AY091855) and UniProtKB (accession: O75469):

```
TGCGAGTTGCCAGAGTCTCTGCAGGCCCCATCGAGGGAAGAAGCTGCCAAGTGGAGCCAG
GTCCGGAAAGATCTGTGCTCTTTGAAGGTCTCTCTGCAGCTGCGGGGGGAGGATGGCAGT
GTCTGGAACTACAAACCCCCAGCCGACAGTGGCGGGAAAGAGATCTTCTCCCTGCTGCCC
CACATGGCTGACATGTCAACCTACATGTTCAAAGGCATCATCAGCTTTGCCAAAGTCATC
TCCTACTTCAGGGACTTGCCCATCGAGGACCAGATCTCCCTGCTGAAGGGGGCCGCTTTC
GAGCTGTGTCAACTGAGATTCAACACAGTGTTCAACGCGGAGACTGGAACCTGGGAGTGT
GGCCGGCTGTCCTACTGCTTGGAAGACACTGCAGGTGGCTTCCAGCAACTTCTACTGGAG
CCCATGCTGAAATTCCACTACATGCTGAAGAAGCTGCAGCTGCATGAGGAGGAGTATGTG
CT
```

```
CELPESLQAPSREEAAKWSQVRKDLCSLKVSLQLRGEDGSVWNYKPPADSGGKEIFSLLP
HMADMSTYMFKGIISFAKVISYFRDLPIEDQISLLKGAAFELCQLRFNTVFNAETGTWEC
GRLSYCLEDTAGGFQQLLLEPMLKFHYMLKKLQLHEEEYV
```

Nucleotide sequence of *Pxr* (mRNA) and amino acid sequence of PXR in mouse from EMBL (AF031814) and UniProtKB (accession: O54915):

```
TGTGAGCTTCCAGAGTTTCTGCAGGCCTCACTGTTGGAAGACCCTGCCACATGGAGTCAA
ATCATGAAAGACAGGGTTCCAATGAAGATCTCTCTGCAGCTGCGCGGAGAAGACGGCAGC
ATCTGGAACTACCAACCCCCTTCCAAGAGCGACGGGAAAGAGATCATCCCTCTTCTGCCA
CACCTGGCCGATGTGTCAACCTACATGTTCAAGGGCGTCATCAACTTCGCCAAAGTCATA
TCCTACTTTAGGGACCTGCCTATTGAGGACCAGATCTCCCTGCTGAAGGGGGCCACTTTT
GAGATGTGCATCCTGAGGTTCAACACGATGTTCGACACGGAAACGGGAACCTGGGAGTGC
GGCCGGCTGGCTTACTGCTTCGAAGACCCTAATGGTGGCTTCCAGAAACTTCTGTTGGAT
CCATTGATGAAATTCCACTGCATGCTGAAGAAGCTACAGCTGCATAAGGAGGAGTATGTG
CT
```

```
CELPEFLQASLLEDPATWSQIMKDRVPMKISLQLRGEDGSIWNYQPPSKSDGKEIIPLLP
HLADVSTYMFKGVINFAKVISYFRDLPIEDQISLLKGATFEMCILRFNTMFDTETGTWEC
GRLAYCFEDPNGGFQKLLLDPLMKFHCMLKKLQLHKEEYV
```

Appendix B

The following supplementary data was taken from the Master's thesis of Richard Davies (Figure 4.11, 2011). Note that SXR refers to PXR, immunogen means antigen, and that hybridoma supernatant 12D5B5C8 was also tested in our study.

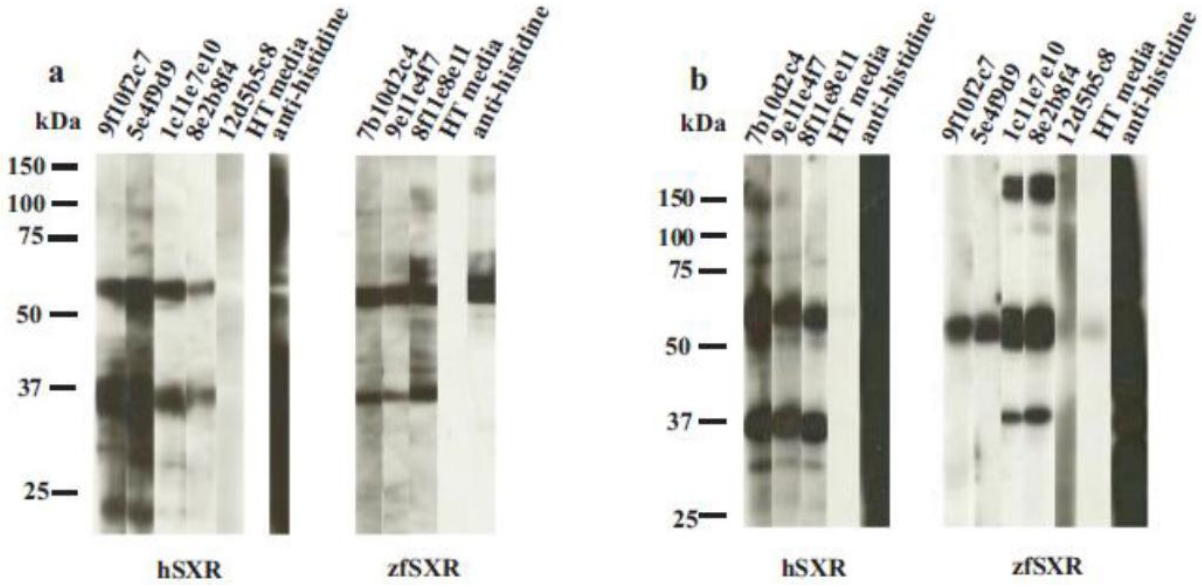

Figure B1. Immunoreactivity of hybridoma supernatants against hSXR and zfSXR orthologs. 300 μg of PXR was separated using a 10% SDS-PAGE gel and transferred to a PVDF membrane. The membrane was cut into strips prior to screening. The primary antibody probes were non-diluted hybridoma culture supernatants 9f10f2c7, 5e4f9d9, 1c11e7e10, 8e2b8f4, 12d5b5c8, 7b10d2c4, 9e11e4f7 and 8f11e8e11 as well as HT medium (no dilution) and anti-hist mAb (1:3000). The supernatants were used to probe the immunogen used in their development (a) and an immunogen containing SXR from a different species (human or zebrafish) (b). Primary Antibodies were detected with polyclonal goat anti-mouse Ig HRP-conjugated antibodies. Respective protein sizes in kDa are labelled on the left of the figure as indicated by a Precision Plus Protein Standard. Development was by Amersham ECL Plus™.

The following supplementary data was taken from work carried out by PhD candidate Roger Lille-Langøy (unpublished data).

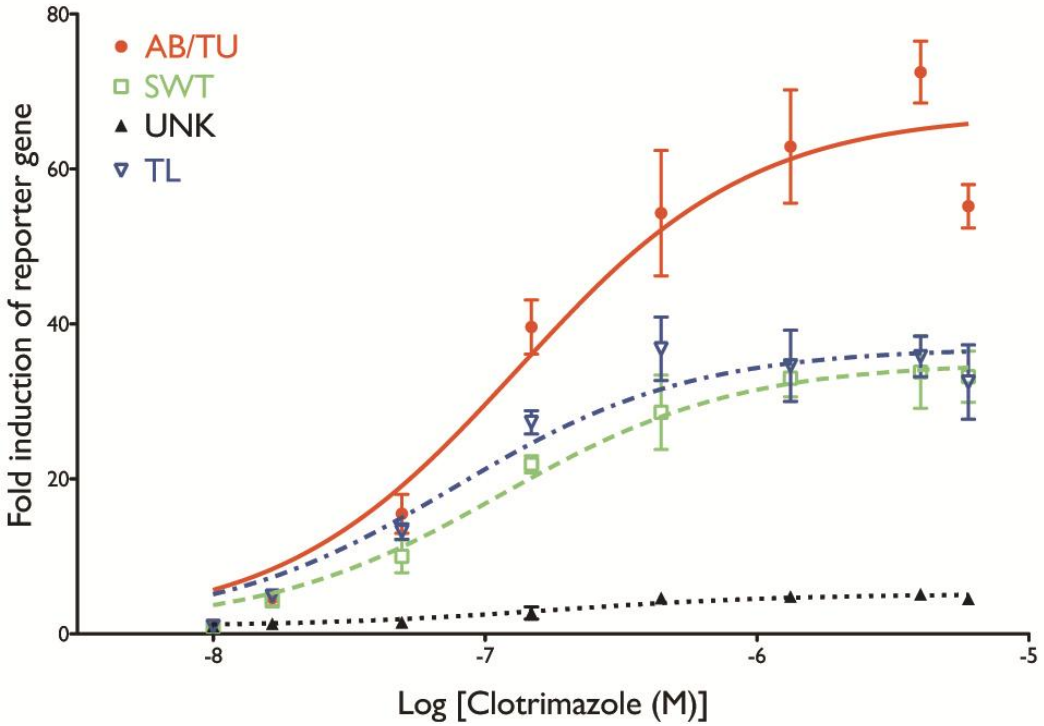

Figure B2. Luciferase reporter gene assay of zebrafish *pxr* variants after exposure to clotrimazole. Ligand activation was reported as a fold change of luciferase activity relative to vehicle control (DMSO). Transfection efficiency was normalised against β-galactosidase activity. Concentrations range from 10 nM to 6 µM, with data points representing the mean of individual triplicate experiments ± standard deviation.

Appendix C

The effect of genotypic variation on promiscuous xenobiotic receptor (Pxr) activation and phenotypic *cyp3a65* transcription in zebrafish

Daniel Hitchcock[1], Roger Lille-Langøy[1], Irene Biancarosa[1,2,3], Marta Eide[1], Ståle Ellingsen[2], Anders Goksøyr[1]
[1] Department of Biology, University of Bergen, Norway; [2] National Institute of Nutrition and Seafood Research (NIFES), Norway; [3] Marche Polytechnic University, Italy
daniel.hitchcock@student.uib.no

INTRODUCTION

The promiscuous xenobiotic receptor (PXR, Nr1i2) is a nuclear receptor which regulates the transcription of genes for enzymes involved in the biotransformation of xenobiotic compounds. Some pollutants are capable of activating Nr1i2 more strongly than others, which in turn can lead to a higher level of enzyme gene expression (Lehmann *et al.*, 1998). One important subfamily of genes activated by Nr1i2 are the cytochrome P450 monooxygenases, including *cyp3a65* involved in metabolism of xenobiotics. This gene has been shown to be strongly expressed in zebrafish after exposure to clotrimazole (Tseng *et al.*, 2005). Nr1i2 in zebrafish contains allelic variation (Bainy *et al.*, 2013) that could affect Nr1i2 function and consequently target gene expression. This study aims to determine whether the genotype of zebrafish Nr1i2 affects its ability to be activated by clotrimazole, and thus affect *cyp3a65* transcription.

METHODS

Sequencing and ligand activation of zebrafish Nr1i2 variants
Zebrafish *nr1i2* variants were cloned and then sequenced from individual livers of zebrafish from four different strains, AB/TU, SWT, TL and a strain of unknown origin (UNK). Ligand activation of each variant was measured *in vitro* using the luciferase reporter gene assay (Grün *et al.*, 2002). *Nr1i2* were transferred into plasmids and transfected to a eukaryotic cell line (COS7) along with a GAL4-UAS luciferase reporter and β-galactosidase control plasmids. Twenty-four hours post transfection, the cells were exposed to clotrimazole (from 10 nM to 6 µM) for another 24 hours. Ligand activation was reported as fold change of luciferase activity relative to a solvent control (DMSO). Transfection efficiency was normalised against β-galactosidase activity.

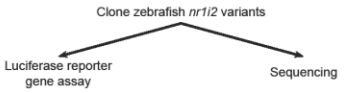

Nr1i2 mediated induction of *cyp3a65* in zebrafish embyos
To assess *in vivo* activation of Nr1i2, zebrafish embryos were maintained in E3 medium and were at 48 hpf, exposed to clotrimazole (from 0.11 to 9 µM) dissolved in 1% DMSO. At 120 hpf, 10 embryos from the same treatment group were pooled and homogenised using a syringe and total RNA extracted (TRIzol® Reagent, Life Technologies). cDNA from each pooled group was synthesised (qScript, Quanta Biosciences), and the transcription of *cyp3a65* was quantified using real-time PCR. Expression levels were then mean normalised to three housekeeping genes (*ef1a*, *rpl13a* and *tuba1*).

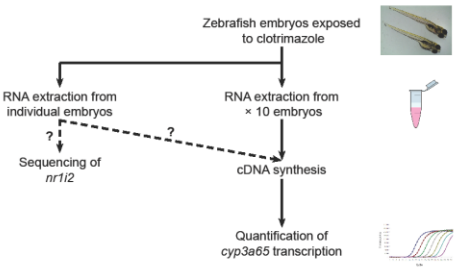

RESULTS

Variants of zebrafish Nr1i2 resulting from allelic variation

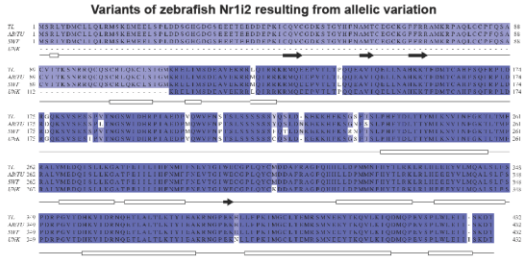

Figure 1. Sequence alignment of zebrafish Nr1i2 variants. Alignments were carried out in Clustal Omega.

***In vitro* activation of zebrafish Nr1i2s is variant dependent**

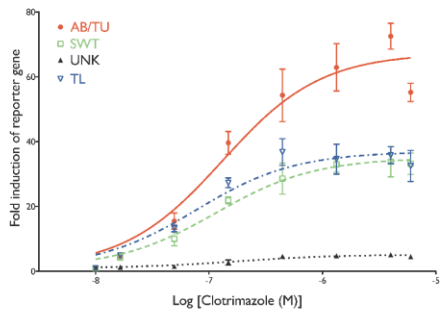

Figure 2. *In vitro* ligand activation of zebrafish Nr1i2 variants after exposure to clotrimazole. Concentrations range from 10 nM to 6 µM. Data points represent the mean of individual triplicate experiments ± SD, and curves are fitted by non-linear regression using GraphPad Prism.

Clotrimazole induces *cyp3a65* in zebrafish embryos

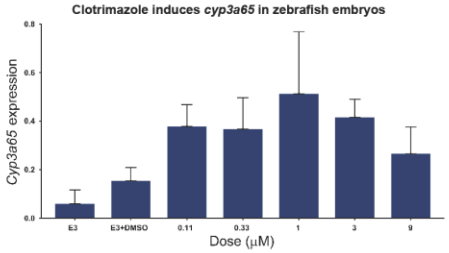

Figure 3. Expression levels of *cyp3a65* from pooled zebrafish embryos after exposure to clotrimazole. Concentrations range from 0.11 to 9 µM. Bars represent the mean of individual triplicates + SD, and data included is representative of one experiment.

CONCLUSIONS

Zebrafish Nr1i2 variants share a high sequence identity but contain some amino acid differences in the ligand-binding domain. This results in differing levels of Nr1i2 activation by clotrimazole. Gene transcription of *cyp3a65* in zebrafish embryos is also induced by clotrimazole.

We are currently trying to determine whether zebrafish *nr1i2* genotype has an effect on the phenotypic transcription of *cyp3a65* in individual embryos. This will involve exposing single embryos to clotrimazole, sequencing *nr1i2* and quantifying *cyp3a65* transcription for each individual. Functional variation among *nr1i2* alleles could have implications for toxicological studies which use zebrafish and exposures to compounds acting through Nr1i2.

REFERENCES

1. Lehmann, JM *et al.* (1998) *J. Clin. Invest.* 102(5):1016-1023.
2. Tseng, HM *et al.* (2005) *Toxicol. Appl. Pharm.* 205(3):247-258.
3. Bainy, EC *et al.* (2013) *Aquat. Toxicol.* 142-143:447-457.
4. Grün, F *et al.* (2002) *J. Biol. Chem.* 207(46): 43691-43697.

Funded by the Norwegian Research Council, Miljø 2015, Project 18188

Figure C1. Poster presented at the Norwegian Society for Pharmacology and Toxicology (NSFT) winter meeting in Beitostølen 2014.